NASA TECHNICAL NOTE

NASA TN D-8472 c.1

NASA TN D-8472

SUBSONIC AND SUPERSONIC LONGITUDINAL STABILITY AND CONTROL CHARACTERISTICS OF AN AFT-TAIL FIGHTER CONFIGURATION WITH CAMBERED AND UNCAMBERED WINGS AND CAMBERED FUSELAGE

Samuel M. Dollyhigh

Langley Research Center
Hampton, Va. 23665

NATIONAL AERONAUTICS AND SPACE ADMINISTRATION · WASHINGTON, D. C. · SEPTEMBER 1977

1. Report No. NASA TN D-8472	2. Government Accession No.	3. Recipient's Catalog No.
4. Title and Subtitle SUBSONIC AND SUPERSONIC LONGITUDINAL STABILITY AND CONTROL CHARACTERISTICS OF AN AFT-TAIL FIGHTER CONFIGURATION WITH CAMBERED AND UNCAMBERED WINGS AND CAMBERED FUSELAGE		5. Report Date September 1977
		6. Performing Organization Code
7. Author(s) Samuel M. Dollyhigh		8. Performing Organization Report No. L-11424
		10. Work Unit No. 505-11-21-03
9. Performing Organization Name and Address NASA Langley Research Center Hampton, VA 23665		11. Contract or Grant No.
		13. Type of Report and Period Covered Technical Note
12. Sponsoring Agency Name and Address National Aeronautics and Space Administration Washington, DC 20546		14. Sponsoring Agency Code
15. Supplementary Notes		

16. Abstract

An investigation has been conducted over a Mach number range from 0.50 to 2.16 to determine the longitudinal aerodynamic characteristics of a fighter airplane concept. The configuration incorporates a cambered fuselage with a single external-compression horizontal-ramp inlet, a clipped arrow wing, twin horizontal tails, and a single vertical tail. The wing camber surface was optimized in drag due to lift and was designed to be self-trimming at Mach 1.40 and at a lift coefficient of 0.20. The fuselage was cambered to preserve the design wing loadings on the part of the theoretical wing enclosed by the fuselage. An uncambered or flat wing of the same planform and thickness ratio distribution was also tested.

17. Key Words (Suggested by Author(s)) Fighter design, Supersonic camber, Longitudinal aerodynamic characteristics		18. Distribution Statement Unclassified - Unlimited. Subject Category 02	
19. Security Classif. (of this report) Unclassified	20. Security Classif. (of this page) Unclassified	21. No. of Pages 77	22. Price* $5.00

* For sale by the National Technical Information Service, Springfield, Virginia 22161

SUBSONIC AND SUPERSONIC LONGITUDINAL STABILITY AND CONTROL CHARACTERISTICS OF AN AFT-TAIL FIGHTER CONFIGURATION WITH CAMBERED AND UNCAMBERED WINGS AND CAMBERED FUSELAGE

Samuel M. Dollyhigh
Langley Research Center

SUMMARY

An investigation has been conducted over a Mach number range from 0.50 to 2.16 to determine the longitudinal aerodynamics of a fighter airplane concept. The configuration incorporates a cambered fuselage with a single external-compression horizontal-ramp inlet, a clipped arrow wing, twin horizontal tails, and a single vertical tail. The wing camber surface was optimized in drag due to lift and was designed to be self-trimming at Mach 1.40 and at a lift coefficient of 0.20. The fuselage was cambered to preserve the design wing loadings on the part of the theoretical wing enclosed by the fuselage. An uncambered or flat wing of the same planform and thickness ratio distribution was also tested.

The results indicate that the configuration possessed linear pitching-moment characteristics over the test Mach number and angle-of-attack ranges, except for a tendency to pitch down at subsonic Mach numbers when the flow over the wing separated at the higher angles of attack. The horizontal-tail control effectiveness was found to be adequate over the test Mach number range. The configuration with the supersonic cambered wing had much better drag polar characteristics at subsonic and transonic Mach numbers, and the drag polar characteristics at supersonic Mach numbers were only slightly better than those for the configuration with the flat wing. Most of the supersonic benefits expected from optimizing the wing camber for minimum drag due to lift and trim were apparently achieved by cambering the fuselage to preserve the design wing loadings on the part of the theoretical wing enclosed by the fuselage. The shape of the trimmed drag polar and the tail deflection necessary to trim at Mach 1.47, 1.80, and 2.16 are fairly accurately predicted by current supersonic theoretical methods. However, the theoretical methods underpredicted the experimentally realized drag level. The difference is primarily attributable to evidence of separated flow not accounted for in the theoretical methods.

INTRODUCTION

As part of a research program in advanced fighter technology, the National Aeronautics and Space Administration has undertaken to study the design of efficient supersonic cruise and maneuver in fighter airplanes. References 1 to 6 give a good general background of this research program. This report presents the results of wind-tunnel tests of a generalized fighter configuration discussed in references 1 and 2. This configuration is designed for maneuver or operation at high lift coefficients at low supersonic speeds.

The configuration concept is as tightly packaged as possible to keep the frontal area low. The configuration incorporates a cambered fuselage with a single external compression horizontal-ramp inlet, a clipped arrow wing, twin horizontal tails, and a single vertical tail. The cockpit features an inclined pilot seat, and as a result, the cross-sectional area at the pilot station is greatly reduced, and the pilot is able to withstand higher g loads. The wing planform was selected to provide linear low-speed pitching-moment characteristics and the potential for good transonic maneuver. The wing camber surface is designed for minimum drag due to lift and also to be self-trimming at Mach 1.40 at a lift coefficient of 0.20 by the method discussed in reference 7. The fuselage was cambered using the method presented in reference 8 so as to preserve the design wing loadings on the part of the theoretical wing that was enclosed by the fuselage. Ideally, when the wing is designed in this manner and the fuselage is cambered so that the wing loadings are maintained, a low drag penalty, associated with trimming the aircraft by keeping the necessary horizontal-tail deflections (horizontal-tail loads) small, should result. An uncambered wing of the same planform and thickness distribution was included in the investigation as a reference.

Wind-tunnel tests on a 0.056-scale model were conducted in the Langley 8-foot transonic pressure tunnel and the Langley Unitary Plan wind tunnel at Mach numbers ranging from 0.50 to 2.16. The results of the wind-tunnel investigation together with some supersonic analytical results are reported in this paper.

SYMBOLS

The longitudinal force and moment coefficients are referenced to the wind-axis system. The moment reference point was located at fuselage station 39.40 cm ($0.40\bar{c}$). Values are given in SI Units.

A aspect ratio

b wing span, cm

C_D drag coefficient, $\frac{\text{Drag}}{qS}$

$C_{D,0}$ drag coefficient at $C_L = 0$

C_L lift coefficient, $\frac{\text{Lift}}{qS}$

C_{L_α} lift-curve slope at $C_L = 0$, $\frac{\partial C_L}{\partial \alpha}$

C_m pitching-moment coefficient, $\frac{\text{Pitching moment}}{qS\bar{c}}$

$\dfrac{\Delta C_D}{C_L^2}$	drag-due-to-lift parameter (determined at $C_L = 0.50$)
$\dfrac{\Delta C_L}{\Delta \delta_h}$	tail control effectiveness at zero moment, per deg
$\dfrac{\partial C_m}{\partial C_L}$	longitudinal stability parameter at $C_L = 0$
$\dfrac{\partial C_m}{\partial \delta_h}$	pitching-moment effectiveness of horizontal tail at $C_L = 0$
c	streamwise chord, cm
$\bar{c}$	wing mean geometric chord, cm
g	acceleration due to gravity
L/D	lift-drag ratio
M	free-stream Mach number
q	free-stream dynamic pressure, Pa
S	reference area of wing including fuselage intercept, cm^2
x	longitudinal distance along center line of model from nose, cm
y	lateral distance from center line of model, cm
z	vertical distance from center line of model, cm
z_c	vertical ordinate of camber surface, positive up, cm
α	angle of attack, deg
Γ	dihedral angle, deg
δ_h	horizontal-tail deflection angle, positive when trailing edge is down, deg
Λ	leading-edge sweep angle, deg

Subscripts:

max	maximum
trim	trimmed

DESCRIPTION OF MODEL

A three-view drawing of the complete model is shown in figure 1(a), and drawings of the wing, vertical tail, and horizontal tail are shown in figures 1(b) to 1(d). Some geometric characteristics are given in table I, and a photograph of the model is presented in figure 1(e). The configuration incorporates a cambered fuselage with a single external compression horizontal-ramp inlet, a clipped arrow wing, twin horizontal tails, and a single vertical tail.

The taper ratio of the theoretical planform was 0.20, and the notch ratio or cutout factor was 0.157. The streamwise airfoil thickness distribution was an NACA 65A004.5. Two wings were tested; each had the same planform and airfoil thickness distribution but differed in camber surface. The first wing had a camber surface that was designed for minimum drag due to lift at $M = 1.40$ and $C_L = 0.20$ by the method of reference 7. The camber surface was also designed so that the wing would be self-trimming about the center of gravity of the configuration at the design point ($M = 1.40$; $C_L = 0.20$). The camber surface ordinates of this wing with respect to the leading edge are given in table II. This wing is hereafter referred to as the cambered wing. The second wing, which was also tested on the same cambered fuselage, was uncambered and untwisted (flat) and is hereafter referred to as the uncambered or flat wing.

The fuselage was cambered by the method presented in reference 2 so as to preserve the wing loading on the part of the theoretical wing enclosed by the fuselage. The configuration employed low twin horizontal tails with a 4-percent biconvex airfoil section. The horizontal tails could be deflected over a range from -15° to 10° and could be removed from the model. The single vertical tail also had a 4-percent biconvex airfoil section.

TEST CORRECTIONS

The tests were conducted in the Langley 8-foot transonic pressure tunnel and the Langley Unitary Plan wind tunnel. The tests were conducted under the following conditions:

Mach number	Stagnation pressure, mPa	Stagnation temperature, K	Reynolds number per meter
0.50	57.46	320	5.18×10^6
.80	57.46	321	7.05
.85	57.46	322	7.22
.90	57.46	323	7.38
.95	57.46	323	7.48
1.03	57.46	323	7.68
1.20	57.46	323	7.81
1.47	66.03	339	8.20
1.47	39.60	339	4.92
1.80	73.07	339	8.20
1.80	43.86	339	4.92
2.16	85.61	339	8.20
2.16	52.38	339	4.92

The presented data taken at Mach 1.03 in the Langley 8-foot transonic pressure tunnel were not corrected for the severe tunnel-wall interference that exists at this test condition. To stay within the balance load limits, the Reynolds number per meter was reduced at angles of attack above 10° at Mach 1.47, 1.80, and 2.16 as indicated by the second value in the preceding table. The dewpoint was maintained sufficiently low to prevent measurable condensation effects in the test section. The angle of attack ranged approximately from -6° to 20°. To insure boundary-layer transition to turbulent flow at conditions between Mach 0.20 to 1.20, transition strips 0.16 cm wide of No. 60 carborundum grit were placed on the body 3.05 cm aft of the nose of the model, and strips of No. 80 carborundum grit were placed streamwise 1.02 cm aft of the leading edge on the wings, tails, inlet ramps, and external inlet surface. At conditions between Mach 1.47 to 2.16, strips of No. 50 carborundum grit were used. These transition strips were shown to be adequate in the conclusions of reference 9.

Aerodynamic forces and moments on the model were measured by a six-component strain-gage balance which was housed within the model. The balance was attached to a sting which in turn was rigidly fastened to the tunnel support system. Balance-chamber static pressure was measured with pressure tubes located in the vicinity of the balance. The model internal-flow total pressures and static pressures were measured with a rake consisting of 12 total-pressure tubes and 4 static-pressure tubes. The rake was placed flush with the base of the model and was removed during the force-measurement tests. The drag data presented have been corrected for internal flow and have been corrected to the condition of free-stream static pressure in the balance chamber. Corrections to the angles of attack of the model have been made for both tunnel airflow misalinement and for the deflection of the balance and sting under load.

PRESENTATION OF RESULTS

	Figure
Longitudinal aerodynamic characteristics with cambered wing	2
Longitudinal aerodynamic characteristics with flat wing	3
Longitudinal aerodynamic characteristics with cambered wing and flat wing	4
Trimmed drag polars and lift-drag ratios with cambered wing and flat wing	5
Summary of pertinent longitudinal data	6
Comparison of experimental and theoretical trim curves for Mach 1.47, 1.80, and 2.16	7

DISCUSSION

Figure 2 shows the longitudinal aerodynamic characteristics of the configuration with the cambered wing. The configuration exhibits linear pitching-moment characteristics at all test conditions except for a tendency to pitch down at the higher angles of attack at subsonic Mach numbers. Although arrow wings tend to pitch up, this behavior is presumably associated with flow separation on the wing. As the flow separates, the downwash on the low horizontal tail is decreased, and an increased positive tail load results. This presumption is supported by the fact that the tail-off lift-curve slope (see figs. 2(a) to 2(c)) indicates that separation is beginning to occur at these angles of attack. The wind-tunnel model did not incorporate any wing devices ordinarily used on a fighter airplane to assist in maintaining the flow on the wing at high angles of attack. The horizontal-tail control effectiveness appears to be adequate at all Mach numbers of the test for the moment reference center used. Additional tail deflection data were taken at supersonic speeds to better define the trim drag polar.

The longitudinal aerodynamic characteristics are shown in figure 2(f) for Mach 1.47, the closest test Mach number to the Mach 1.40 design point of the wing and fuselage camber. Note that in figure 2(f), the configuration with the horizontal tail off is trimmed (has zero pitching moment) at a lift coefficient of approximately 0.20. As discussed earlier, the wing camber surface was designed for minimum drag due to lift so that the wing would be self-trimming at the design point ($M = 1.40$; $C_L = 0.20$). The fuselage was then cambered by the method presented in reference 8 to preserve the wing loadings on the part of the theoretical wing enclosed by the fuselage. The pitching-moment curves in figure 2(f) indicate that the self-trimming feature was achieved. The significance of the feature can be seen in the drag polars presented in figure 2(f). Note that the drag levels are approximately the same for a number of tail deflections which result in no trim drag penalty over a lift coefficient range. By designing for no tail load at $C_L = 0.20$, the tail deflection necessary to trim and the resulting tail loads are kept relatively small for a substantial part of the operating lift coefficient range.

A second wing identical to the cambered wing in planform and thickness except that it was uncambered (flat) was tested on the model. Tail-deflection data were limited on the flat-wing configuration since this configuration was a baseline for the effects of exposed wing camber. The longitudinal aerodynamic characteristics for the configuration with the flat wing are shown in figure 3. The effects noted about pitching-moment characteristics and tail control effectiveness for the configuration with the cambered wing are also true for the configuration with the flat wing. The comparison of differences between the two wings is limited to the discussion of figures 4 to 7.

A comparison of the longitudinal aerodynamic characteristics of the cambered-wing configuration with the flat-wing configuration is shown in figure 4. The data presented are for the configuration with zero horizontal-tail deflection and for horizontal tail off. As expected, the configuration with the cambered wing and horizontal tail off has a greater pitching-moment coefficient at a given lift coefficient across the Mach number range than the flat-wing tail-off configuration. However, both configurations with the tail on at 0° deflection tend to have the same pitching moment at low lift coefficients for subsonic speeds and at all lift coefficients for supersonic speeds. Apparently, at all test Mach numbers the horizontal-tail loads are slightly different behind the two wings; the horizontal tail behind the cambered wing is slightly more down loaded than the tail behind the flat wing. This speculation is supported by the fact that for the cambered-wing configuration at Mach 1.47, which is closest to the design Mach number, the trim point for the tail-on 0° deflection (fig. 4(f)) is at a lower lift coefficient than the tail-off (no tail load) trim point. For the flat-wing configuration, the tail-on 0° deflection and the tail-off trim points are the same. Drag polars for the cambered-wing configuration show a much lower drag due to lift than the flat-wing configuration at subsonic and transonic speeds. Increases in $(L/D)_{max}$ of over one are common for the configuration with the cambered wing when compared with the flat wing for subsonic and transonic speeds. But there are very few differences in the drag polars and $(L/D)_{max}$ at supersonic speeds. These results are not as surprising as they may seem. As discussed previously, the fuselage was cambered to preserve the design wing loading ($M = 1.40$; $C_L = 0.20$) on the part of the theoretical wing planform enclosed by the fuselage. The region of the theoretical wing planform enclosed by the fuselage is the most highly cambered part of a supersonic wing and, therefore, has a major influence on the drag-due-to-lift and pitching-moment characteristics of the wing. Since the fuselage is the same for both wings, the drag and pitching-moment characteristics are similar. This situation holds much promise for fighter aircraft because if the fuselage is cambered properly, major benefits of supersonic wing design are realized. The airplane designer is allowed a degree of freedom in exposed wing design to improve the subsonic and transonic aerodynamic characteristics where large influences of exposed wing camber were observed. Then a minimum acceptable supersonic design would allow the wing to be decambered at supersonic speeds to remove any adverse subsonic-transonic camber. The results of a wind-tunnel test using the same wing planform but without fuselage camber are presented in reference 10. The discussion in reference 10 reinforces the statements made earlier about exposed wing camber.

Trimmed drag polars and L/D curves for the configuration with the cambered wing and the flat wing are presented in figure 5. The discussion of figure 4 has already suggested that the drag characteristics of the cambered-wing configuration are superior to those of the flat-wing configuration at subsonic and transonic speeds; these characteristics are only slightly better at supersonic speeds.

A summary plot of the variation of the more pertinent longitudinal parameters with Mach number for the configuration with the cambered wing and with the flat wing is shown in figure 6. Except for $(L/D)_{max}$, which is trimmed, and for tail control effectiveness, the data for the configurations are untrimmed with zero horizontal-tail deflection.

Correlations between the experimental and theoretical trimmed drag and tail deflection necessary to trim are given in figure 7 for the configuration with the cambered wing at Mach 1.47, 1.80, and 2.16. The method used in reference 11, modified to include control surfaces, was employed to calculate the camber drag, drag due to lift, and tail control characteristics. The wave drag and skin friction calculated by methods of references 12 and 13, respectively, were added to the camber drag and drag due to lift to obtain the total drag. Poor agreement exists in the correlation of the drag levels, and fairly good agreement exists in the shape of the drag polar. The experimental and theoretical polars tend to diverge somewhat as the experimental tail-control effectiveness weakens with increasing tail-deflection angle. There are several drag sources such as grit drag and separated flow that are not accounted for in the theoretical drag polars, and these drag sources could be the cause of some of the differences. On this particular model, there was evidence in vapor screen photographs (flow visualization by the induction of fog in the tunnel) of separated flow on the aft side of the canopy. This region of separated flow was evident at zero lift coefficient and increased in magnitude with increasing lift coefficient. Local streamline tailoring of the fuselage aft of the canopy would probably eliminate this problem.

CONCLUDING REMARKS

An investigation has been conducted over a Mach number range from 0.50 to 2.16 to determine characteristics of a fighter airplane concept. The configuration incorporates a cambered fuselage with a single external-compression horizontal-ramp inlet, a clipped arrow wing, twin horizontal tails, and a single vertical tail. The wing camber surface was optimized in drag due to lift and was designed to be self-trimming at Mach 1.40 and at a lift coefficient of 0.20. The fuselage was cambered to preserve the design wing loadings on the part of the theoretical wing enclosed by the fuselage. An uncambered or flat wing of the same planform and thickness ratio distribution was also tested.

The results indicate that the configuration possessed linear pitching-moment characteristics over the test Mach number and angle-of-attack ranges, except for a tendency to pitch down at subsonic Mach numbers when the flow over the wing separated at the higher angles of attack. The horizontal-tail control effectiveness was found to be adequate over the test Mach number range. The configuration with the supersonic cambered wing had much better drag polar characteristics at subsonic and transonic Mach numbers, and the drag polar characteristics at supersonic Mach numbers were only slightly better than those for the configuration with the flat wing. Most of the supersonic benefits expected from optimizing the wing camber for minimum drag due to lift and trim were apparently achieved by cambering the fuselage so as to preserve the design wing loadings on the part of the theoretical wing enclosed by the fuselage. The shape of the trimmed drag polar and the tail deflection necessary to trim at Mach 1.47, 1.80, and 2.16 are fairly accurately predicted by current supersonic theoretical methods. However, the theoretical drag underpredicted the experimentally realized drag level. The difference is primarily attributable to the evidence of separated flow not accounted for in the theoretical methods.

Langley Research Center
National Aeronautics and Space Administration
Hampton, VA 23665
May 26, 1977

REFERENCES

1. Dollyhigh, Samuel M.; Ayers, Theodore G.; Morris, Odell A.; and Miller, David M.: Designing for Supersonic Cruise and Maneuver. Design Conference Proceedings - Technology for Supersonic Cruise Military Aircraft, Volume I, AFFDL TR-77-85, U.S. Air Force, 1976.

2. Shrout, Barrett L.; Morris, Odell A.; Robins, A. Warner; and Dollyhigh, Samuel M.: Review of NASA Supercruise Configuration Studies. Design Conference Proceedings - Technology for Supersonic Cruise Military Aircraft, Volume I, AFFDL TR-77-85, U.S. Air Force, 1976.

3. Berrier, Bobby L.; and Propulsion Integration Section: Propulsion Superintegration = Supercruiser. Design Conference Proceedings - Technology for Supersonic Cruise Military Aircraft, Volume I, AFFDL TR-77-85, U.S. Air Force, 1976.

4. Campbell, J. F.; Gloss, B. B.; and Lamar, J. E.: Vortex Maneuver Lift for Super-Cruise Configurations. Design Conference Proceedings - Technology for Supersonic Cruise Military Aircraft, Volume I, AFFDL TR-77-85, U.S. Air Force, 1976.

5. Coe, Paul L., Jr.; and Gilbert, William P.: Application of Low-Speed Aerodynamic Characteristics of Highly Swept Arrow-Wing Configurations to Supersonic Cruise Tactical Fighter Designs. Design Conference Proceedings - Technology for Supersonic Cruise Military Aircraft, Volume I, AFFDL TR-77-85, U.S. Air Force, 1976.

6. Sorrells, Russell B.; and Foss, Willard E.: Trade Studies on a Long Range Mach 2.7 Supercruiser. Design Conference Proceedings - Technology for Supersonic Cruise Military Aircraft, Volume I, AFFDL TR-77-85, U.S. Air Force, 1976.

7. Carlson, Harry W.; and Middleton, Wilbur D.: A Numerical Method for the Design of Camber Surface of Supersonic Wings With Arbitrary Planforms. NASA TN D-2341, 1964.

8. Dollyhigh, Samuel M.; Morris, Odell A.; and Adams, Mary S.: Experimental Effects of Fuselage Camber on Longitudinal Aerodynamic Characteristics of a Series of Wing-Fuselage Configurations at a Mach Number of 1.41. NASA TM X-3411, 1976.

9. Braslow, Albert L.; Hicks, Raymond M.; and Harris, Roy V., Jr.: Use of Grit Type Boundary-Layer-Transition Trips on Wind-Tunnel Models. NASA TN D-3579, 1966.

10. Dollyhigh, Samuel M.: Subsonic and Supersonic Longitudinal Stability and Control Characteristics of an Aft Tail Fighter Configuration With Cambered and Uncambered Wings and Uncambered Fuselage. NASA TM X-3078, 1974.

11. Middleton, Wilbur D.; and Carlson, Harry W.: A Numerical Method for Calculating the Flat-Plate Pressure Distributions on Supersonic Wings of Arbitrary Planform. NASA TN D-2570, 1965.

12. Harris, Roy V., Jr.: An Analysis and Correlation of Aircraft Wave Drag. NASA TM X-947, 1964.

13. Sommer, Simon C.; and Short, Barbara J.: Free-Flight Measurements of Turbulent-Boundary-Layer Skin Friction in the Presence of Severe Aerodynamic Heating at Mach Numbers From 2.8 to 7.0. NASA TN 3391, 1955.

TABLE I.- COMPONENT GEOMETRY

Wing:	
A	2.758
Λ, deg	50
Γ, deg	0
$\bar{c}$, cm	19.185
b, cm	45.552
S, including fuselage intercept, cm^2	752.398
Airfoil section	NACA 65A004.5
Horizontal tails (exposed):	
A	2.586
Λ, deg	42.5
Γ, deg	0
Mean geometric chord, cm	9.025
Semispan, cm	11.026
Area, cm^2	188.038
Airfoil	4-percent biconvex
Vertical tail:	
A	3.435
Λ, deg	61
Mean geometric chord, cm	13.467
Semispan, cm	10.483
Area, cm^2	127.977
Airfoil	4-percent biconvex
Inlet area, cm^2	13.344
Exit area, cm^2	16.821
Chamber area, cm^2	11.401

TABLE II.- CAMBERED SURFACE ORDINATES

[Fuselage juncture at $\frac{y}{b/2} = 0.15$; wing sections were sheared so that $\frac{x}{c} = 0.25$ was at $z = 0$ in model reference axis]

$\frac{x}{c}$	$\frac{z_c}{c}$, in percent, with respect to leading edge at $\frac{y}{b/2}$ of -															
	0	0.020	0.040	0.060	0.080	0.100	0.150	0.200	0.300	0.400	0.500	0.600	0.700	0.800	0.900	1.000
0	0	0	0	0	0	0	0	0	0	0	0	0	0	0	0	0
.05	-.732	-.331	-.235	-.194	-.164	-.134	.259	.253	.313	.360	.400	.451	.521	.365	.316	.328
.10	-1.951	-.976	-.712	-.582	-.487	-.408	.349	.389	.513	.612	.697	.795	.888	.799	.809	.840
.15	-3.292	-1.732	-1.303	-1.067	-.907	-.783	.356	.459	.656	.810	.942	1.067	1.199	1.148	1.155	1.383
.20	-4.683	-2.558	-1.945	-1.616	-1.387	-1.204	.314	.485	.759	.962	1.137	1.307	1.468	1.445	1.518	1.988
.25	-6.080	-3.415	-2.626	-2.198	-1.900	-1.666	.244	.474	.829	1.096	1.311	1.521	1.723	1.742	1.836	2.593
.30	-7.471	-4.278	-3.325	-2.799	-2.433	-2.147	.149	.442	.884	1.203	1.475	1.711	1.950	2.005	2.134	3.198
.35	-8.831	-5.147	-4.037	-3.407	-2.978	-2.642	.041	.394	.921	1.301	1.608	1.890	2.163	2.250	2.409	3.833
.40	-10.154	-6.004	-4.736	-4.021	-3.524	-3.144	-.078	.332	.943	1.381	1.741	2.057	2.362	2.479	2.684	4.469
.50	-12.652	-7.661	-6.116	-5.229	-4.615	-4.140	-.323	.209	.978	1.523	1.976	2.367	2.747	2.936	3.212	5.740
.55	-13.822	-8.449	-6.777	-5.818	-5.148	-4.629	-.439	.147	.992	1.584	2.078	2.510	2.862	3.148	3.443	6.406
.60	-14.923	-9.119	-7.413	-6.387	-5.661	-5.104	-.551	.085	.998	1.646	2.180	2.653	3.089	3.343	3.674	7.042
.65	-15.957	-9.919	-8.023	-6.930	-6.160	-5.565	-.649	.038	1.011	1.708	2.282	2.785	3.274	3.537	3.927	7.677
.70	-16.923	-10.594	-8.601	-7.447	-6.640	-6.013	-.740	.010	1.033	1.770	2.384	2.916	3.431	3.731	4.137	8.313
.75	-17.815	-11.232	-9.148	-7.944	-7.094	-6.435	-.813	-.042	1.055	1.840	2.476	3.047	3.589	3.926	4.346	8.979
.80	-18.628	-11.819	-9.663	-8.410	-7.521	-6.843	-.870	-.068	1.084	1.902	2.578	3.179	3.746	4.120	4.555	9.614
.85	-19.366	-12.364	-10.133	-8.843	-7.922	-7.217	-.912	-.071	1.123	1.973	2.681	3.310	3.903	4.298	4.742	10.250
.90	-20.020	-12.852	-10.572	-9.244	-8.297	-7.572	-.928	-.067	1.169	2.053	2.783	3.430	4.046	4.475	4.929	10.916
.95	-20.597	-13.290	-10.968	-9.606	-8.646	-7.900	-.929	-.041	1.223	2.142	2.895	3.561	4.203	4.652	5.094	11.552
1.00	-21.089	-13.677	-11.316	-9.935	-8.955	-8.201	-.908	0	1.293	2.231	3.008	3.693	4.361	4.830	5.260	12.187

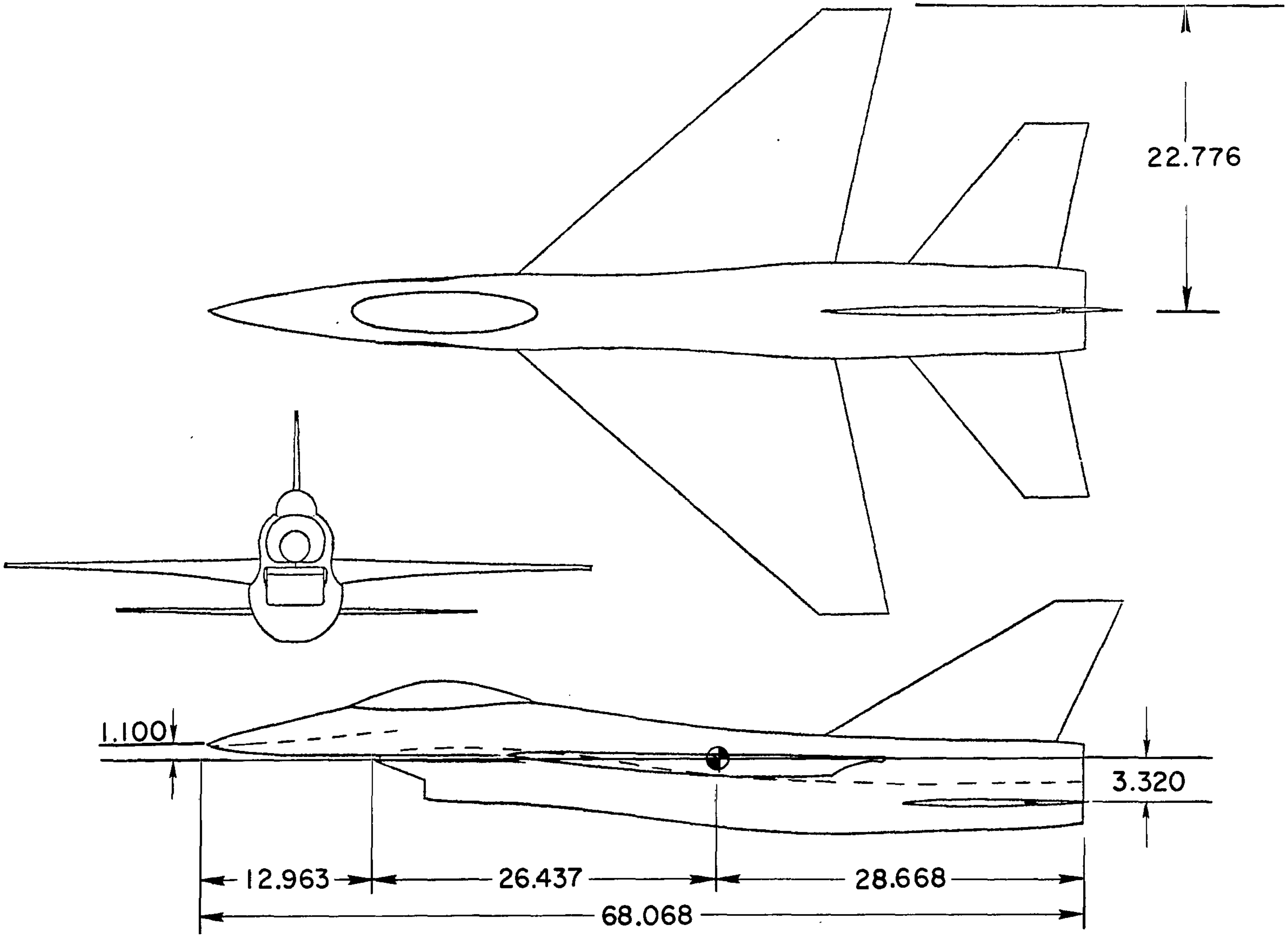

(a) Three-view drawing of complete model. Dashed line indicates centroid of fuselage cross-sectional area.

Figure 1.- Drawing of model. Dimensions in cm.

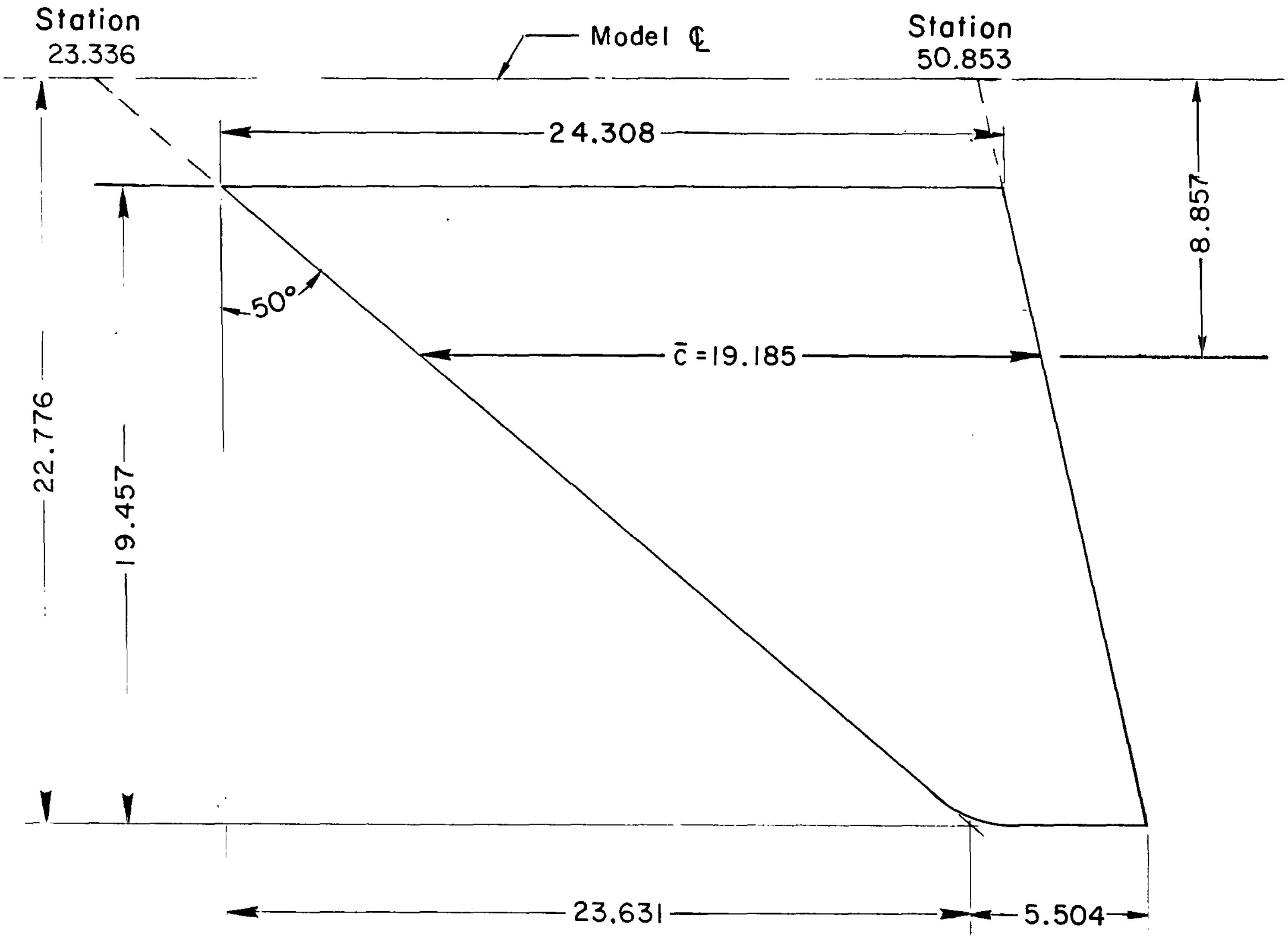

(b) Details of wing.

Figure 1.- Continued.

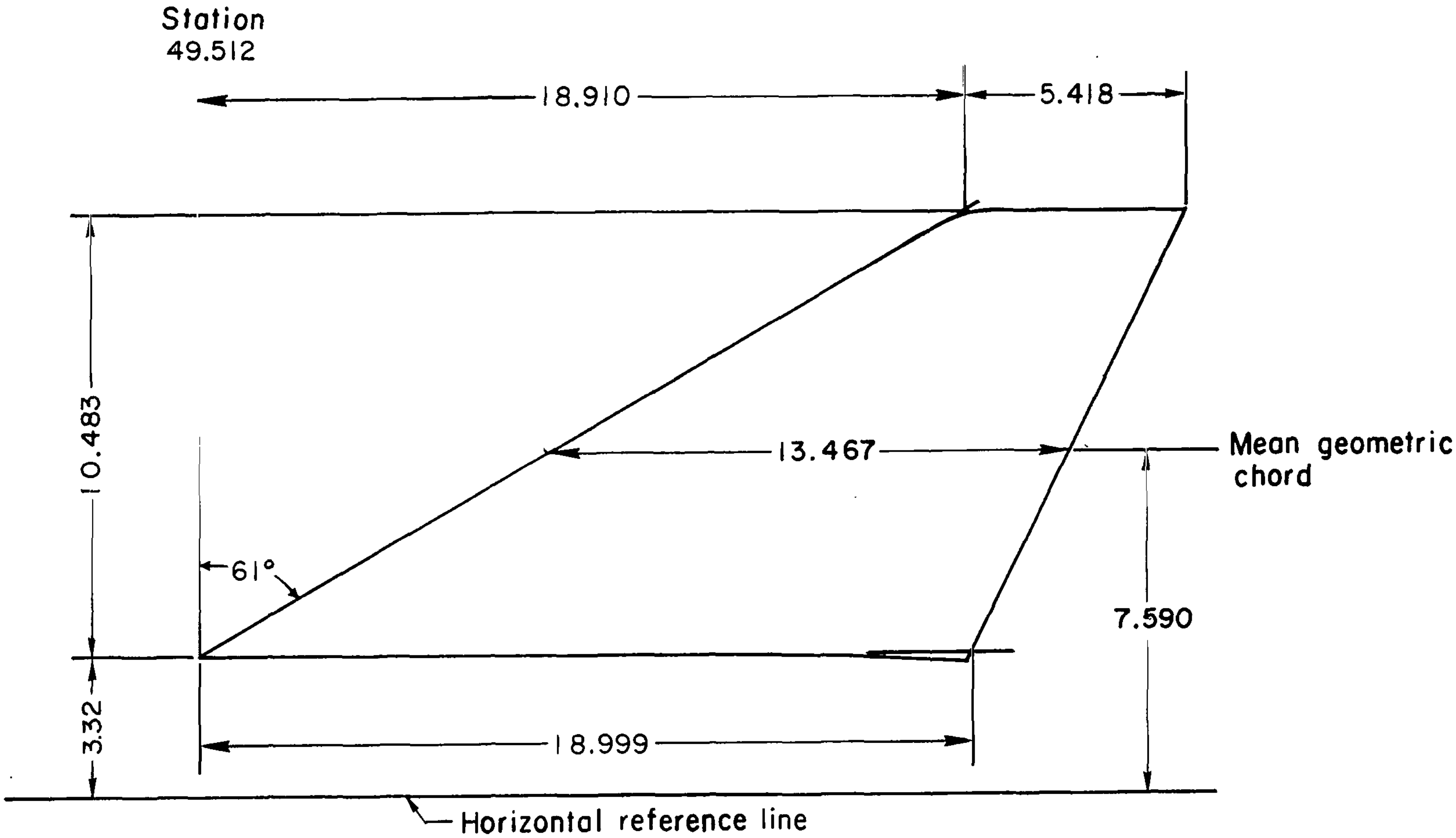

(c) Details of vertical tail.

Figure 1.- Continued.

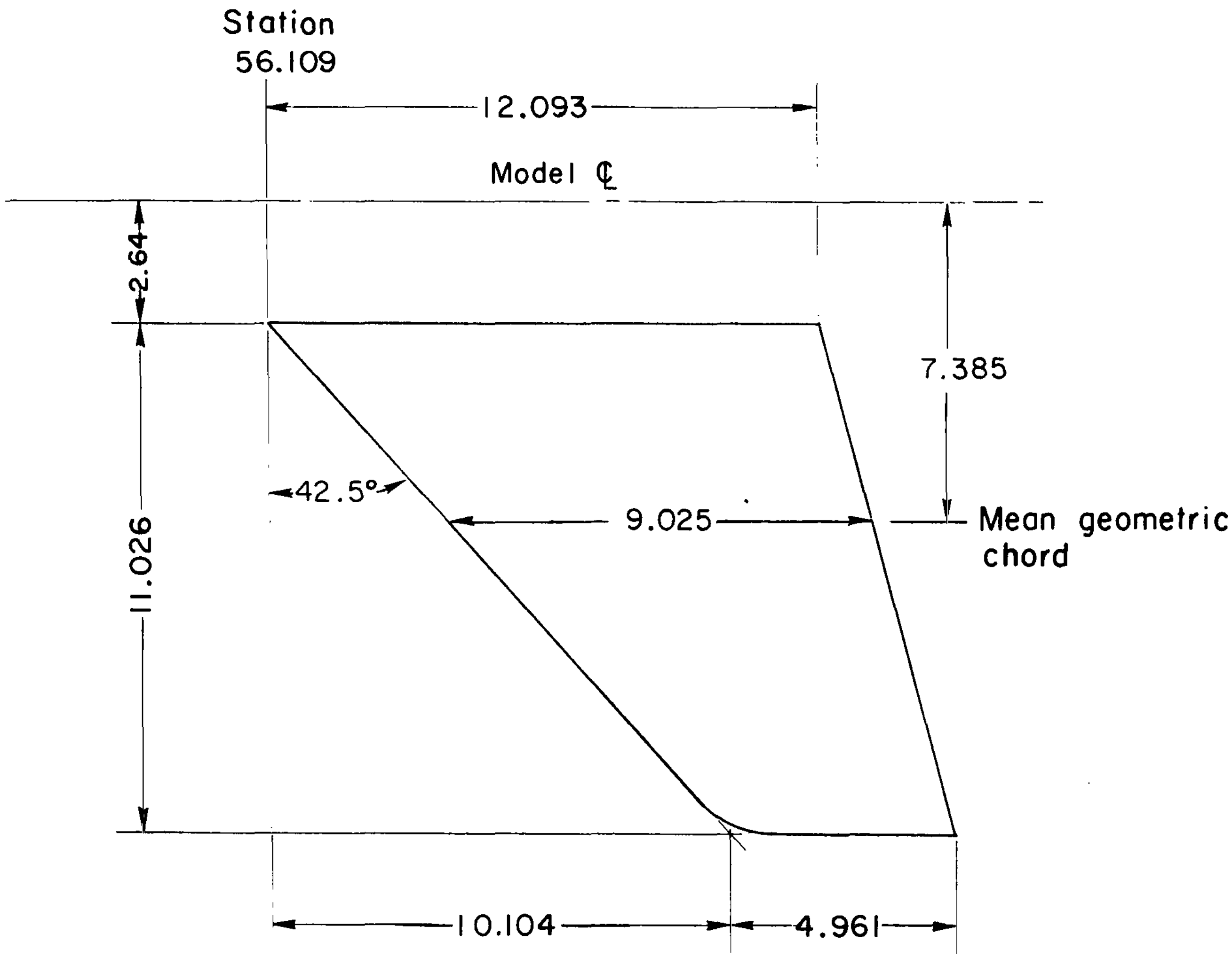

(d) Details of horizontal tail.

Figure 1.- Continued.

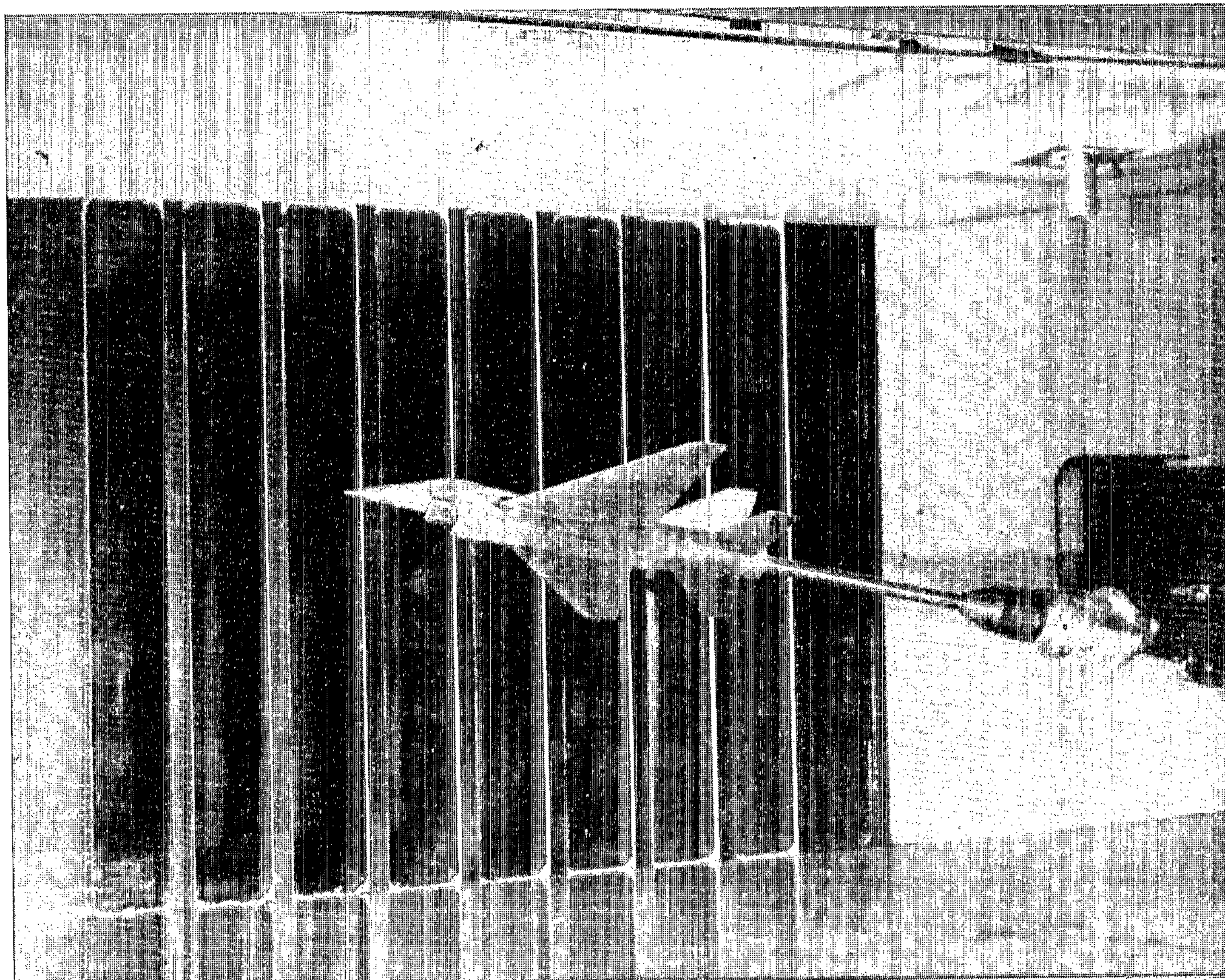

L-76-813

(e) Photograph of model.

Figure 1.- Concluded.

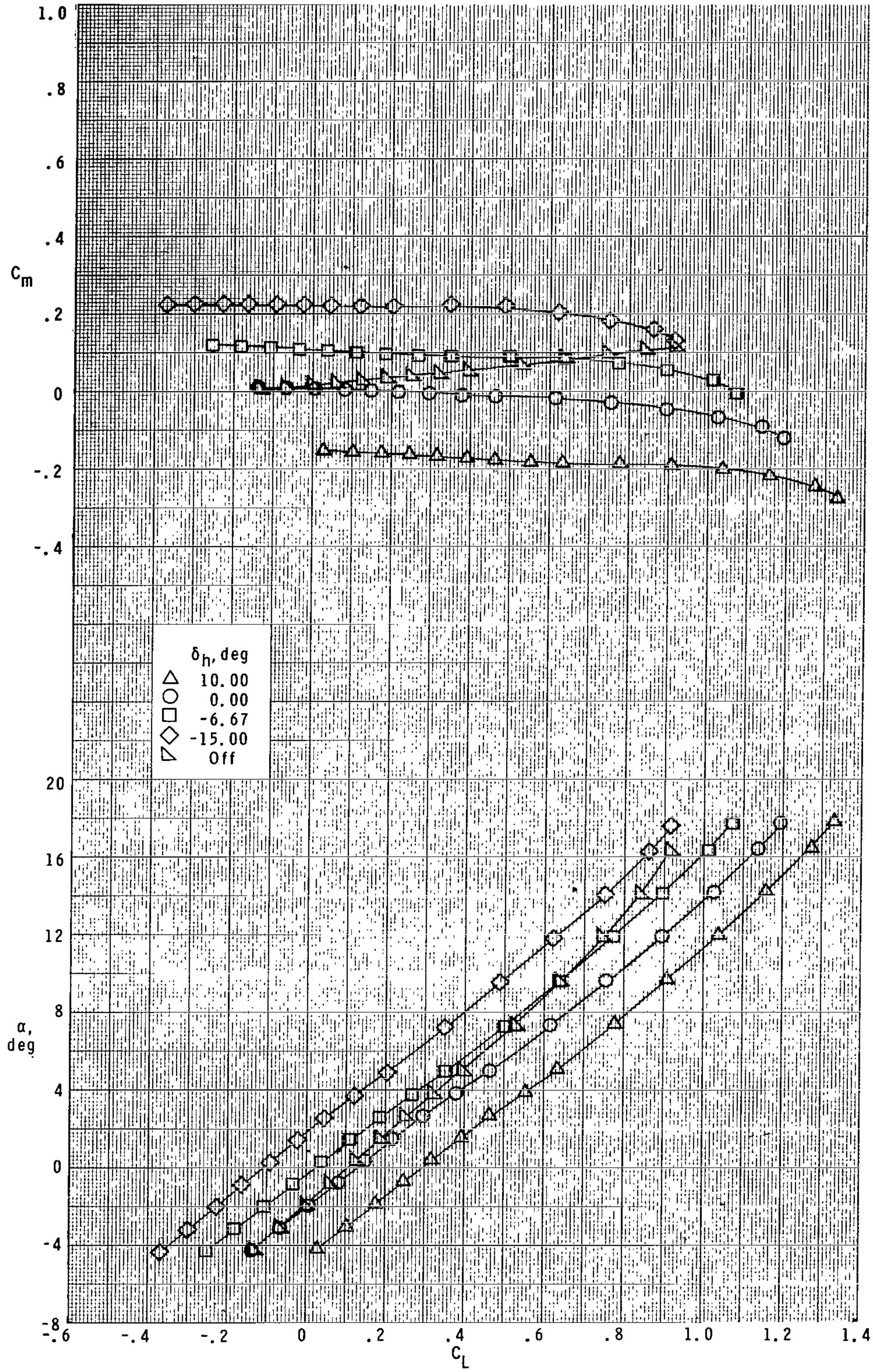

(a) M = 0.50.

Figure 2.- Longitudinal aerodynamic characteristics with cambered wing.

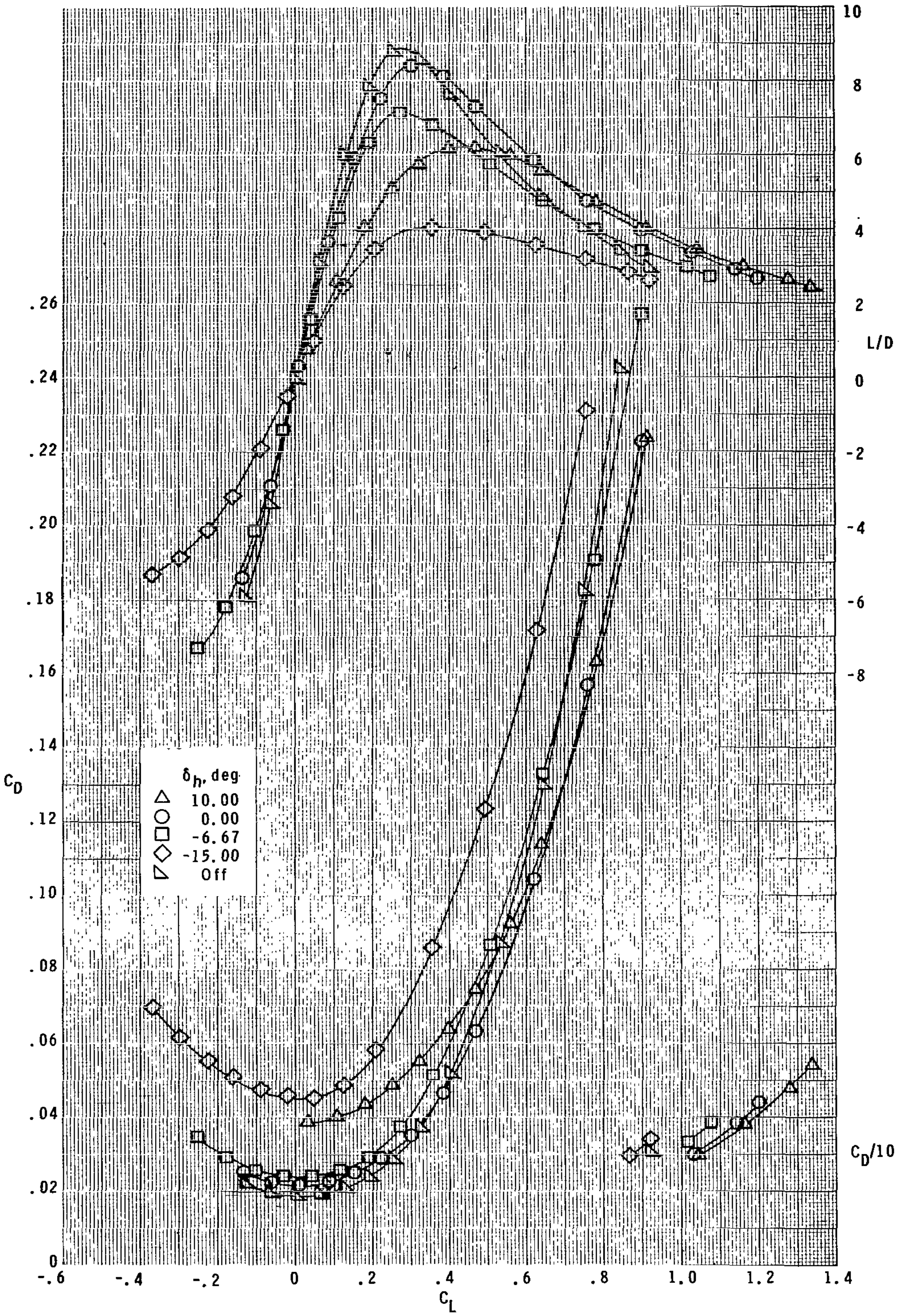

(a) M = 0.50. Concluded.

Figure 2.- Continued.

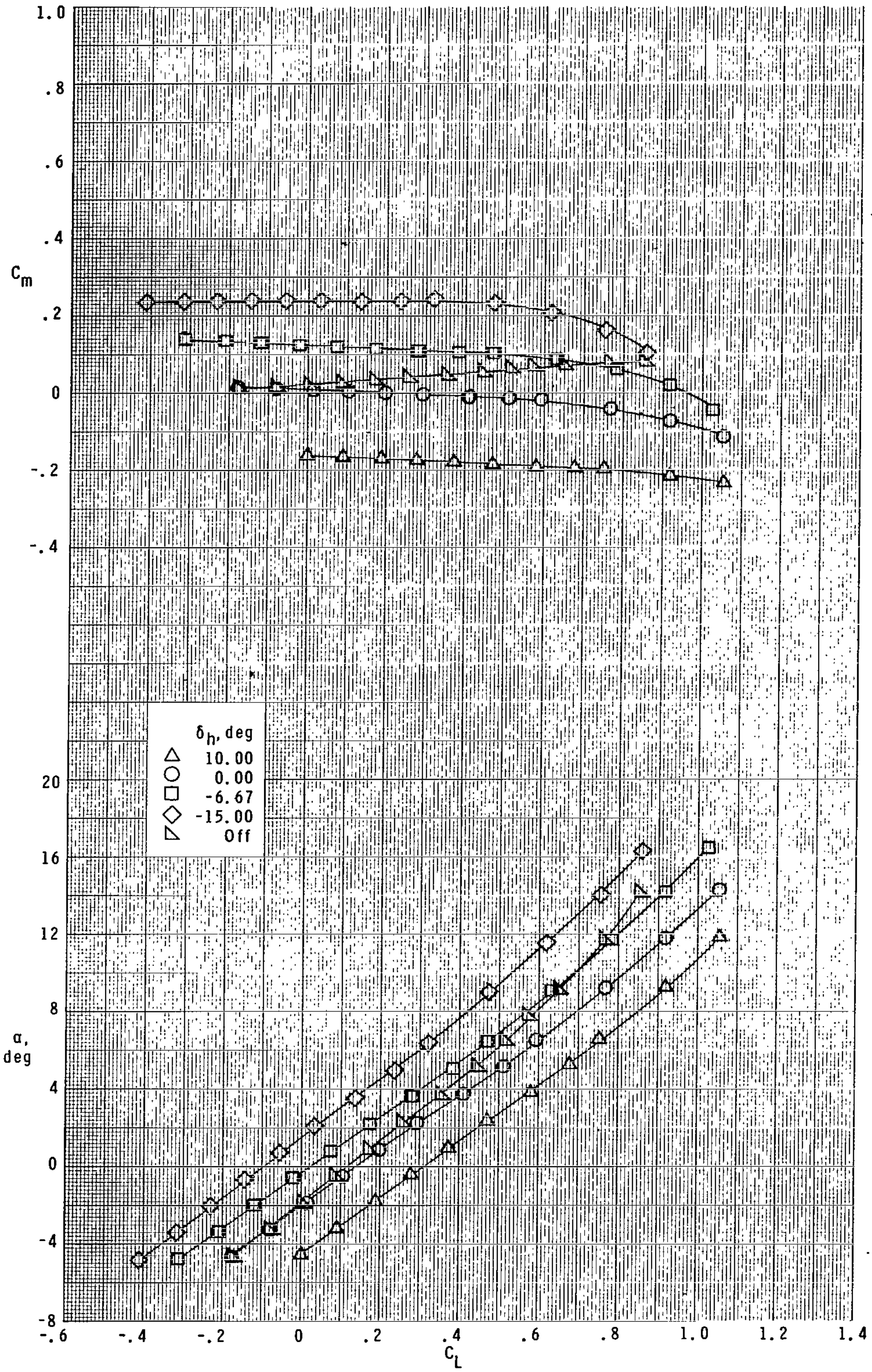

(b) M = 0.80.

Figure 2.- Continued.

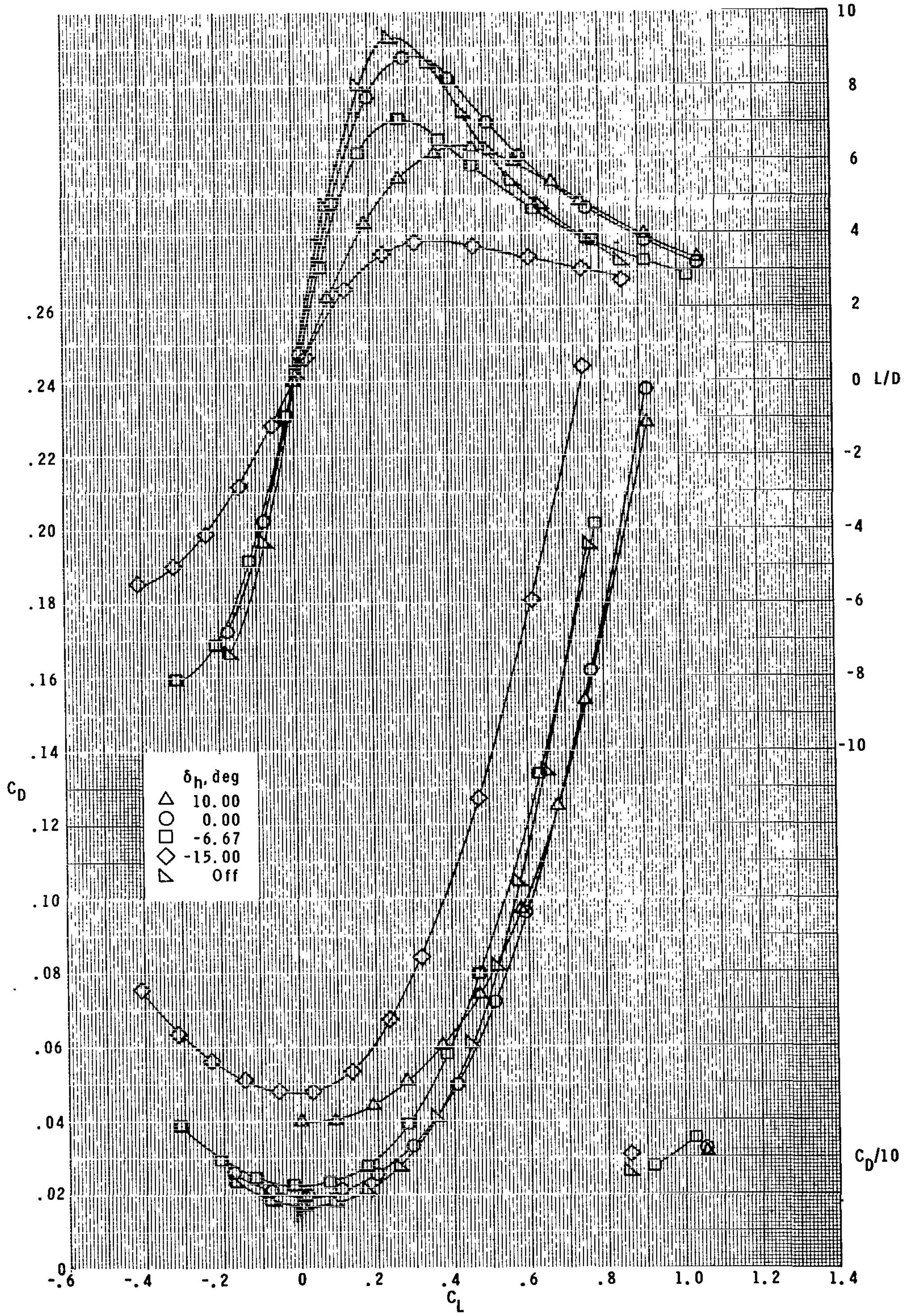

(b) M = 0.80. Concluded.

Figure 2.- Continued.

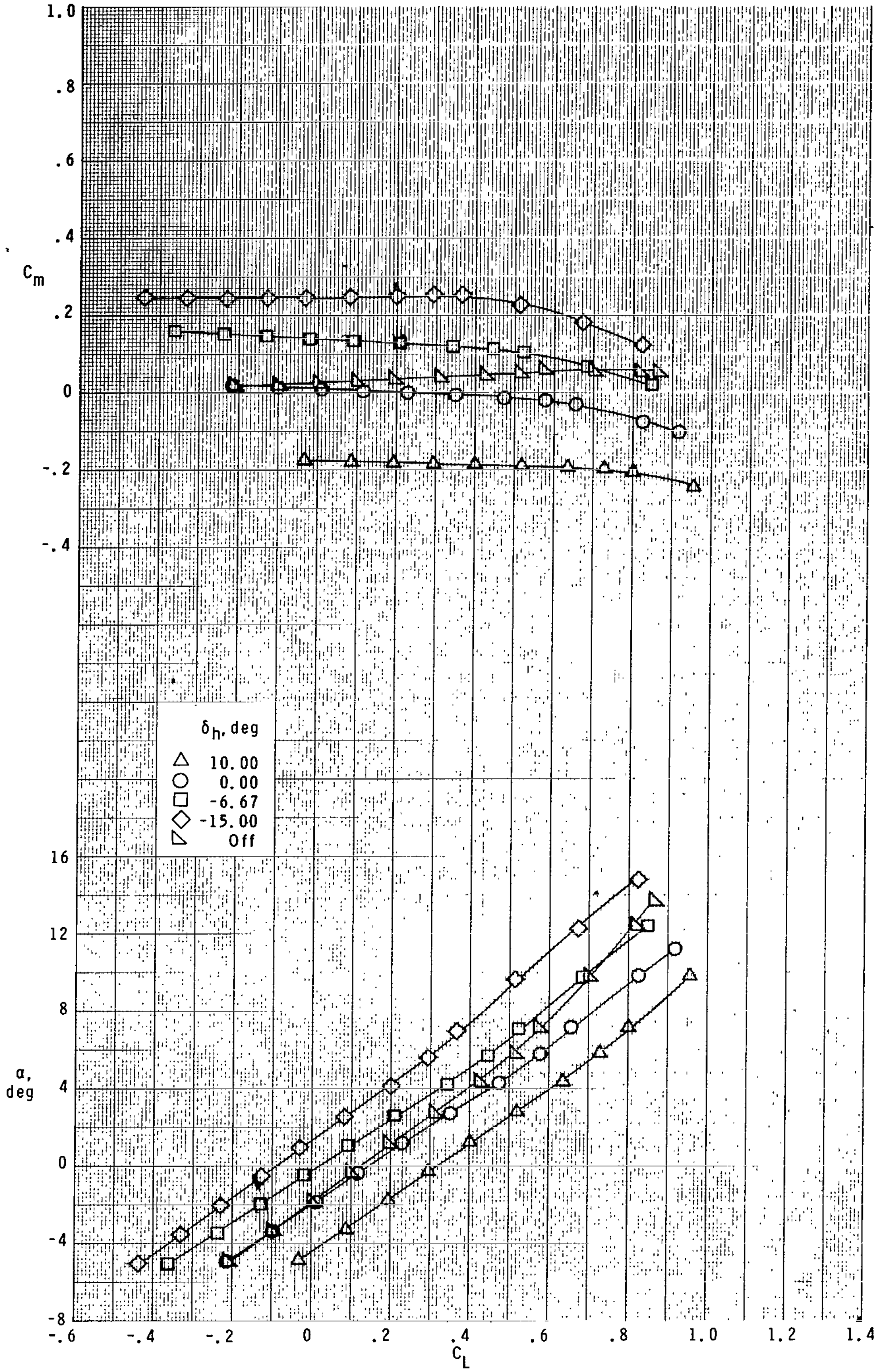

(c) M = 0.90.

Figure 2.- Continued.

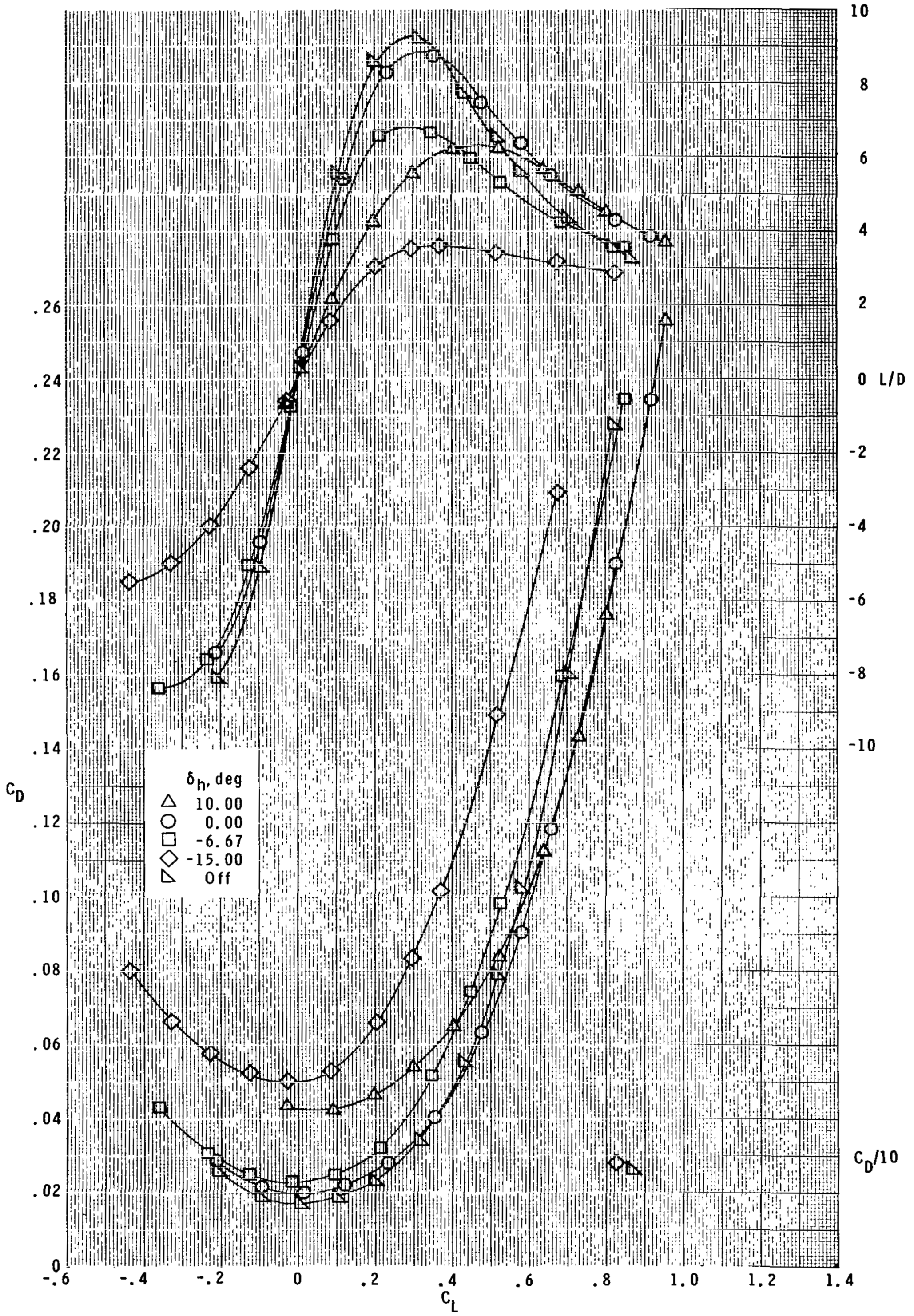

(c) M = 0.90. Concluded.

Figure 2.- Continued.

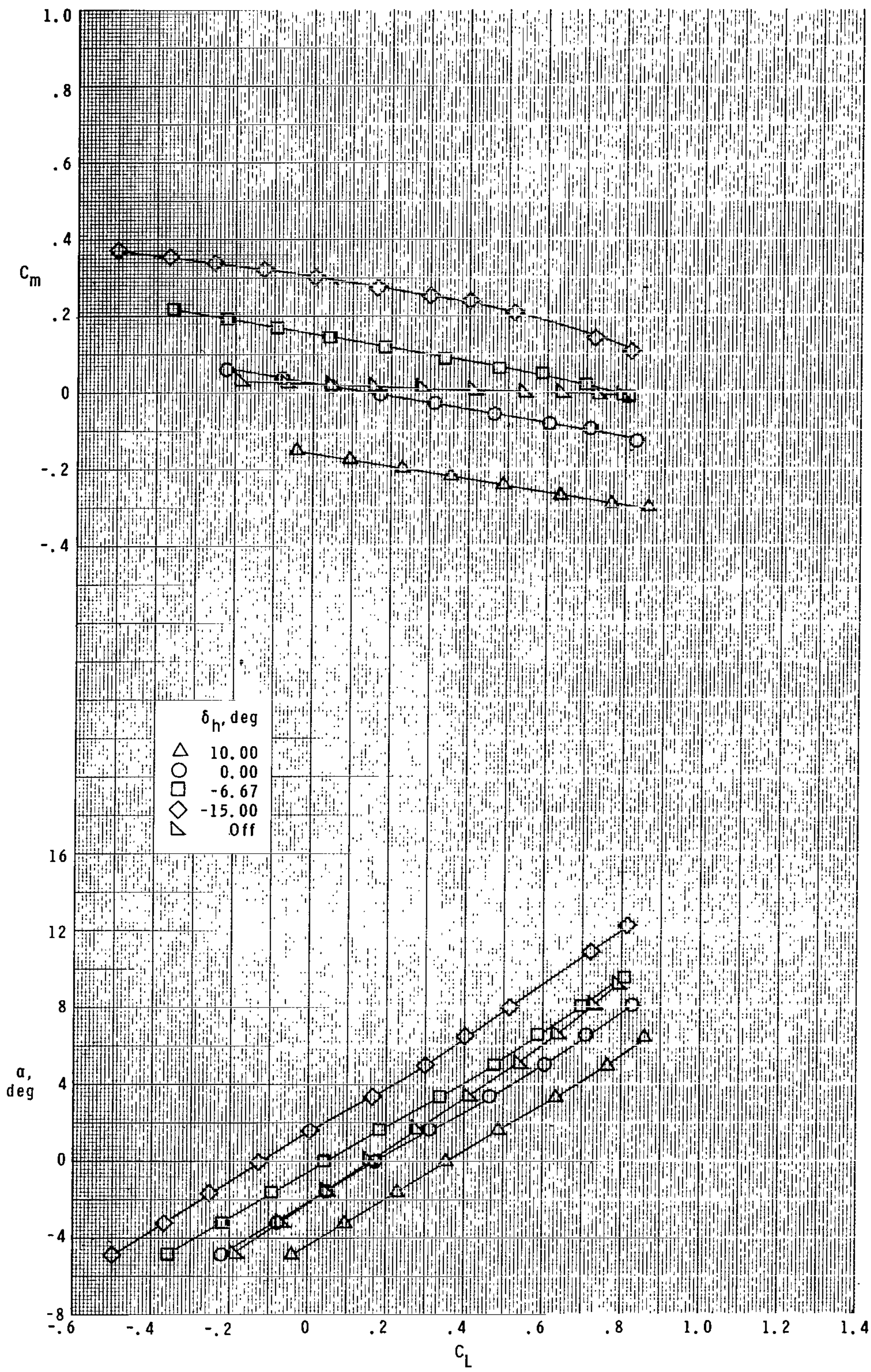

(d) M = 1.03.

Figure 2.- Continued.

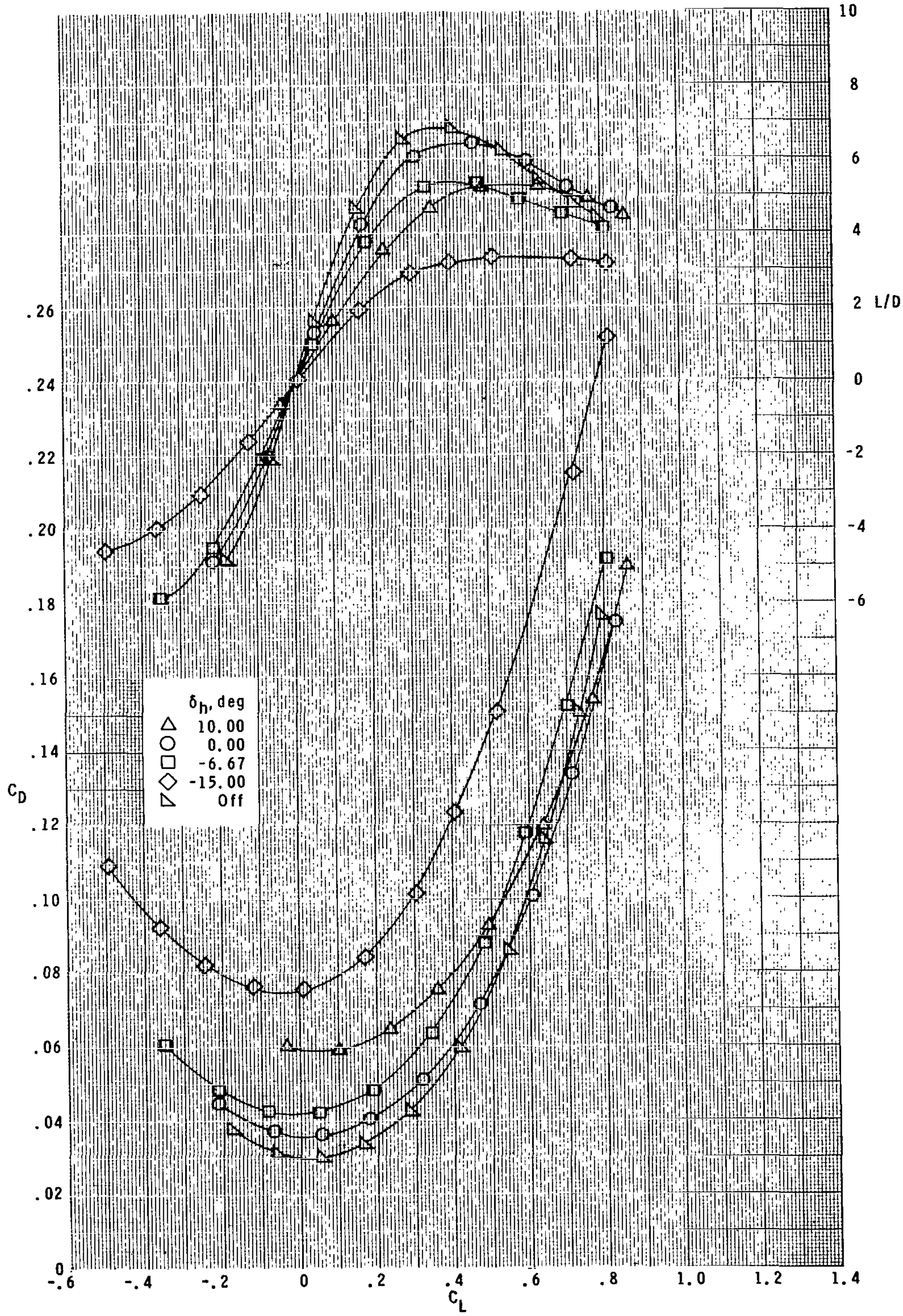

(d) M = 1.03. Concluded.

Figure 2.- Continued.

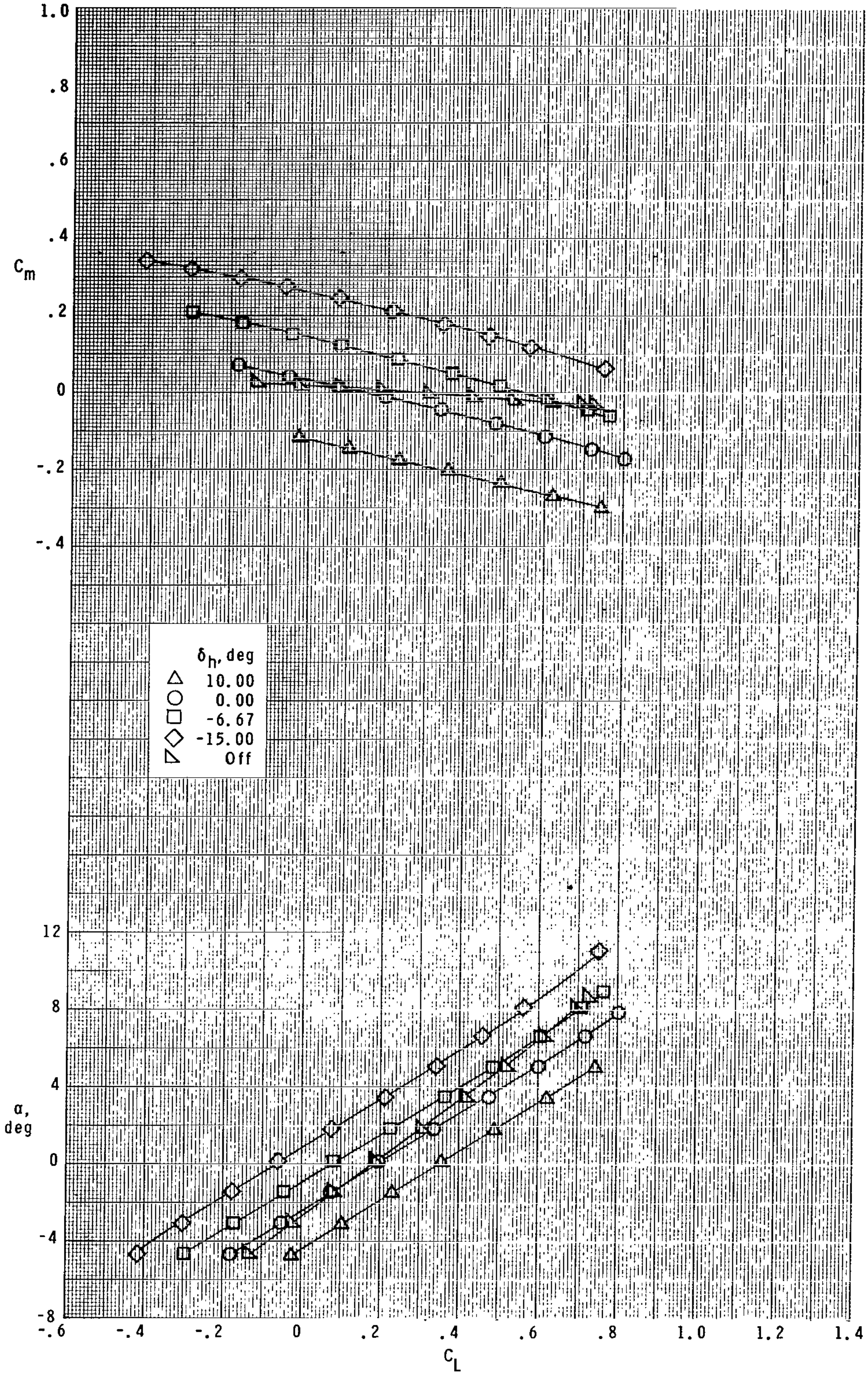

(e) M = 1.20.

Figure 2.- Continued.

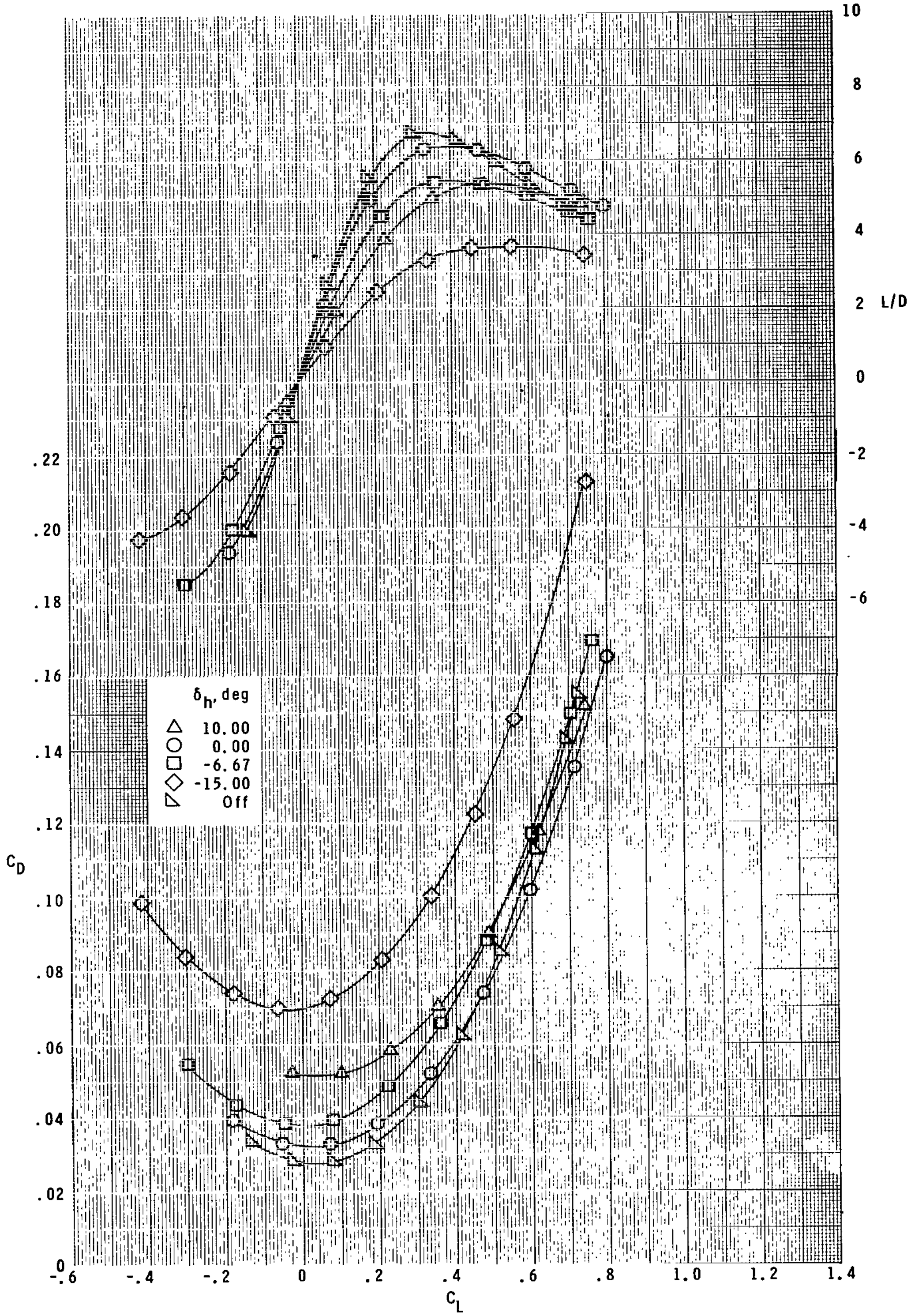

(e) M = 1.20. Concluded.

Figure 2.- Continued.

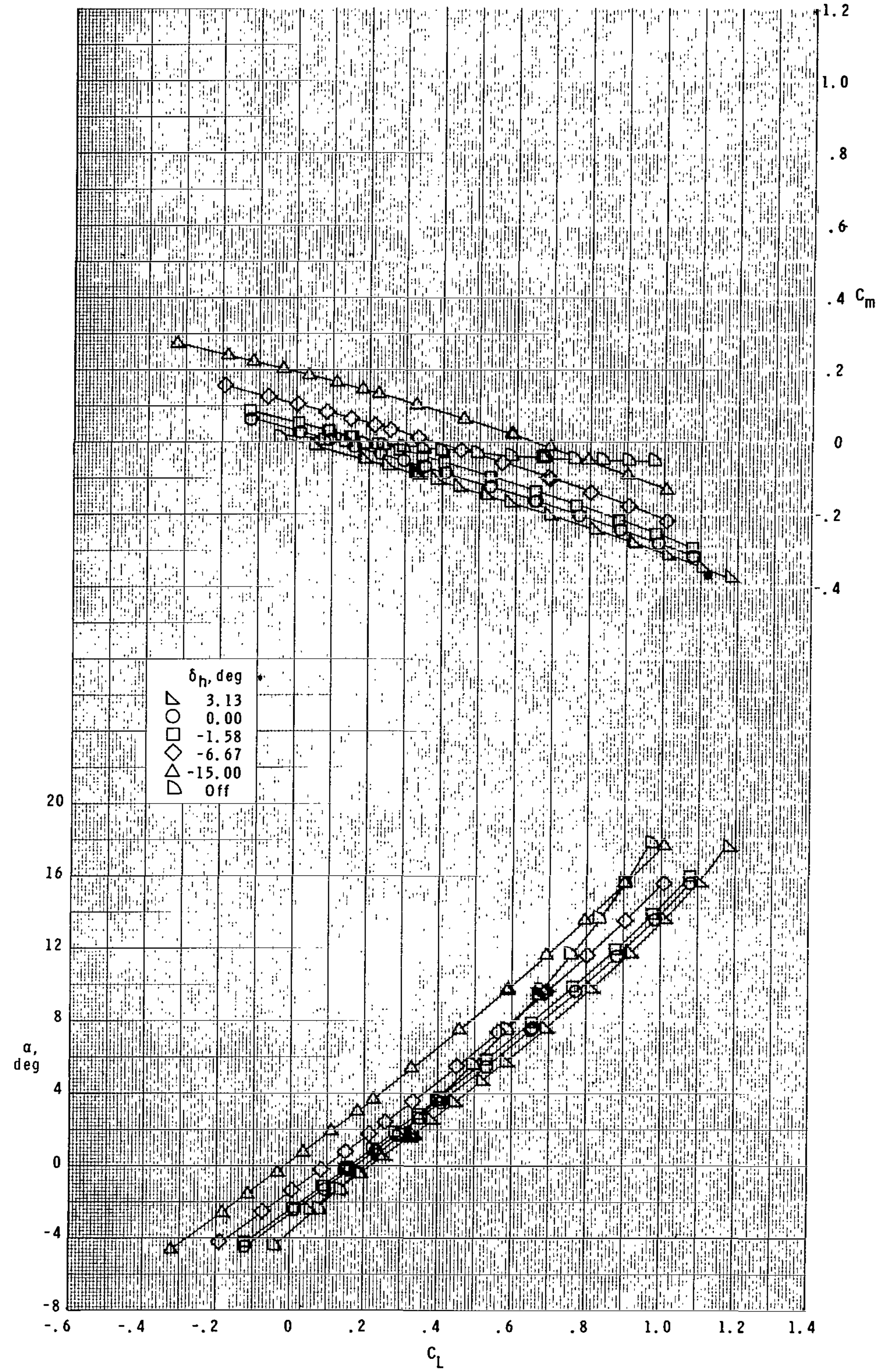

(f) M = 1.47.

Figure 2.- Continued.

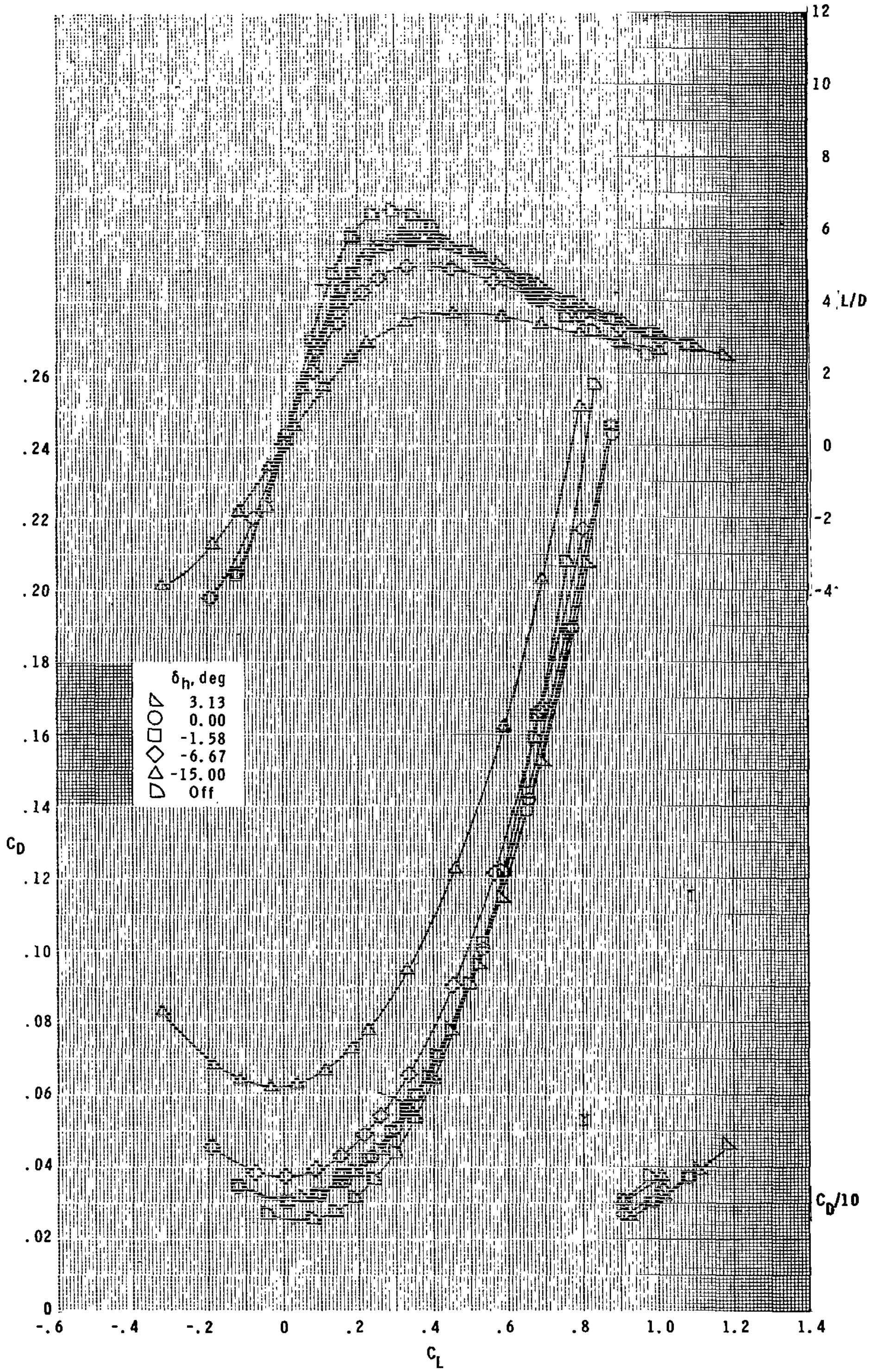

(f) M = 1.47. Concluded.

Figure 2.- Continued.

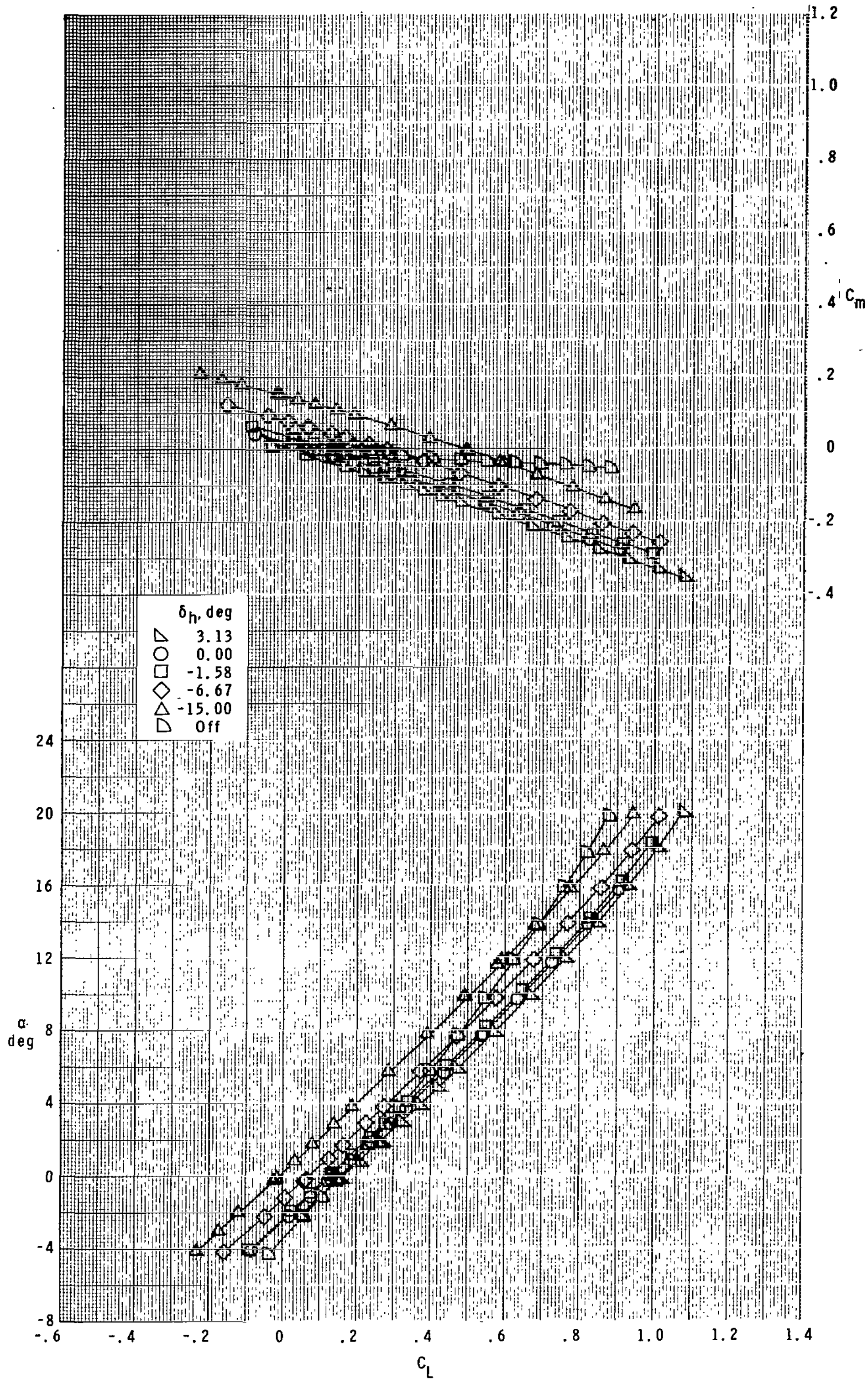

(g) M = 1.80.

Figure 2.- Continued.

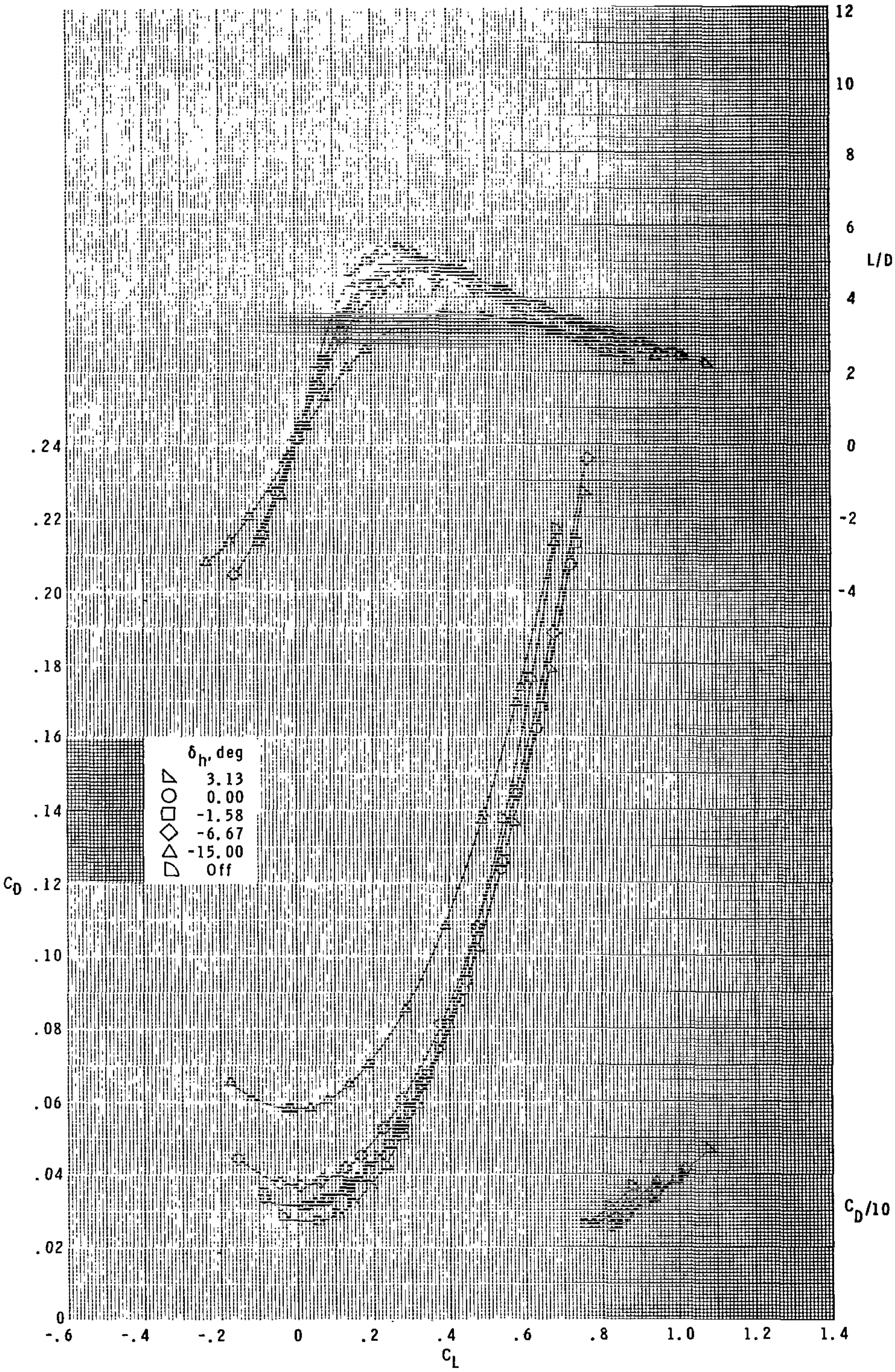

(g) M = 1.80. Concluded.

Figure 2.- Continued.

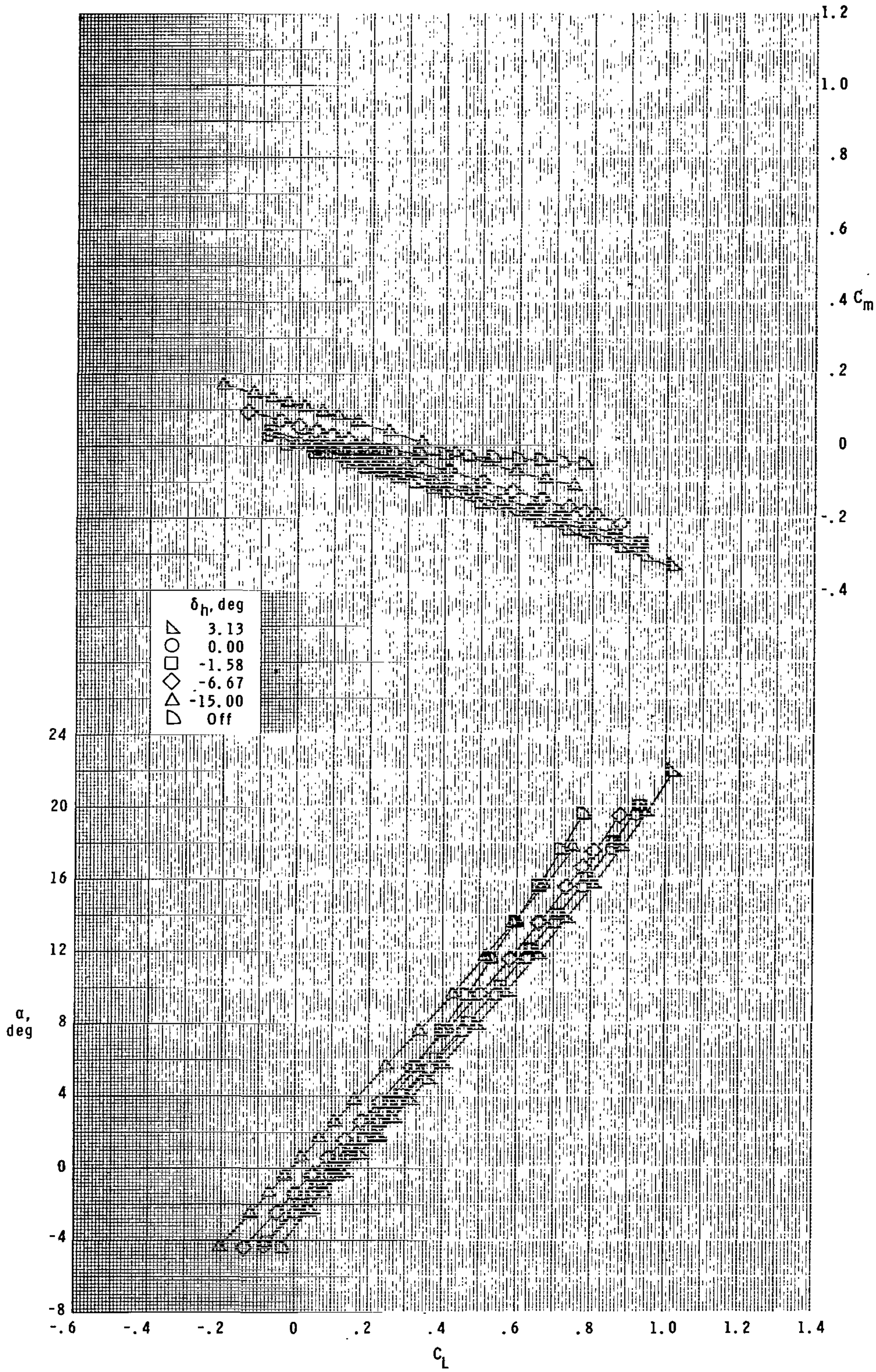

(h) M = 2.16.

Figure 2.- Continued.

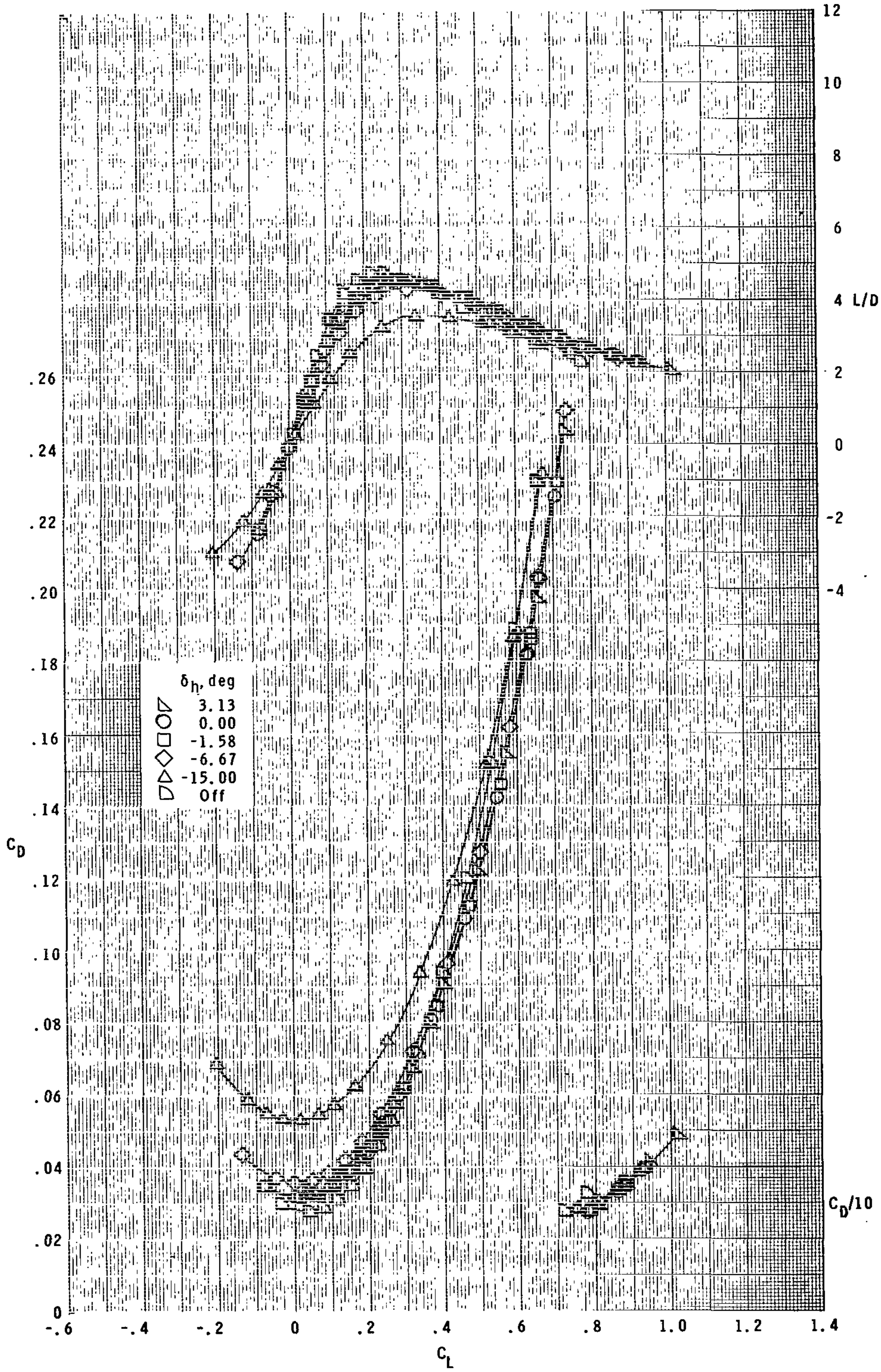

(h) M = 2.16. Concluded.

Figure 2.- Concluded.

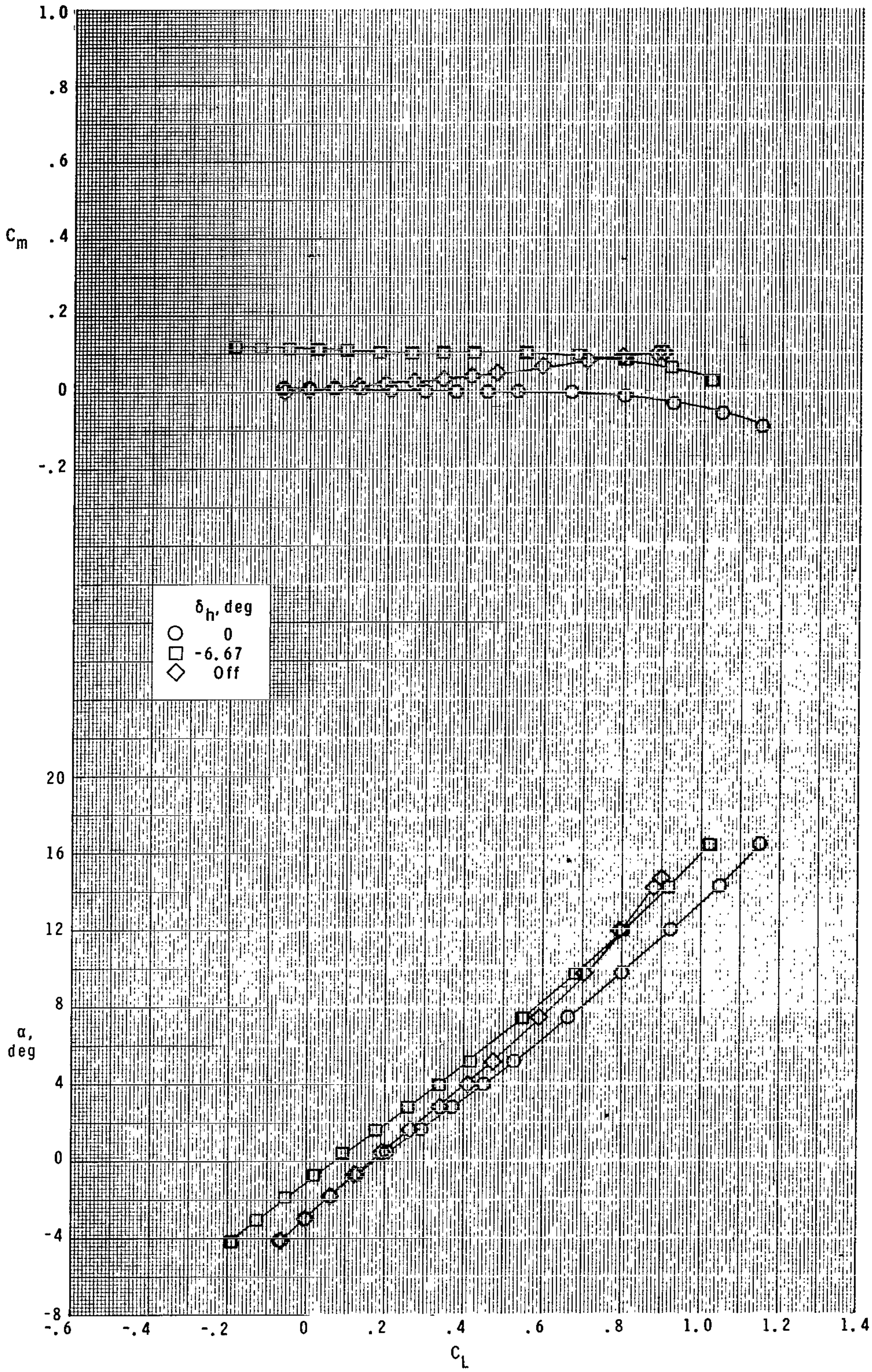

(a) M = 0.50.

Figure 3.- Longitudinal aerodynamic characteristics with flat wing.

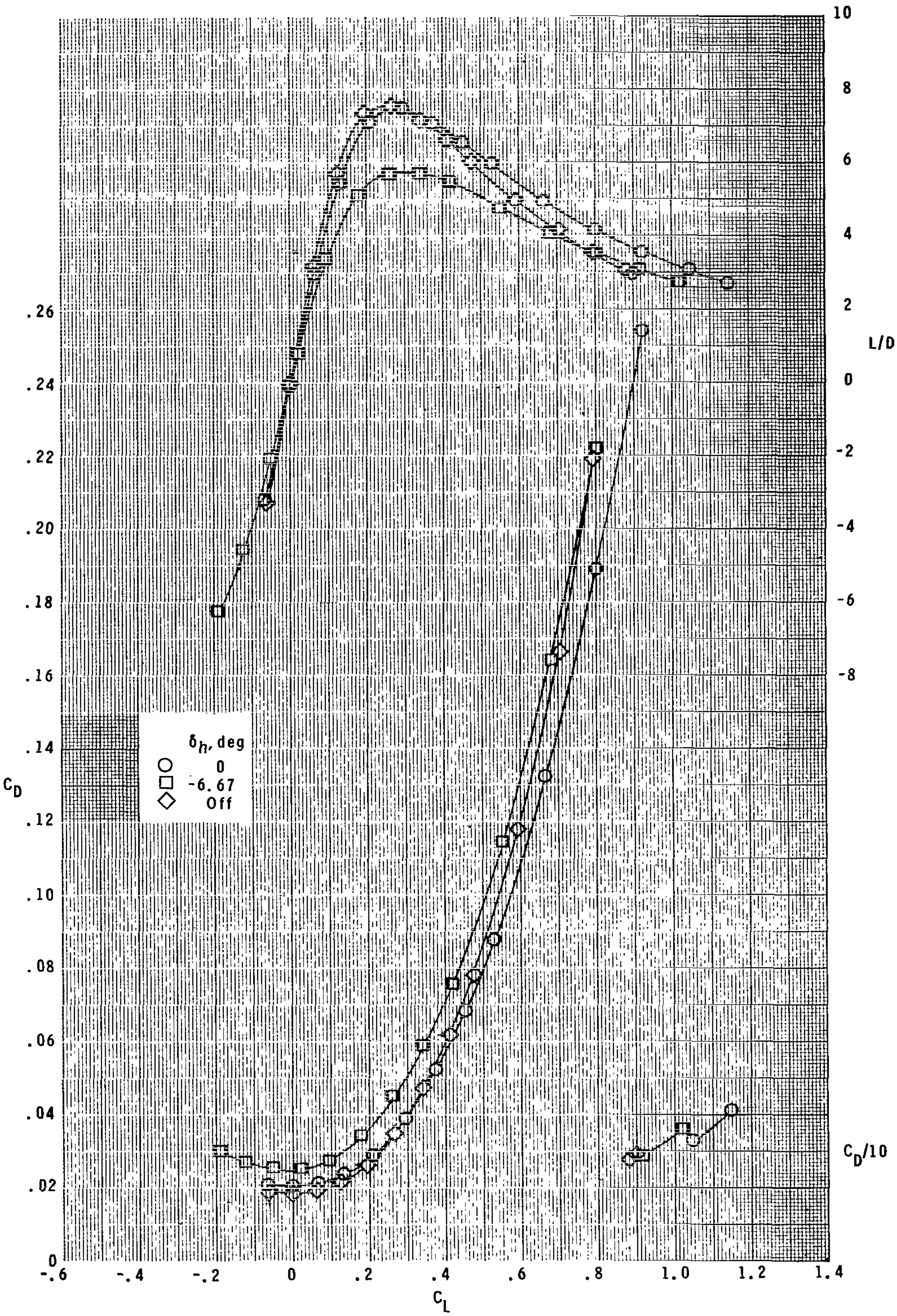

(a) M = 0.50. Concluded.

Figure 3.- Continued.

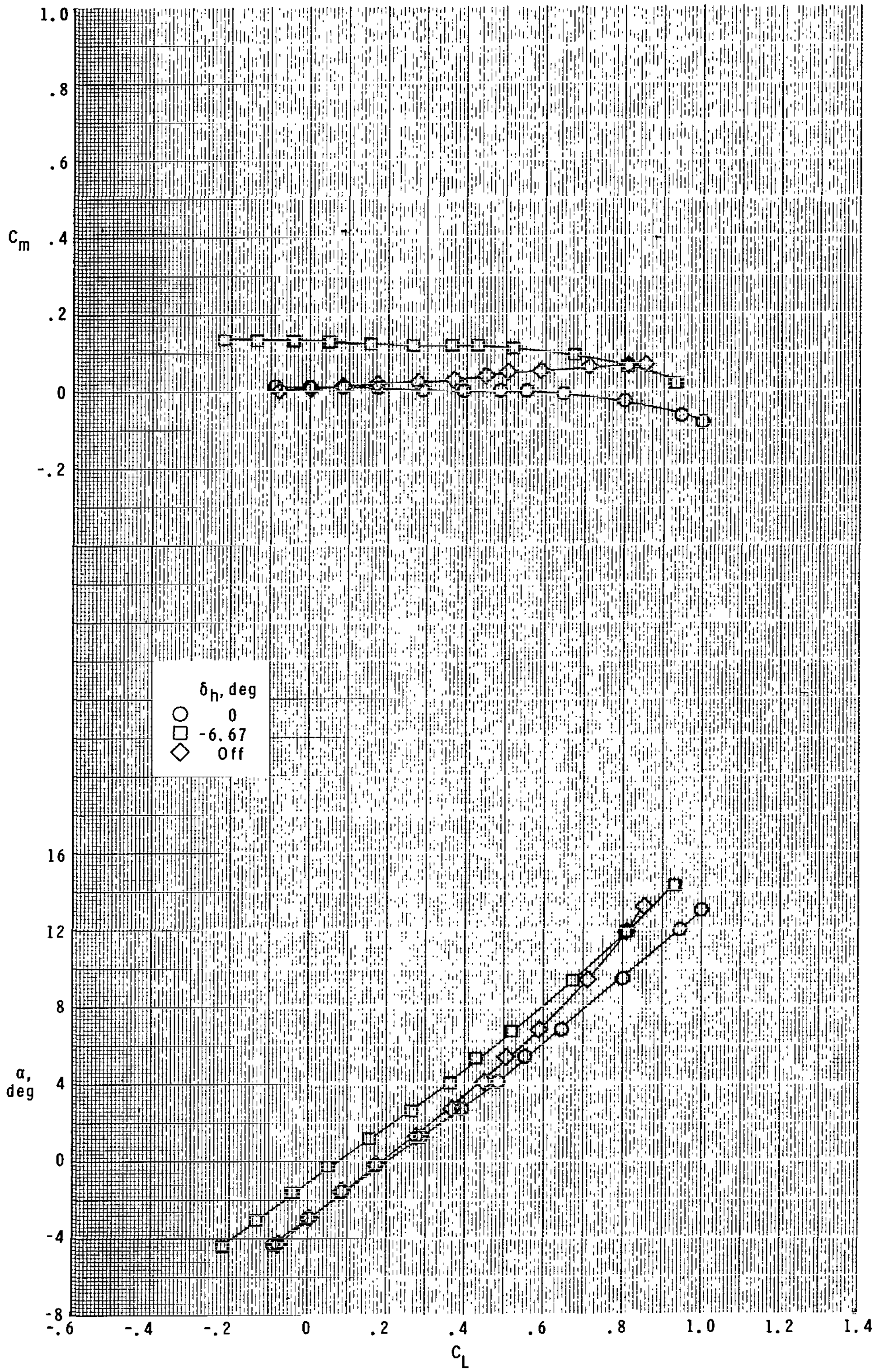

(b) M = 0.80.

Figure 3.- Continued.

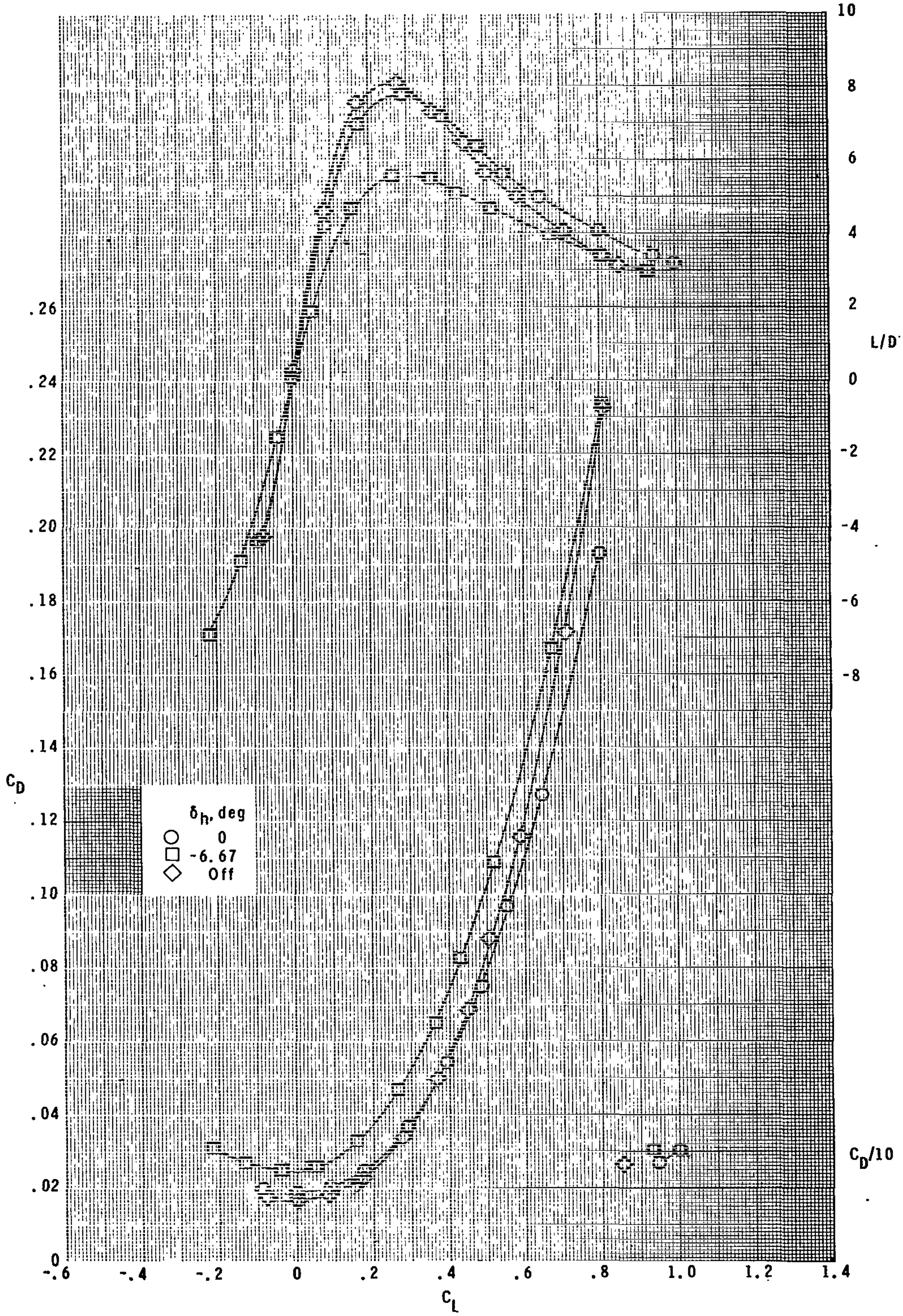

(b) M = 0.80. Concluded.

Figure 3.- Continued.

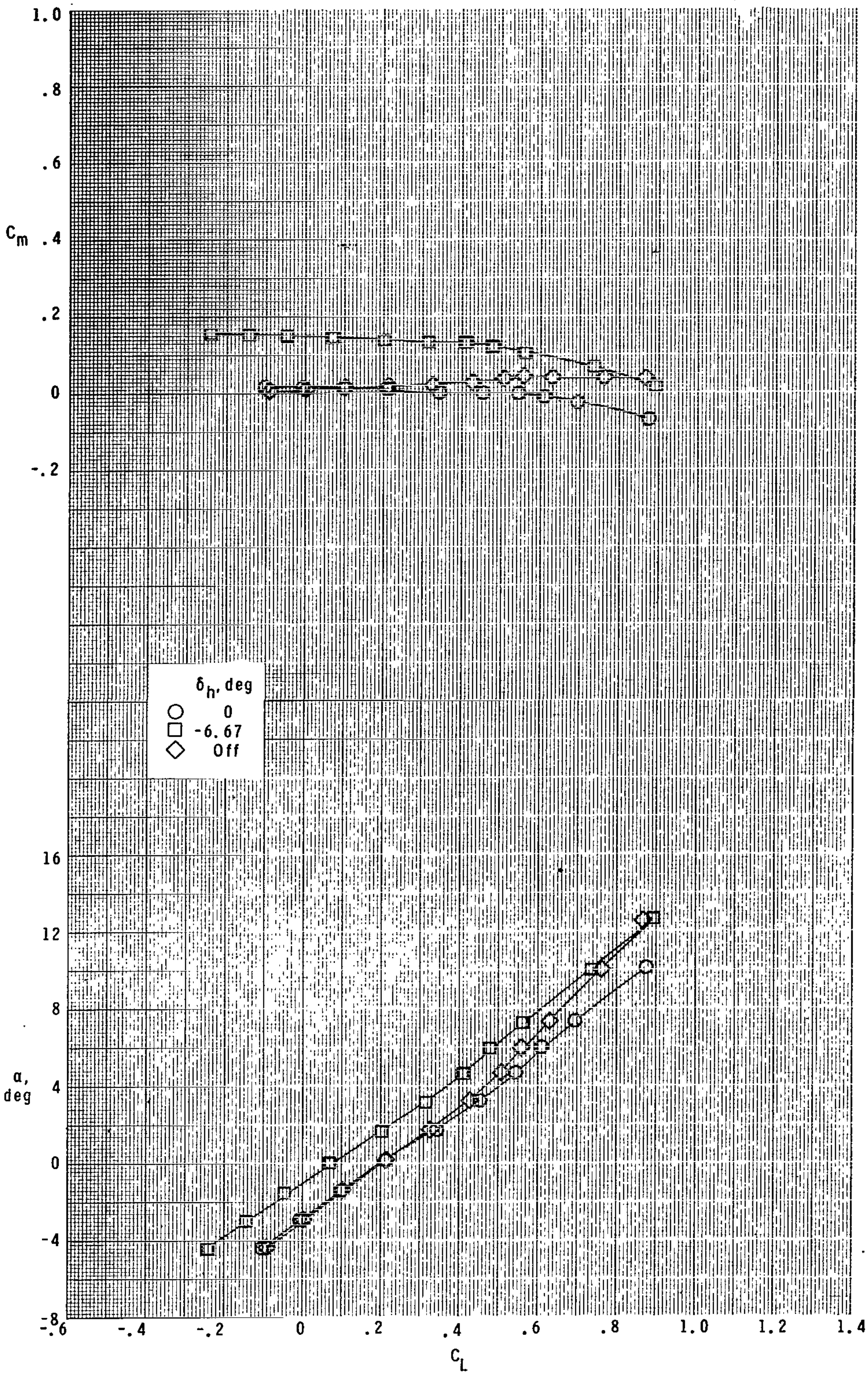

(c) M = 0.90.

Figure 3.- Continued.

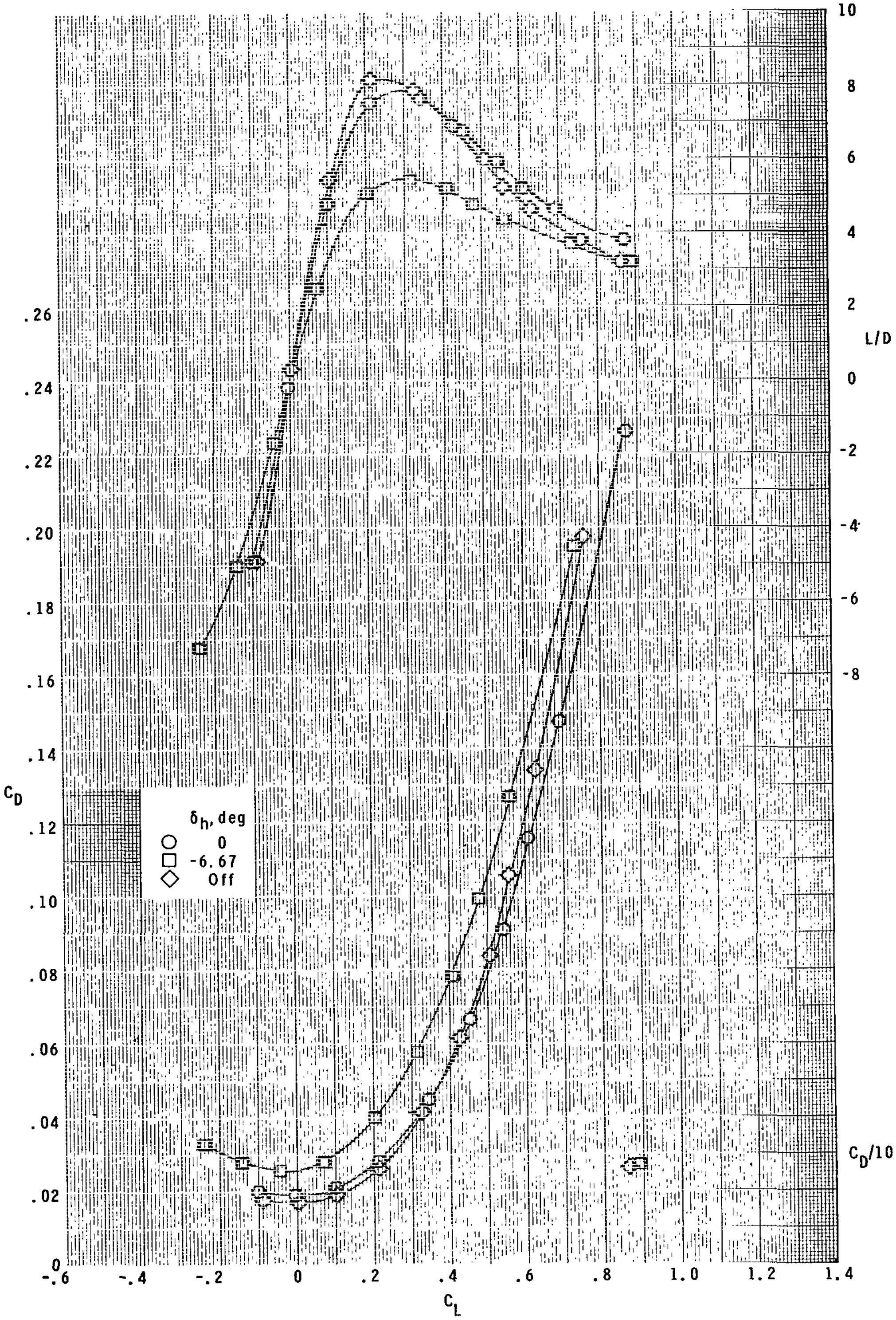

(c) M = 0.90. Concluded.

Figure 3.- Continued.

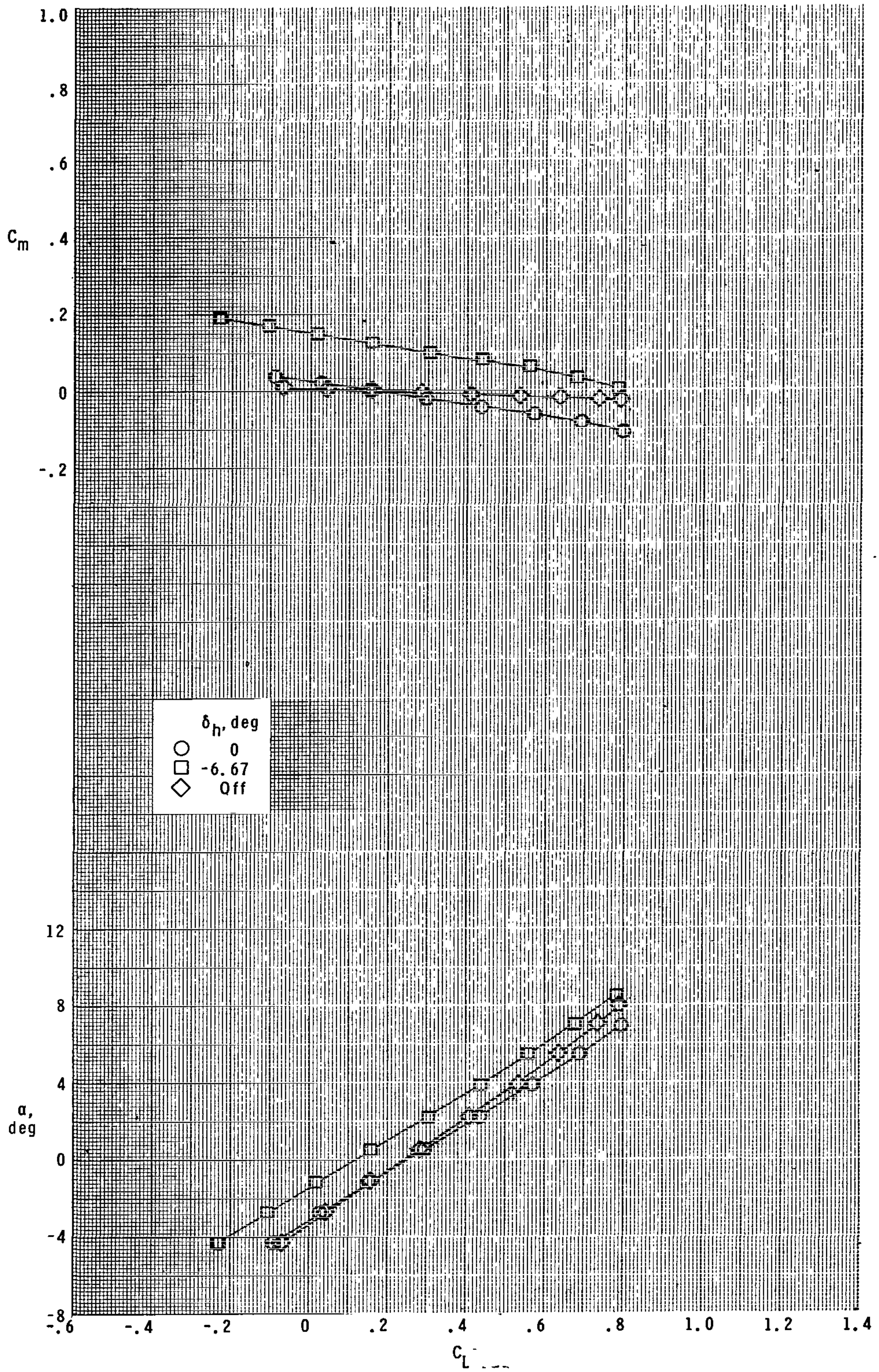

(d) M = 1.03.

Figure 3.- Continued.

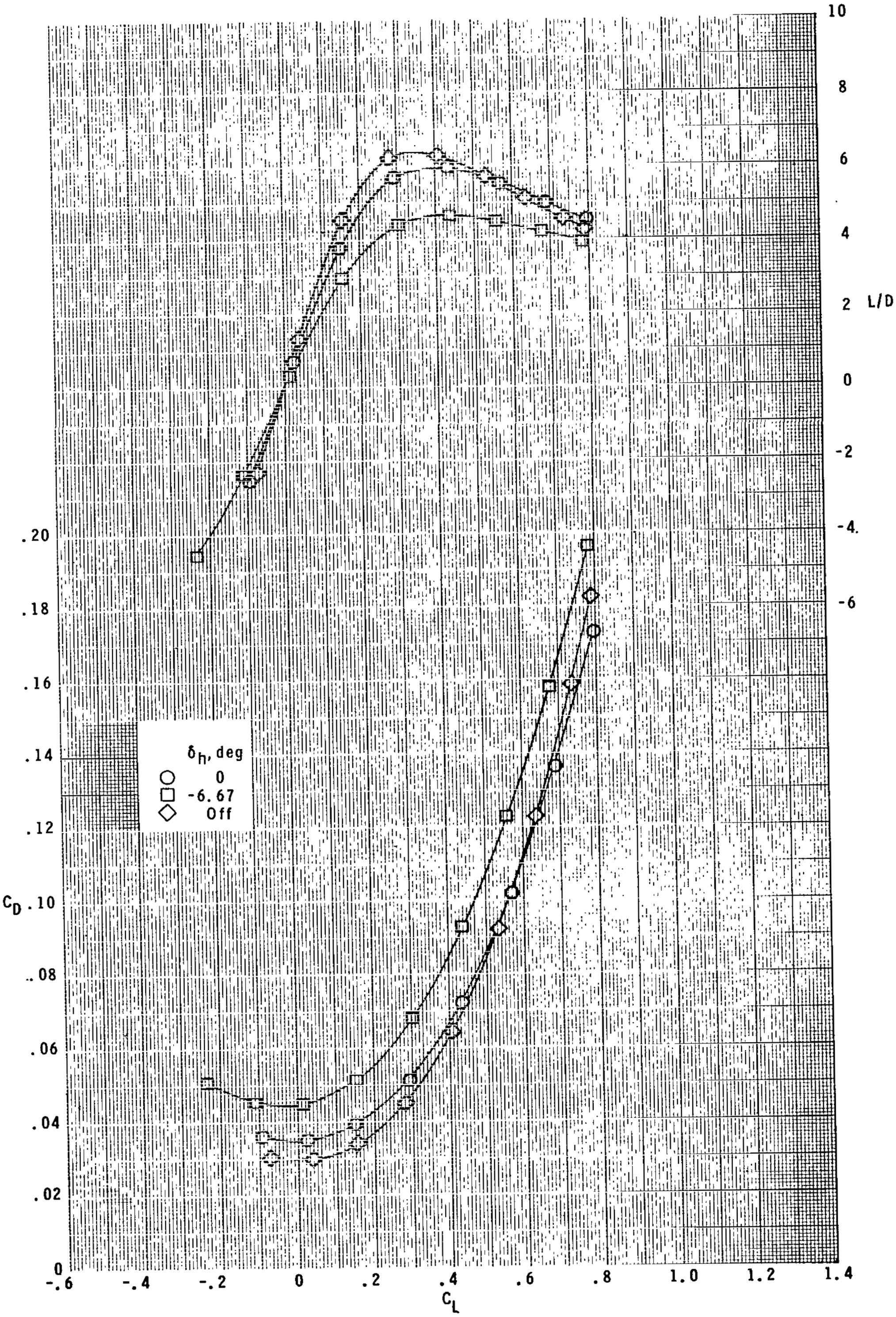

(d) M = 1.03. Concluded.

Figure 3.- Continued.

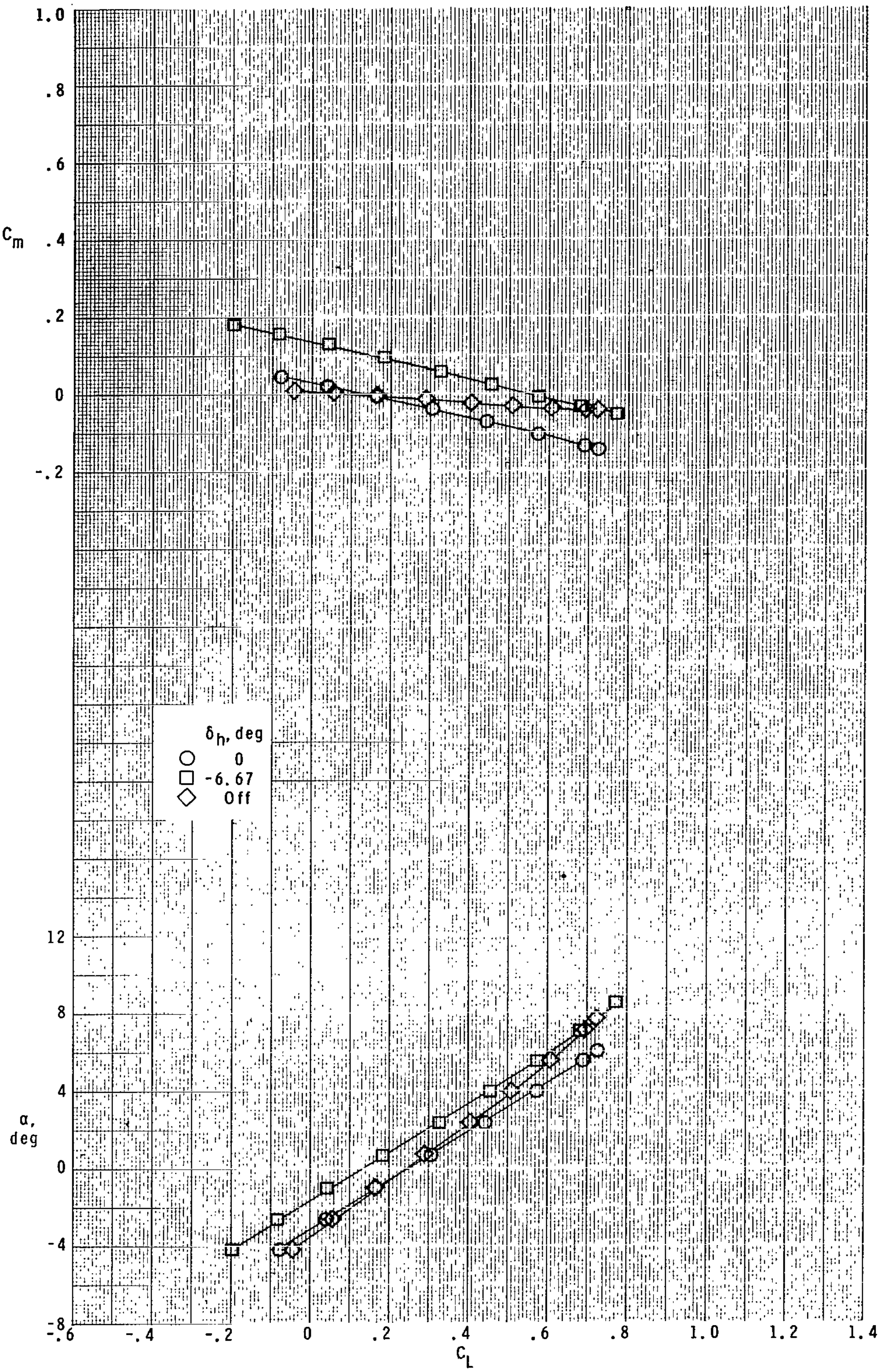

(e) M = 1.20.

Figure 3.- Continued.

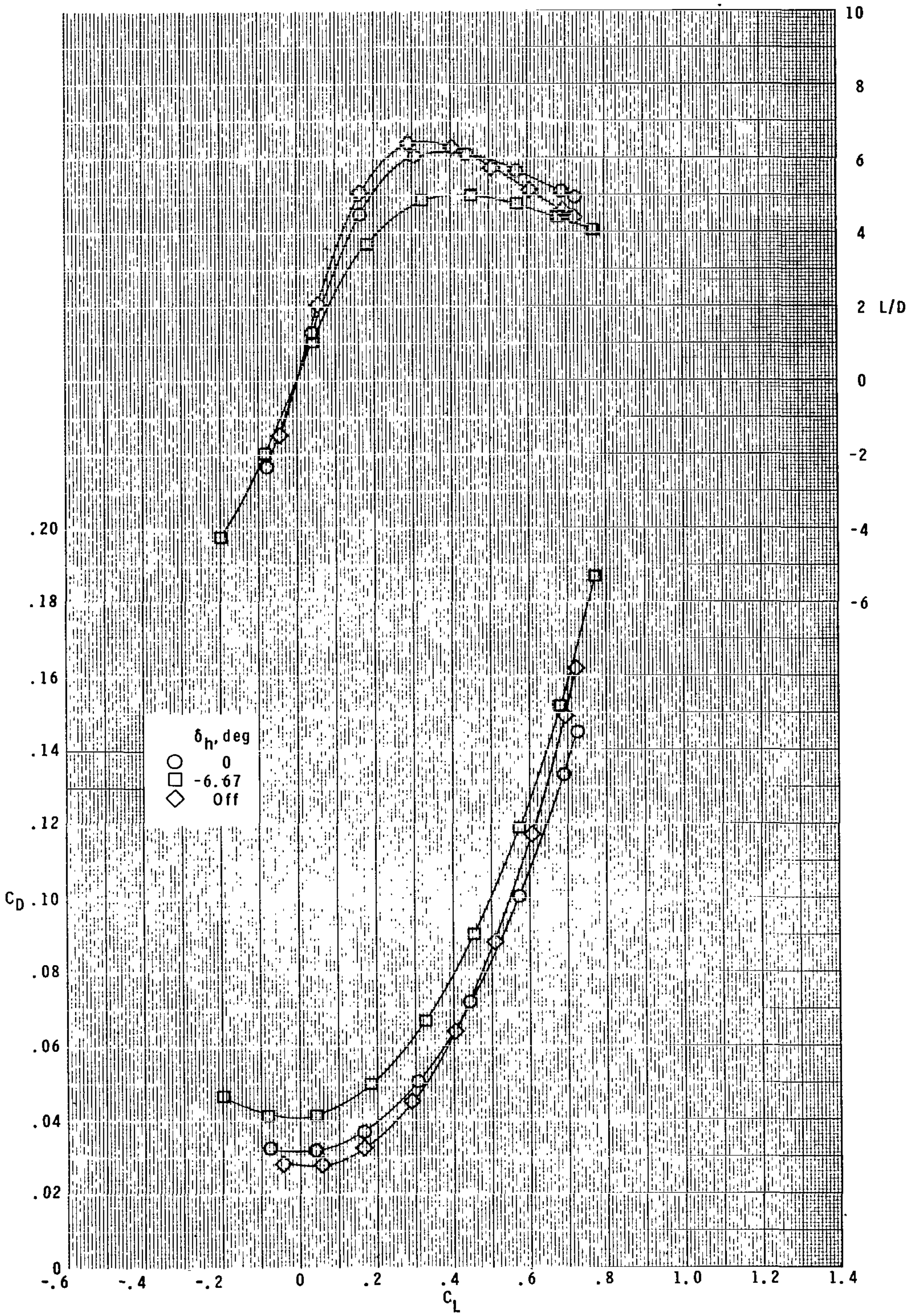

(e) M = 1.20. Concluded.

Figure 3.- Continued.

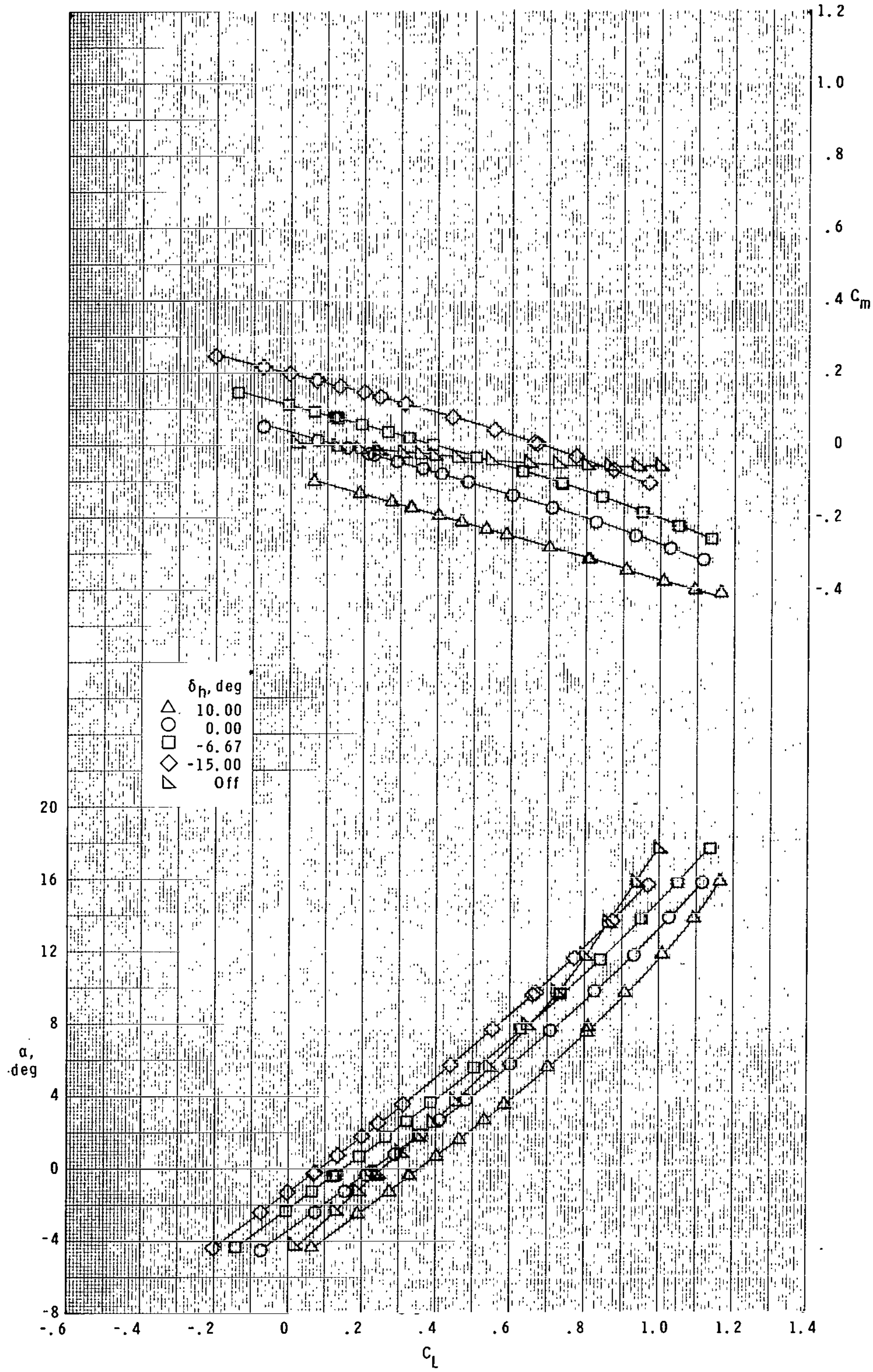

(f) M = 1.47.

Figure 3.- Continued.

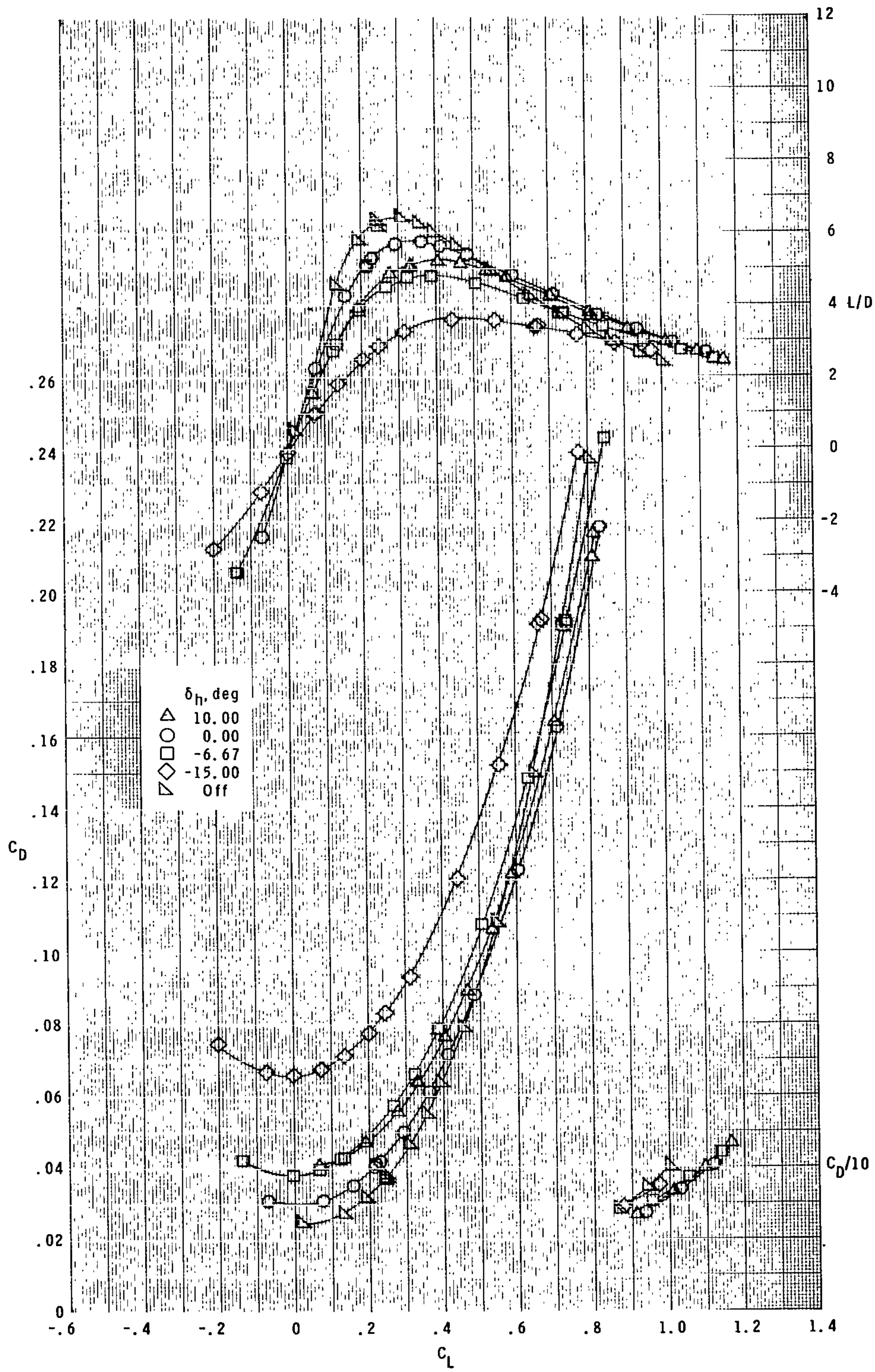

(f) M = 1.47. Concluded.

Figure 3.- Continued.

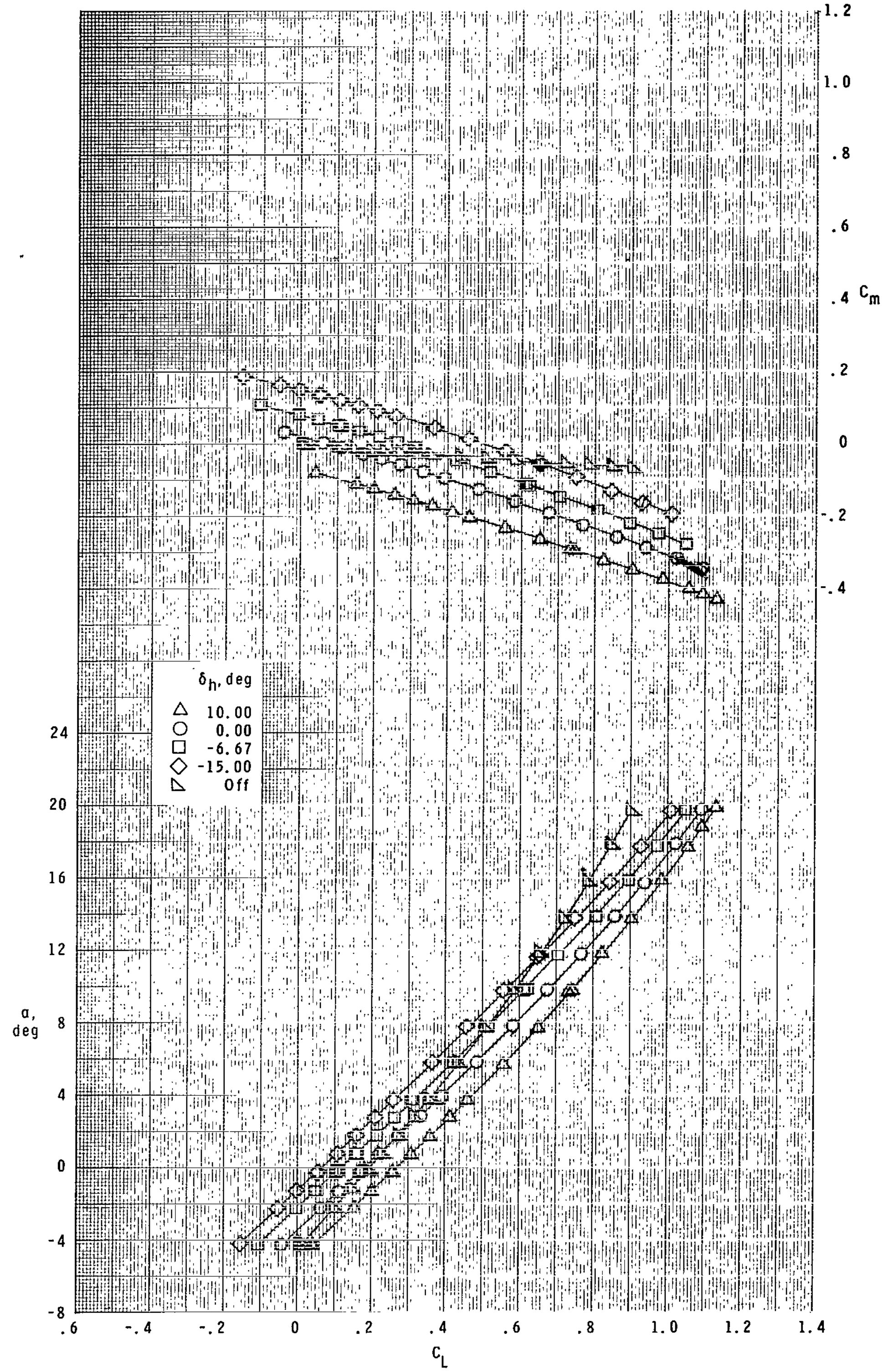

(g) M = 1.80.

Figure 3.- Continued.

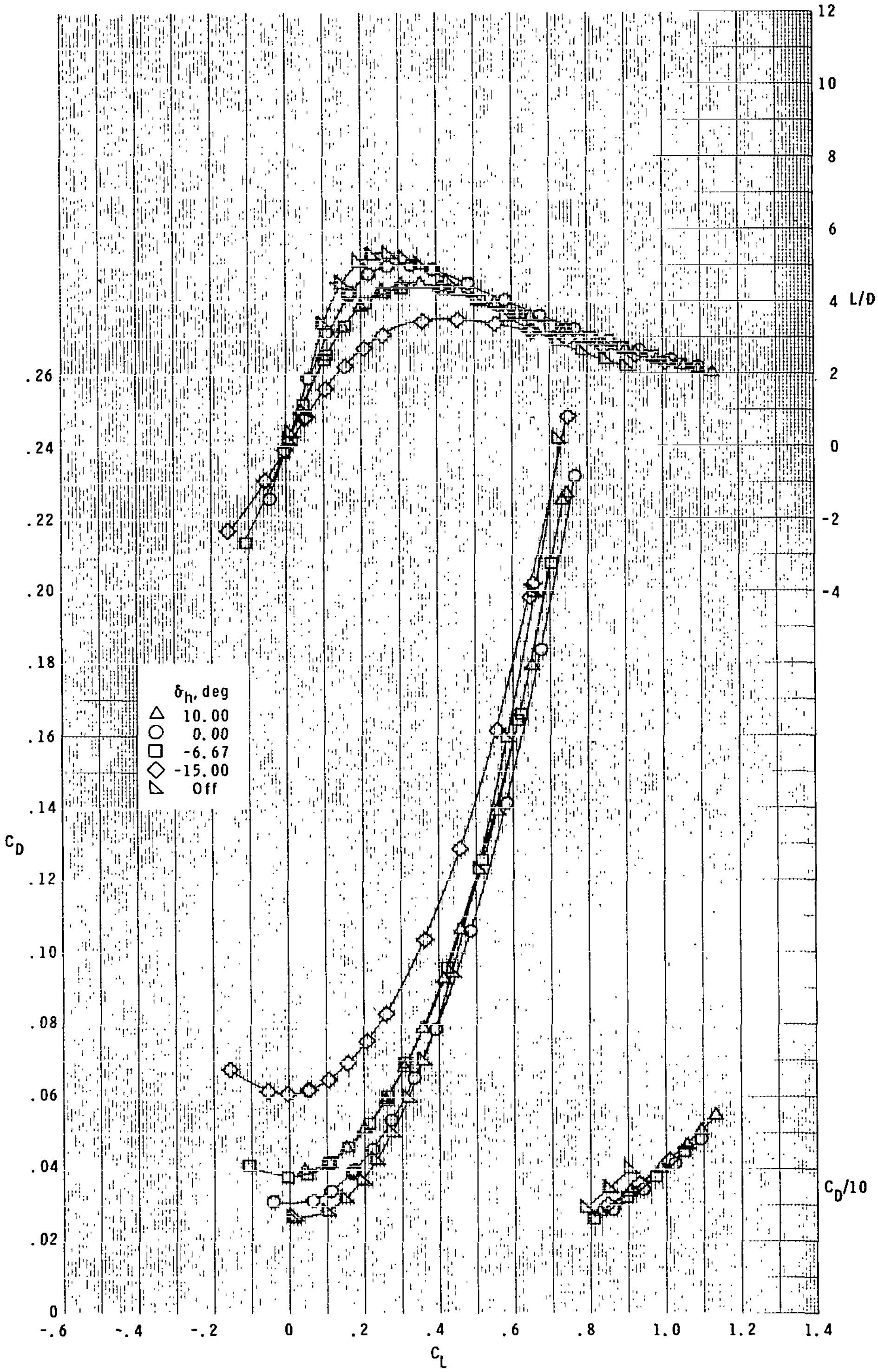

(g) M = 1.80. Concluded.

Figure 3.- Continued.

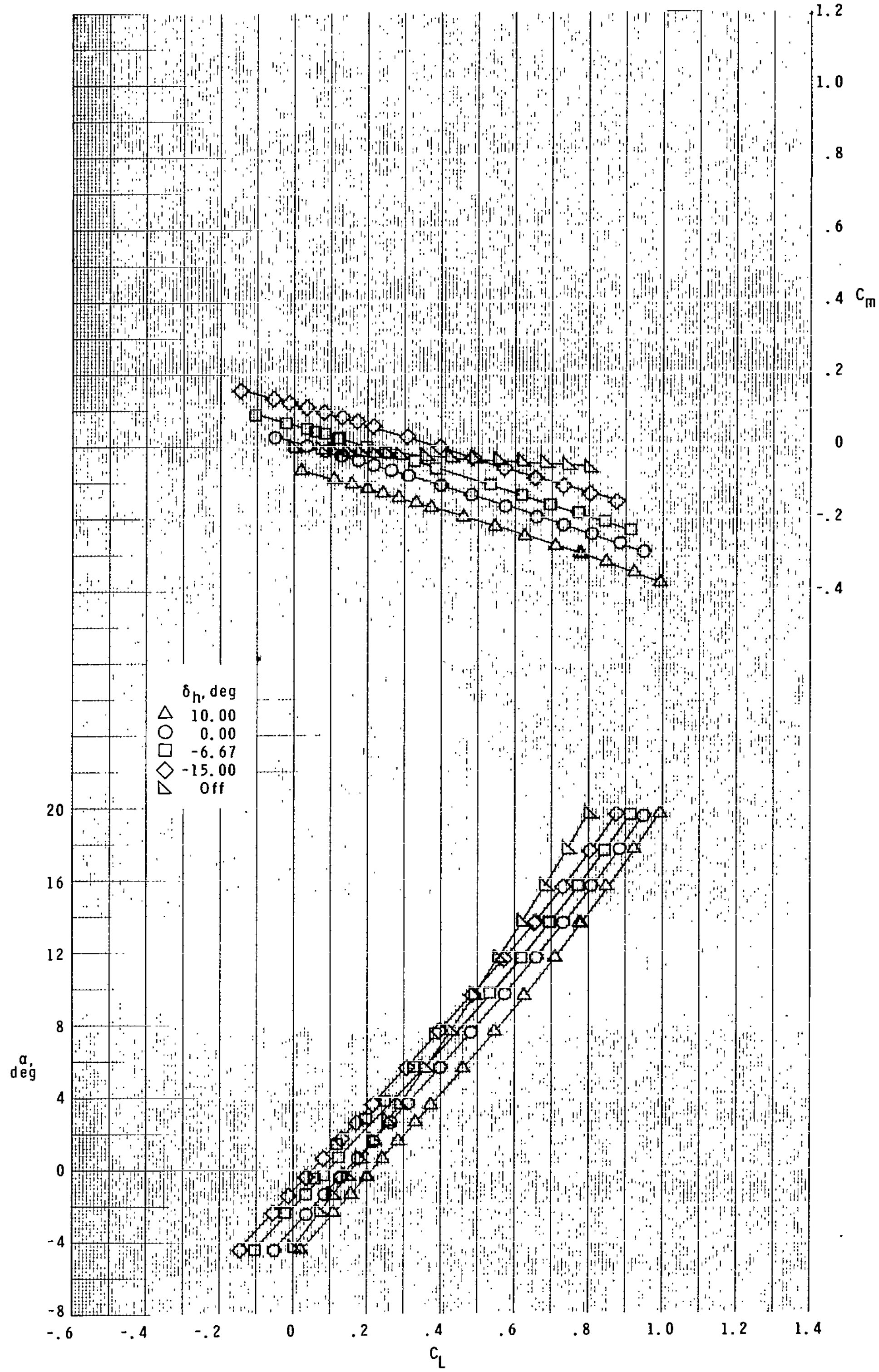

(h) M = 2.16.

Figure 3.- Continued.

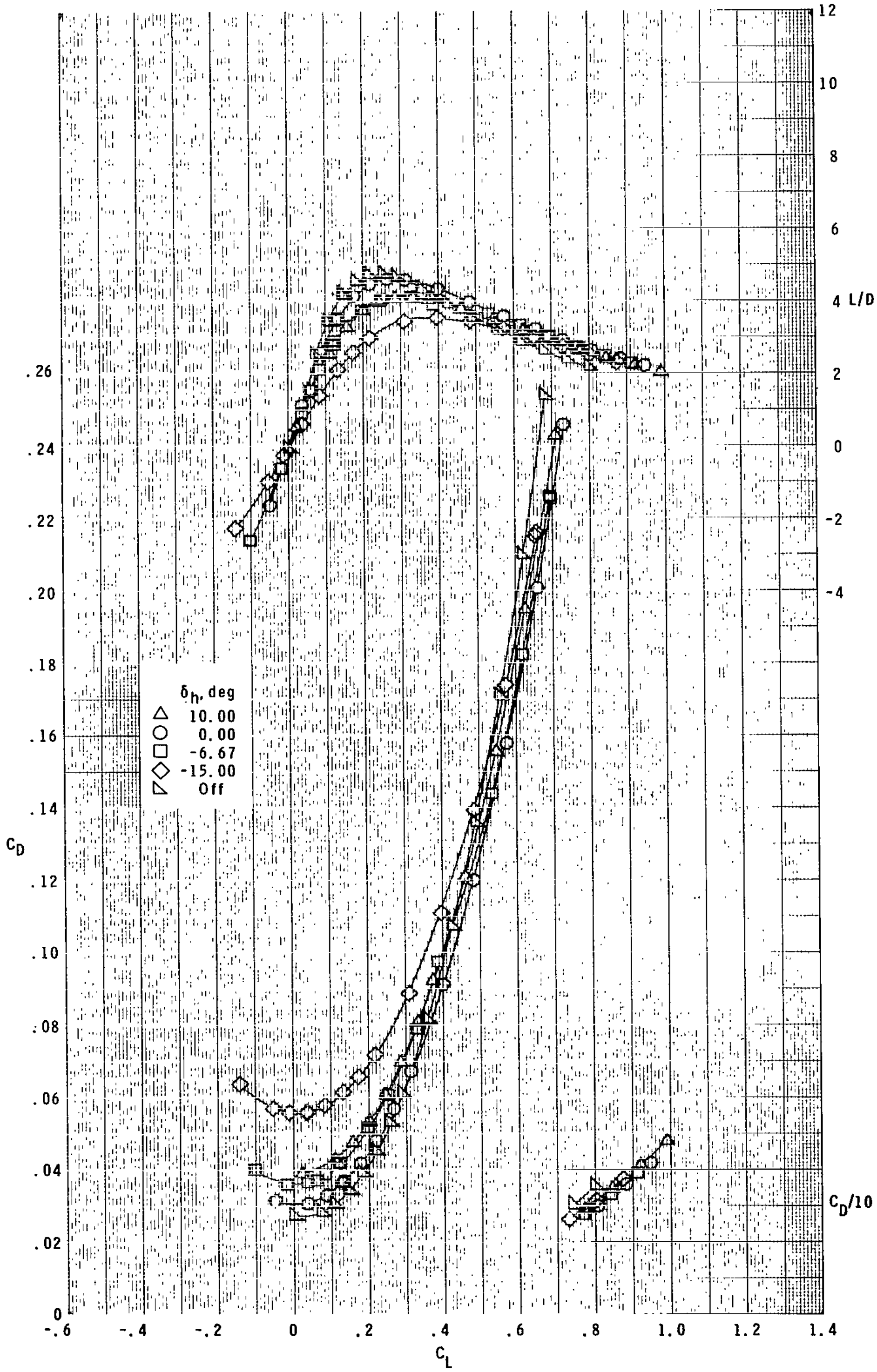

(h) M = 2.16. Concluded.

Figure 3.- Concluded.

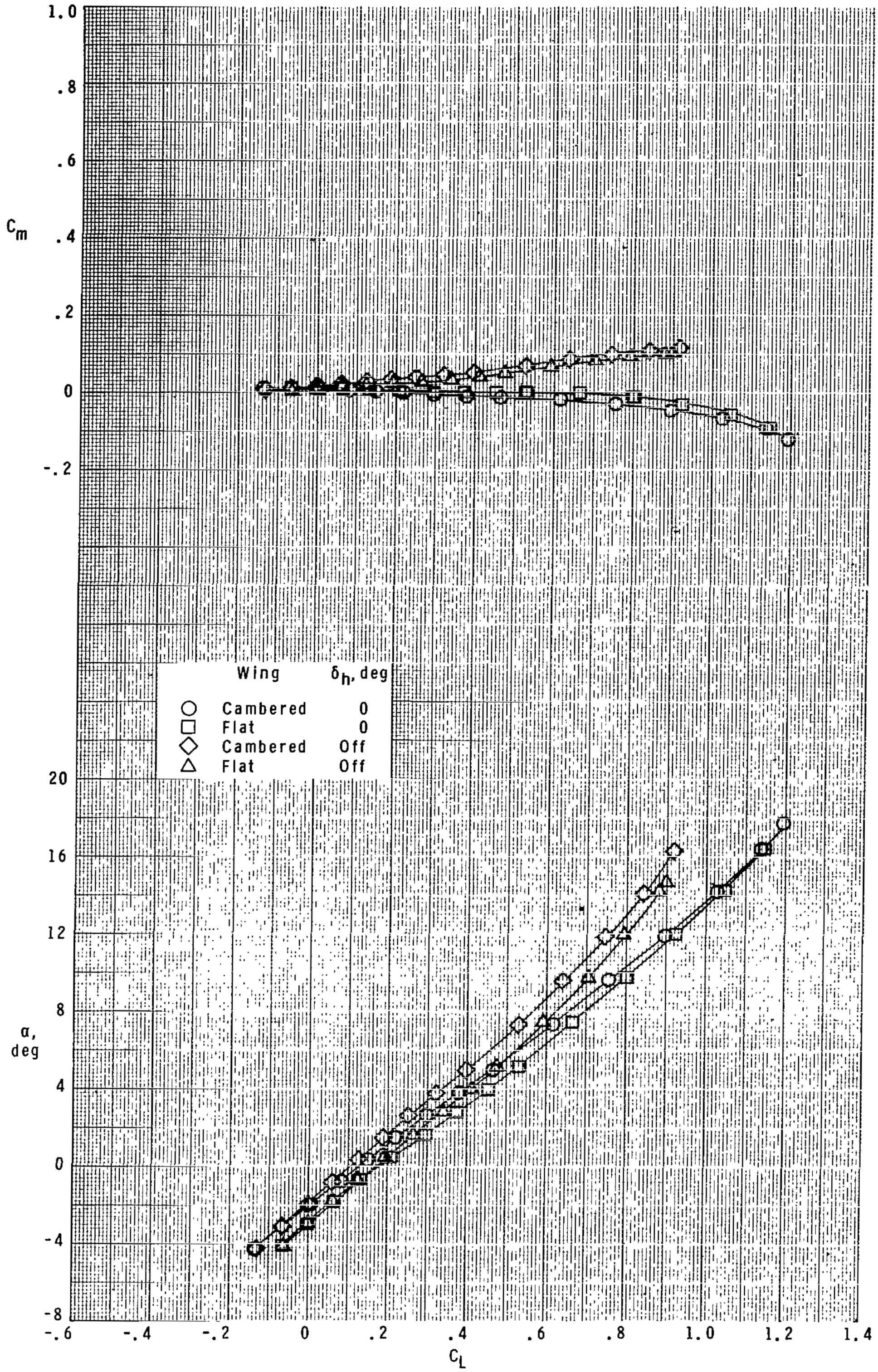

(a) M = 0.50.

Figure 4.- Longitudinal aerodynamic characteristics with cambered wing and flat wing.

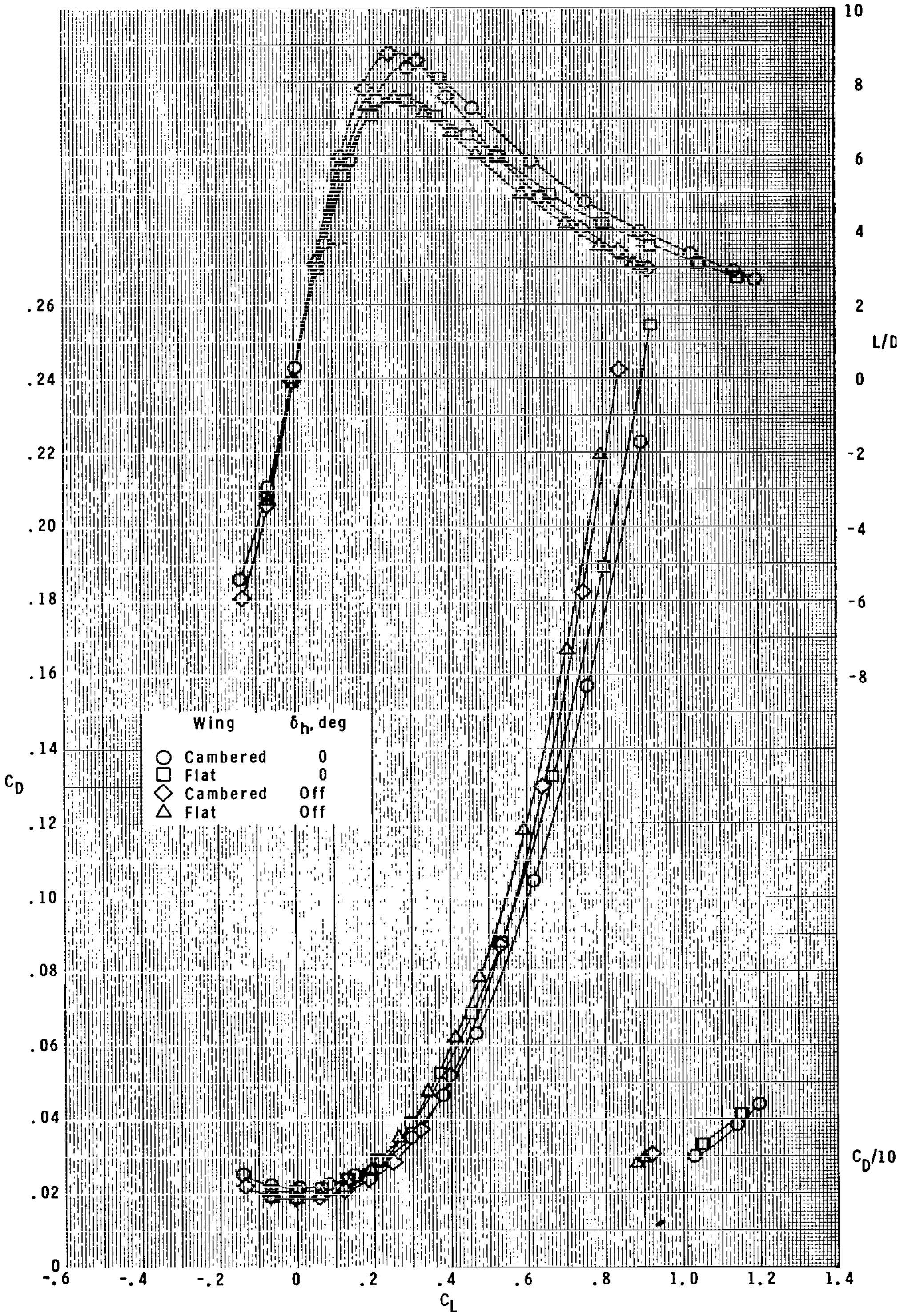

(a) M = 0.50. Concluded.

Figure 4.- Continued.

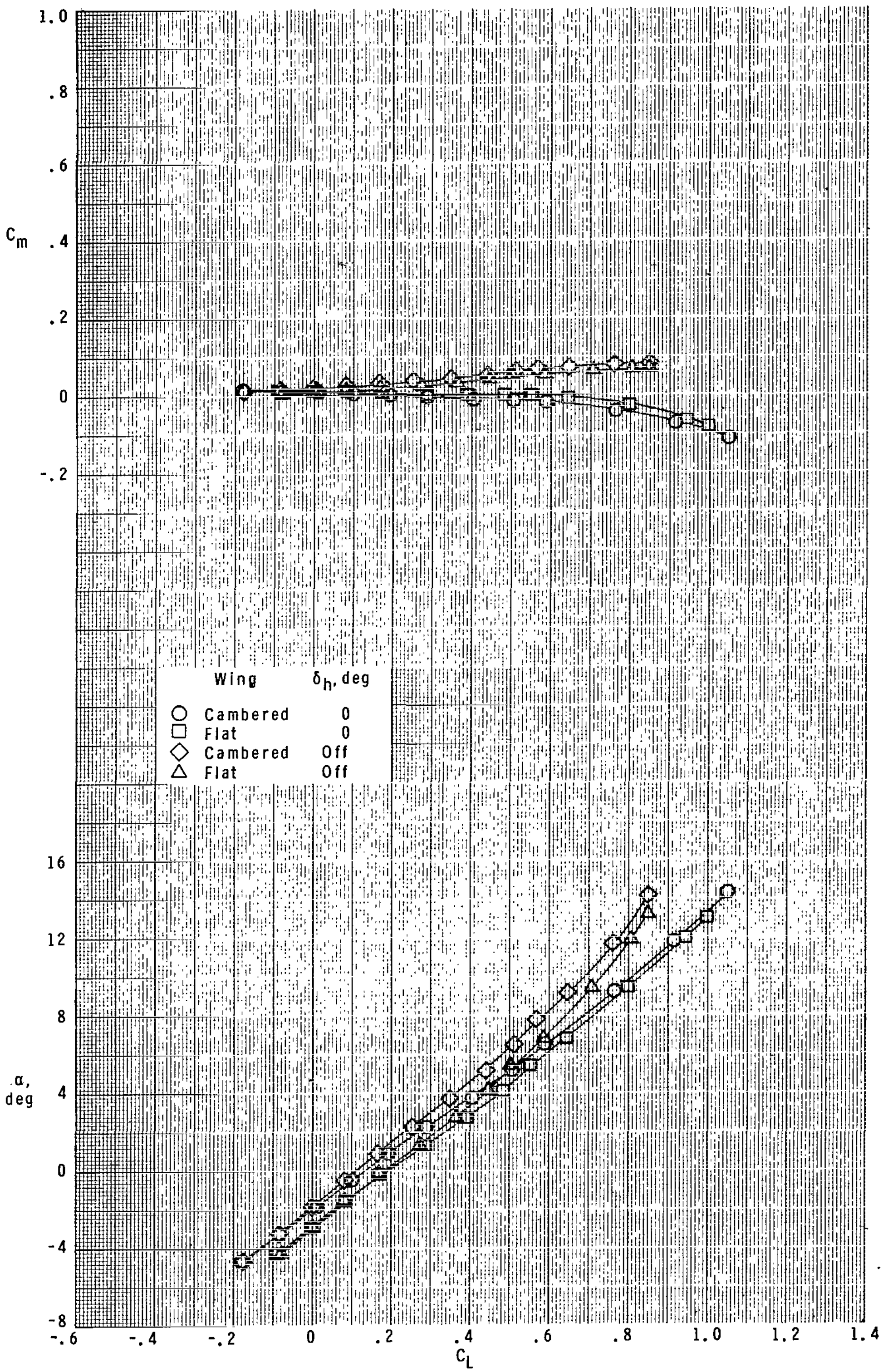

(b) M = 0.80.

Figure 4.- Continued.

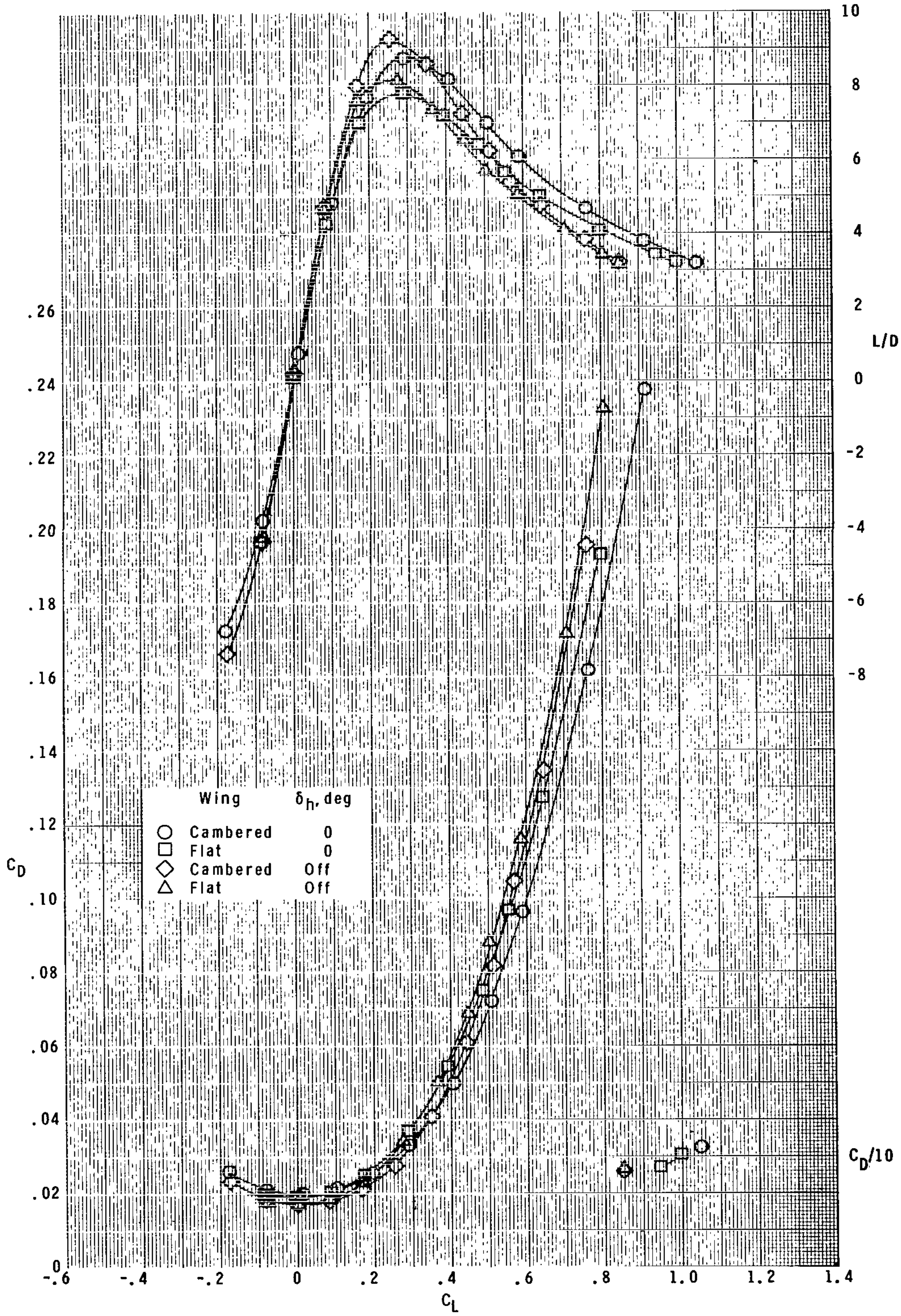

(b) M = 0.80. Concluded.

Figure 4.- Continued.

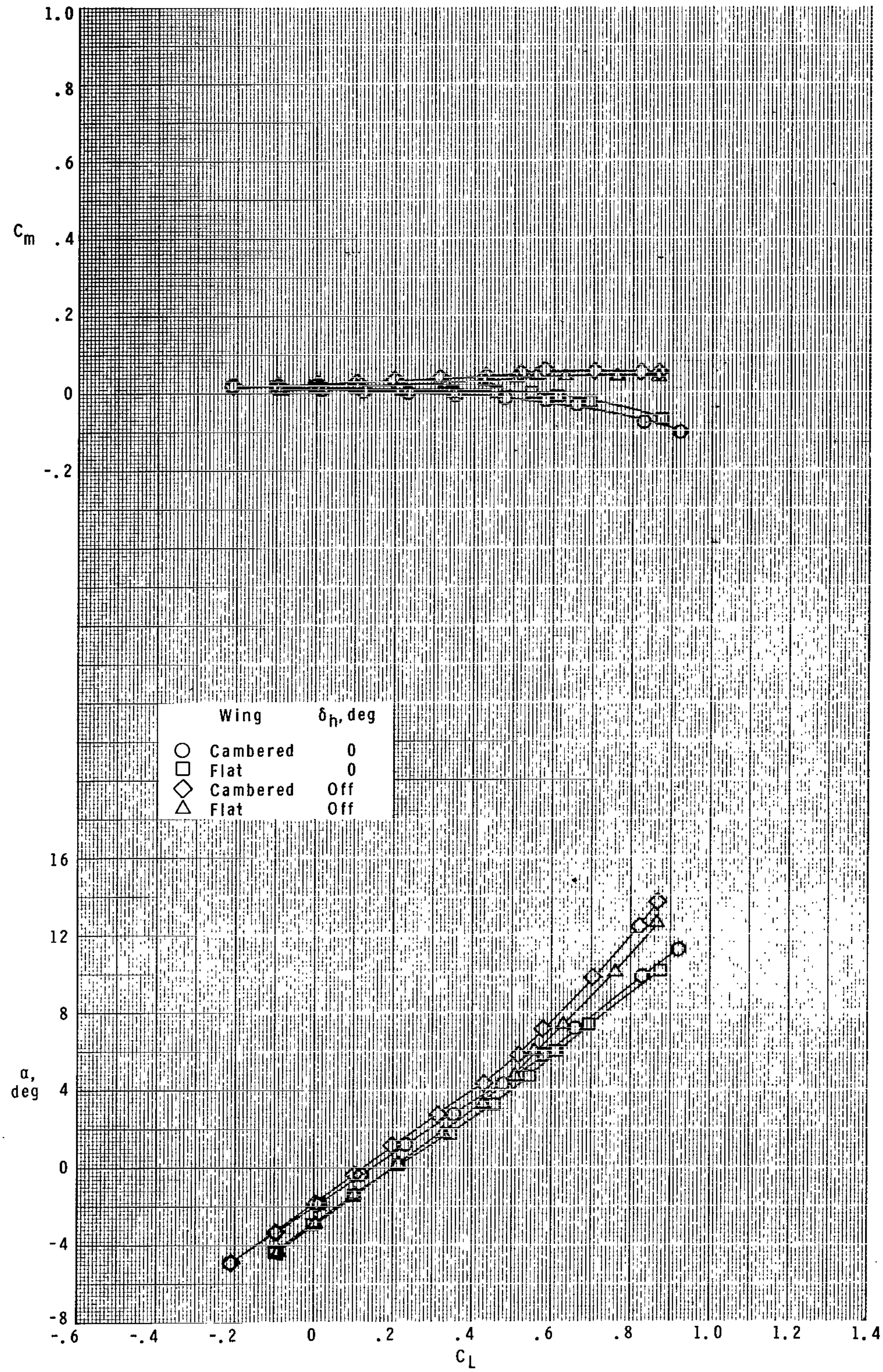

(c) M = 0.90.

Figure 4.- Continued.

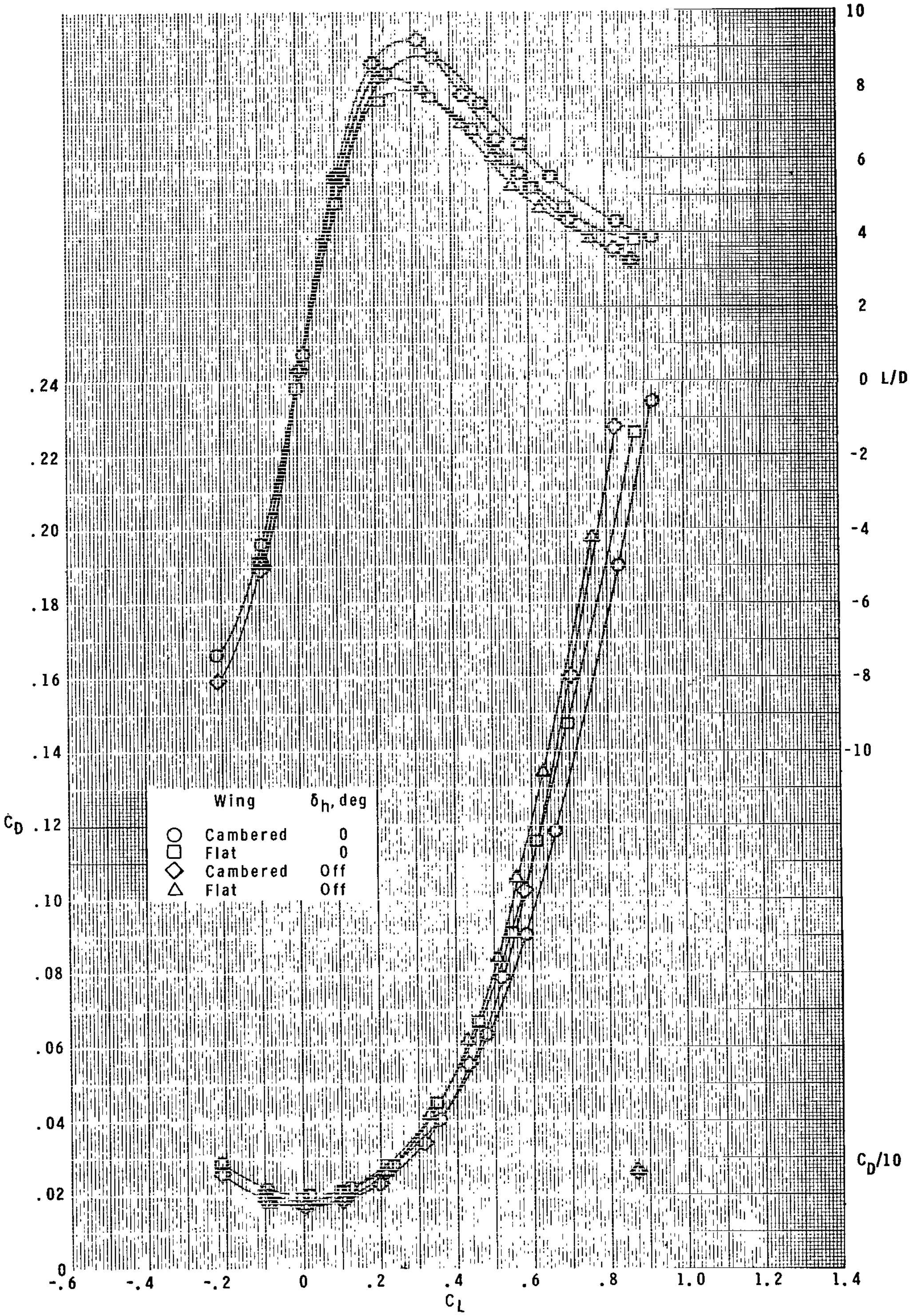

(c) M = 0.90. Concluded.

Figure 4.- Continued.

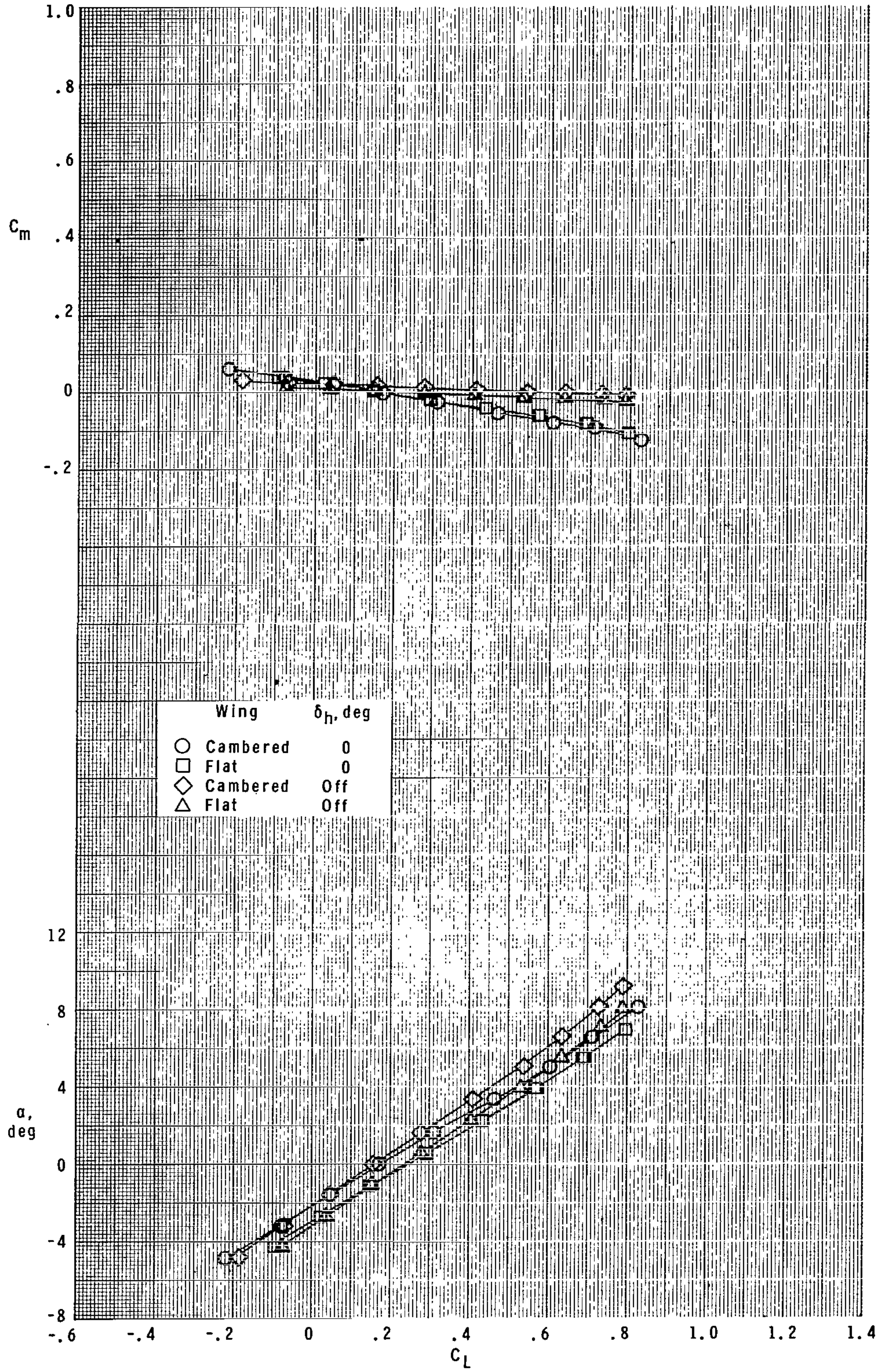

(d) M = 1.03.

Figure 4.- Continued.

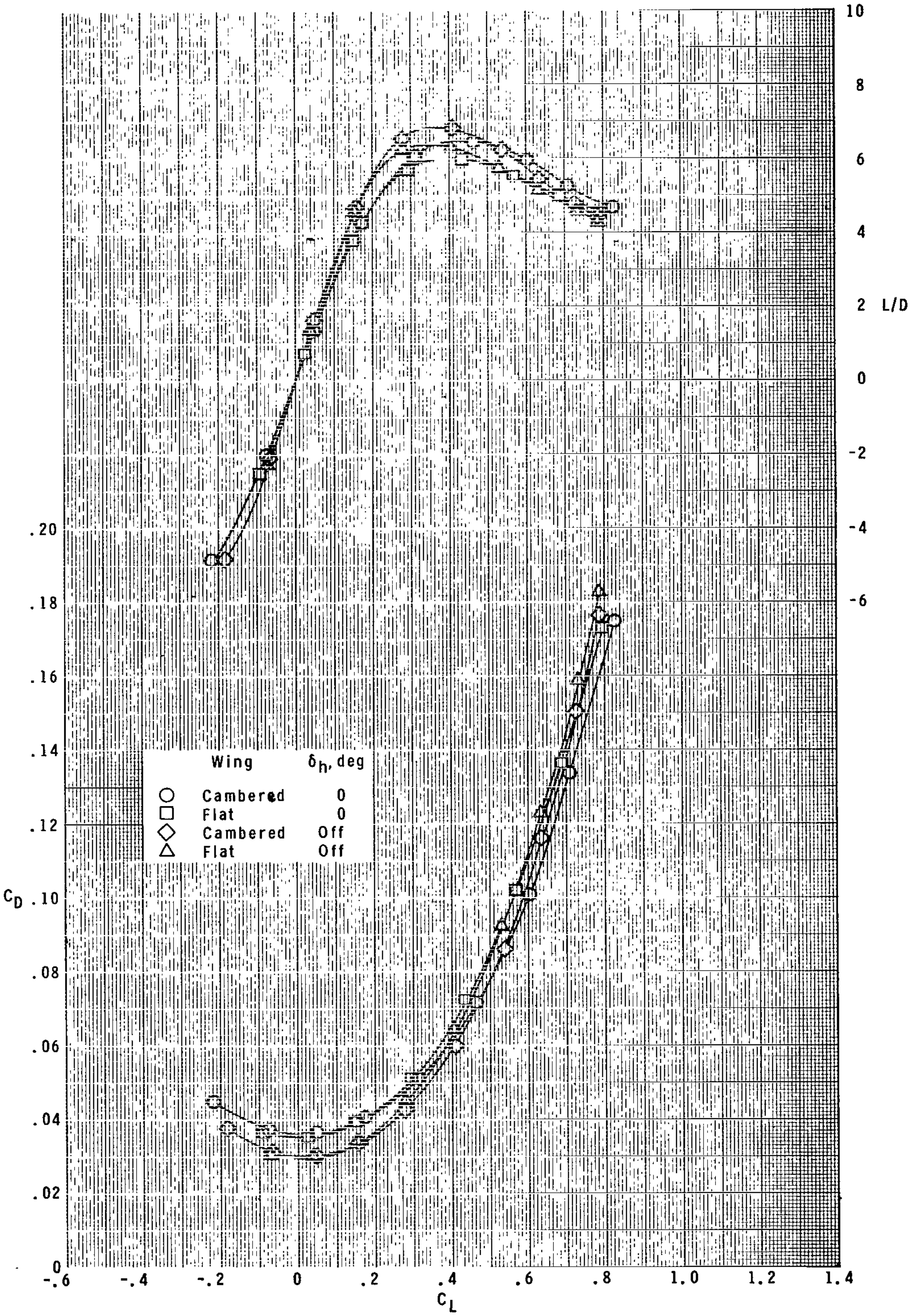

(d) M = 1.03. Concluded.

Figure 4.- Continued.

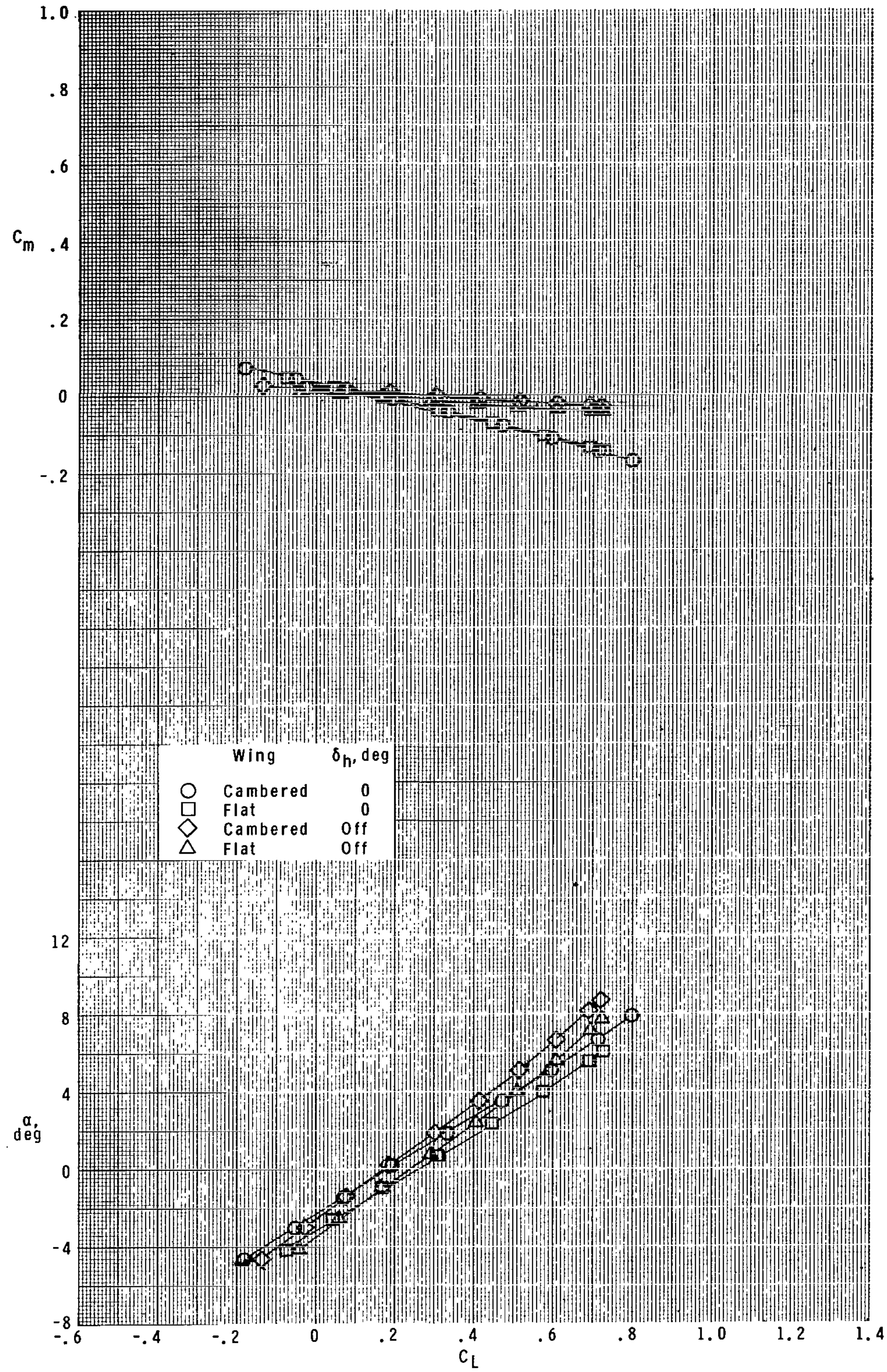

(e) M = 1.20.

Figure 4.- Continued.

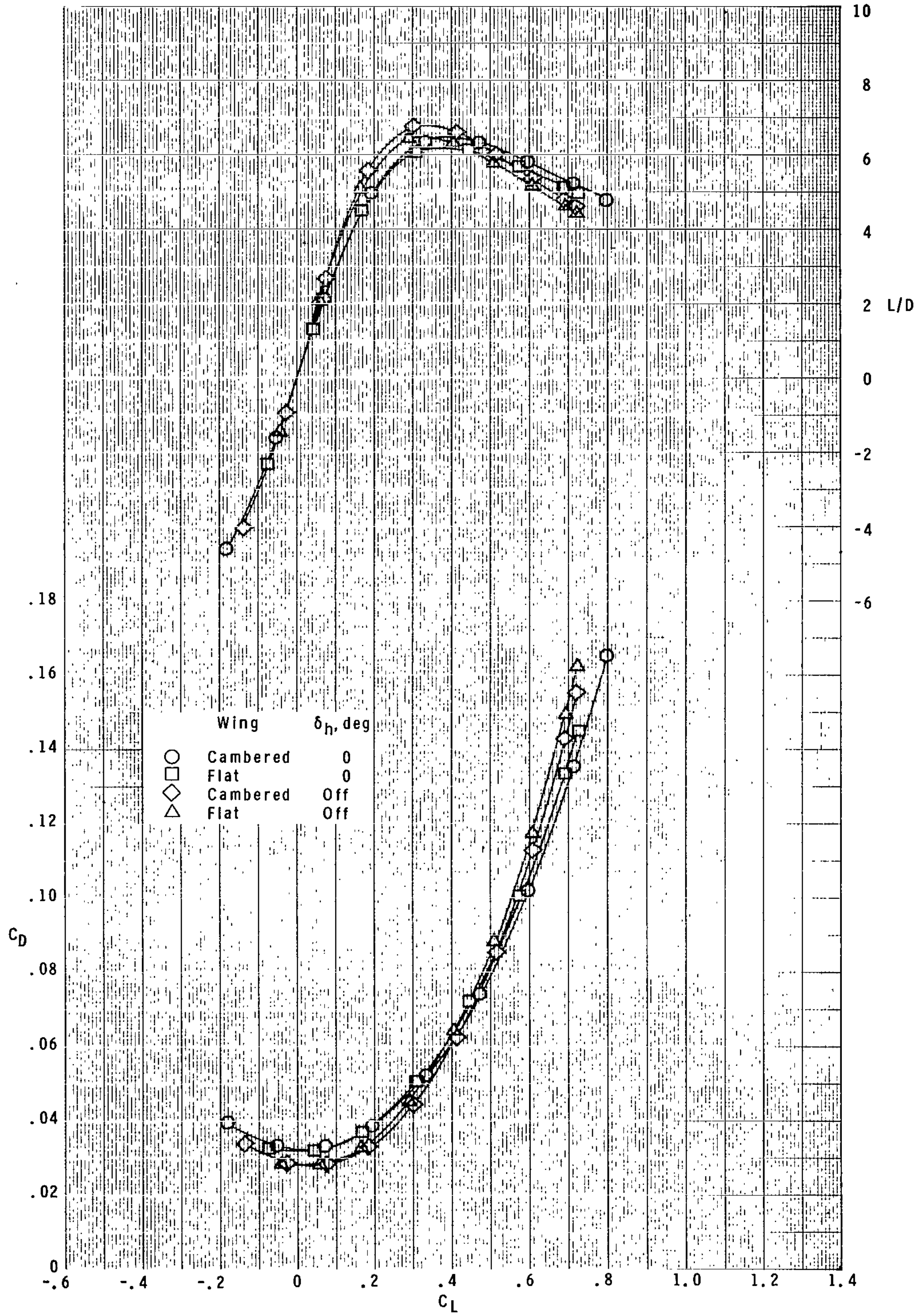

(e) M = 1.20. Concluded.

Figure 4.- Continued.

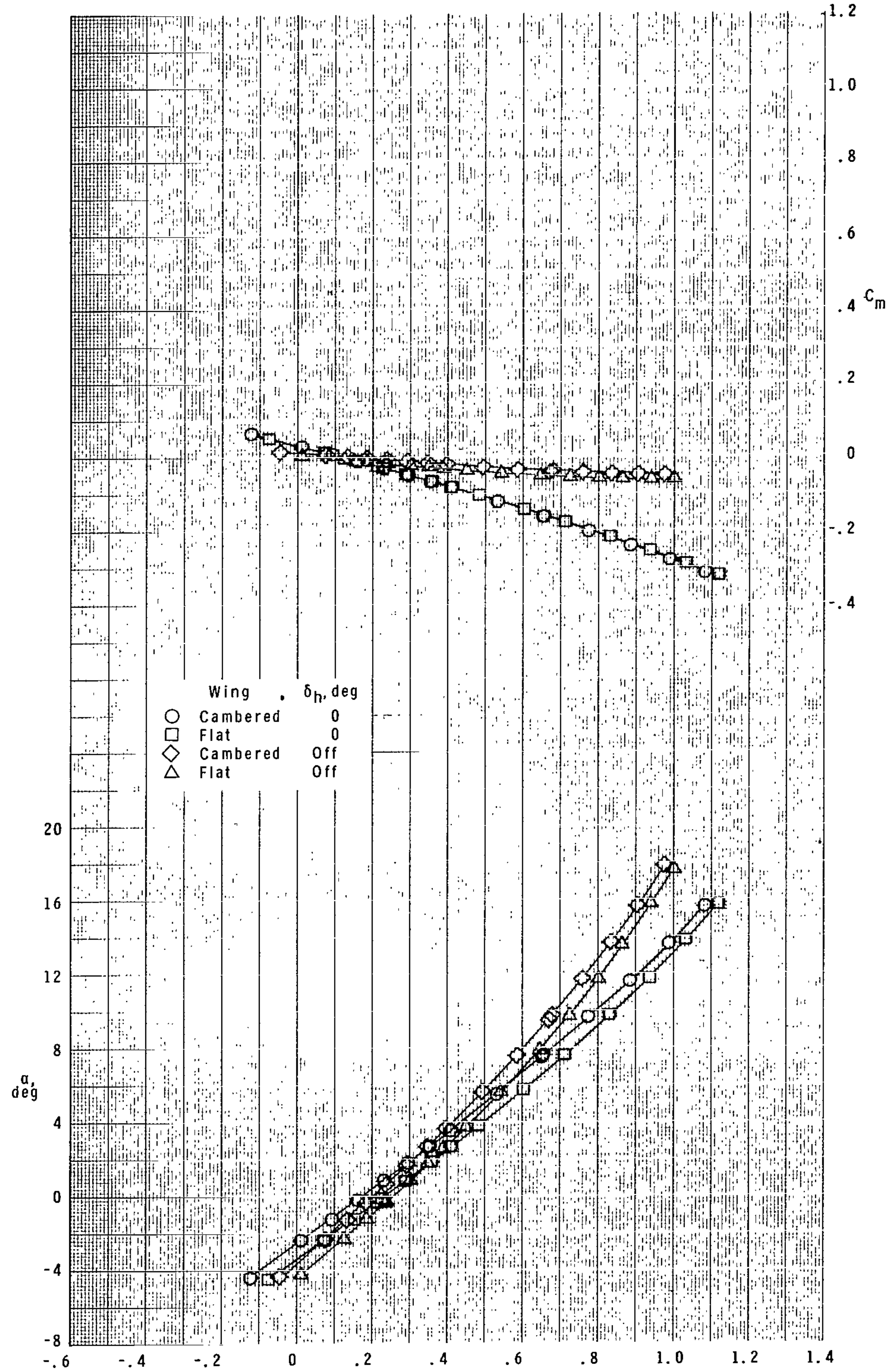

(f) M = 1.47.

Figure 4.- Continued.

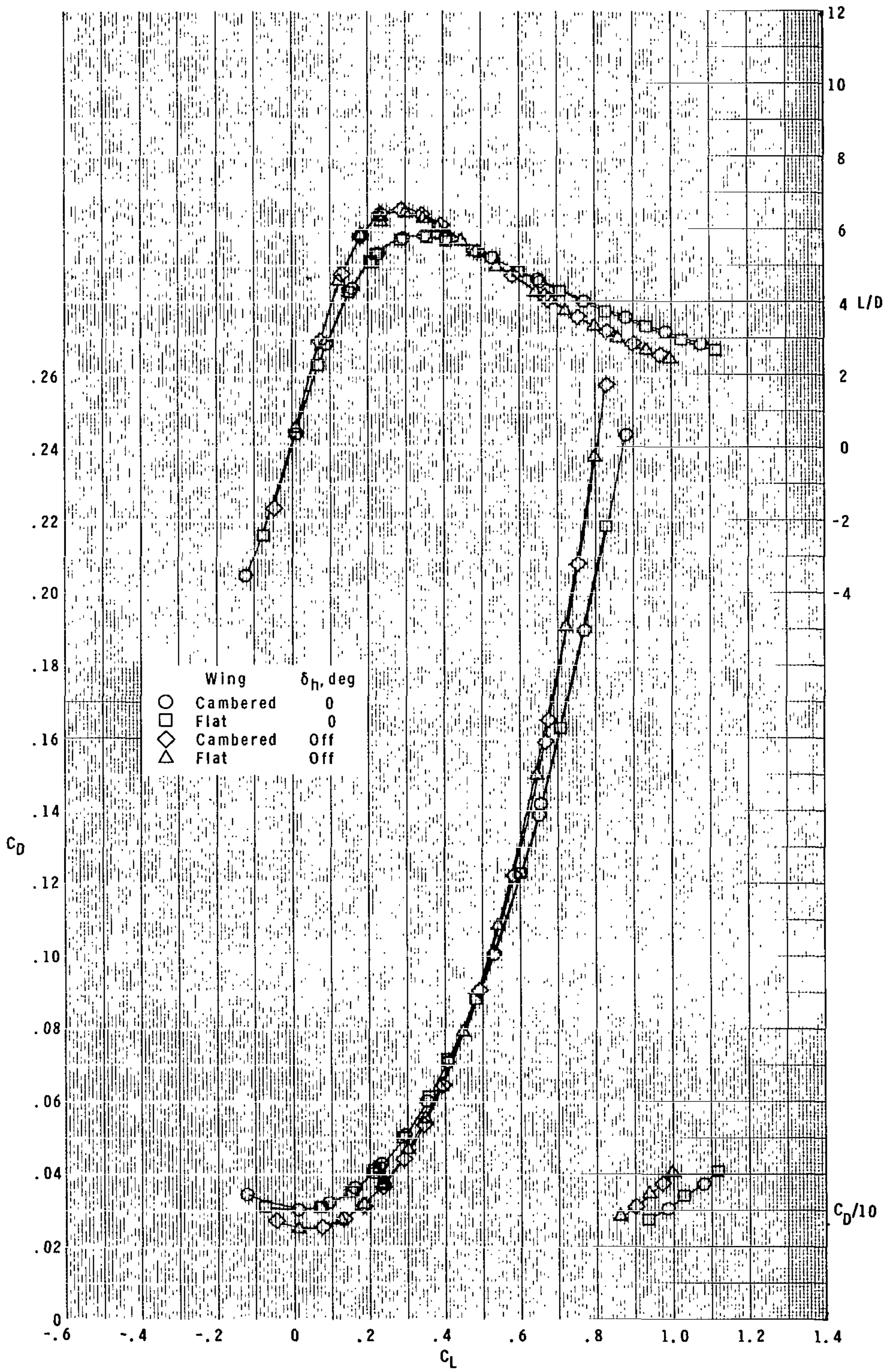

(f) M = 1.47. Concluded.

Figure 4.- Continued.

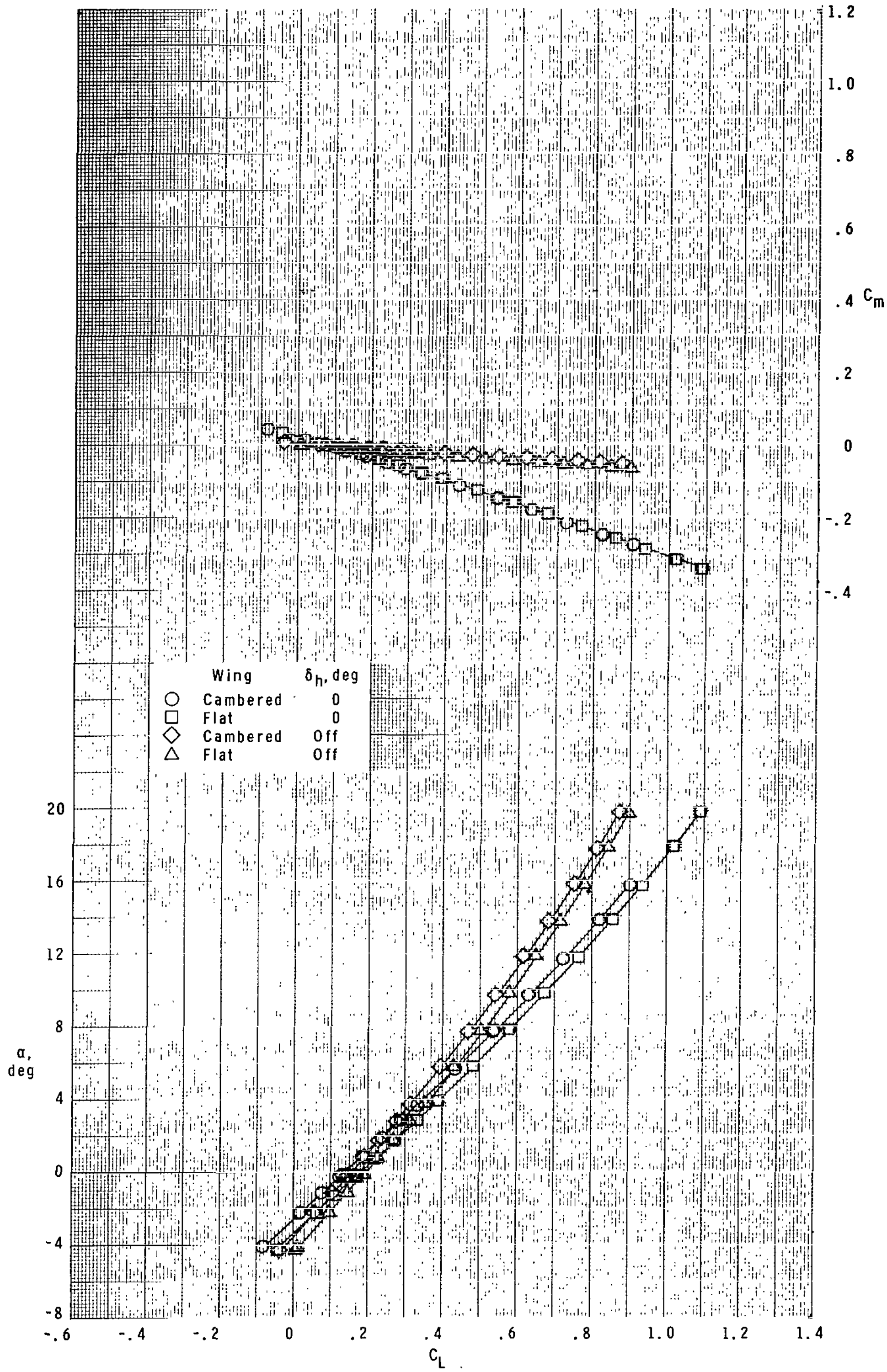

(g) M = 1.80.

Figure 4.- Continued.

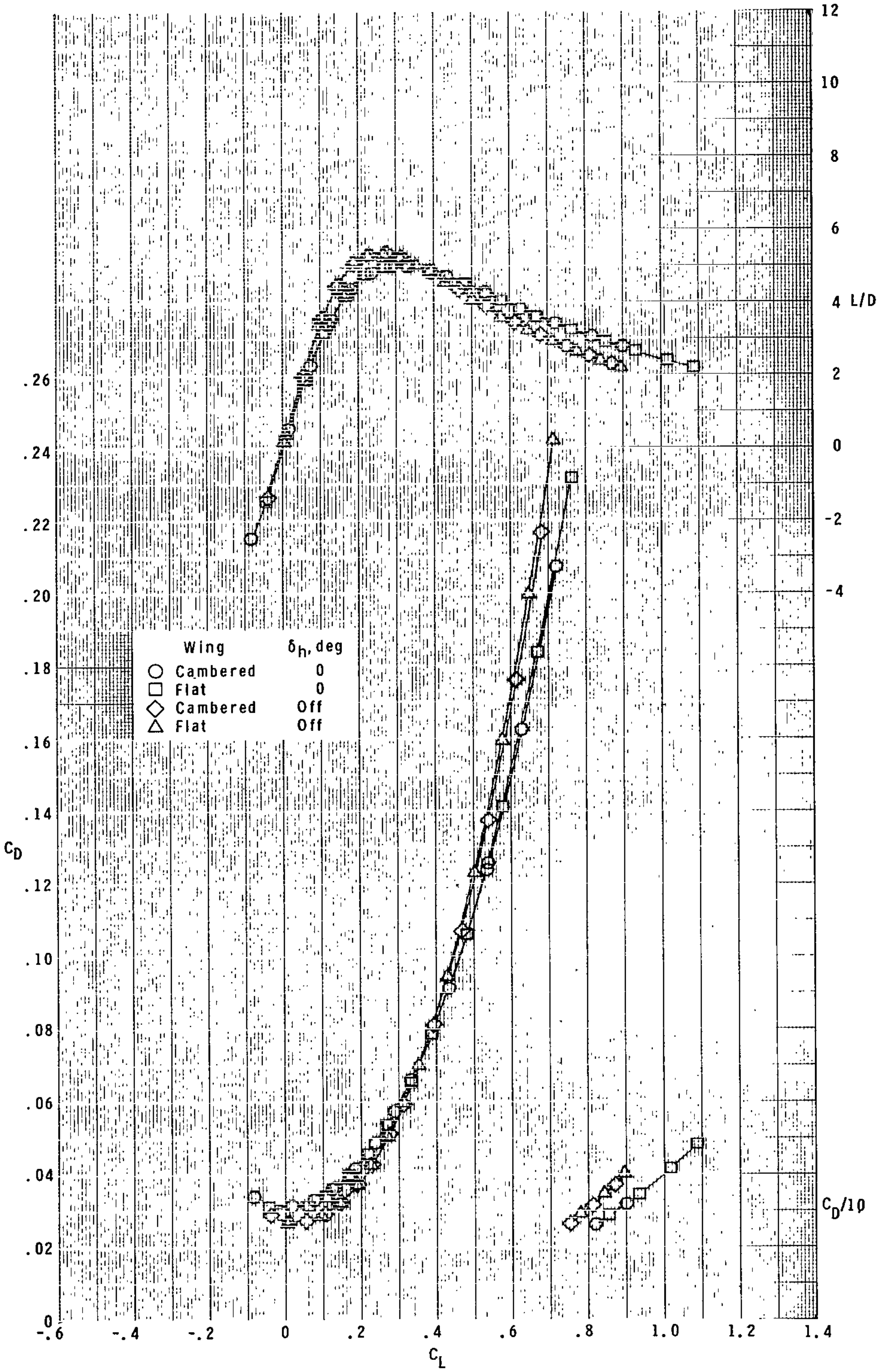

(g) M = 1.80. Concluded.

Figure 4.- Continued.

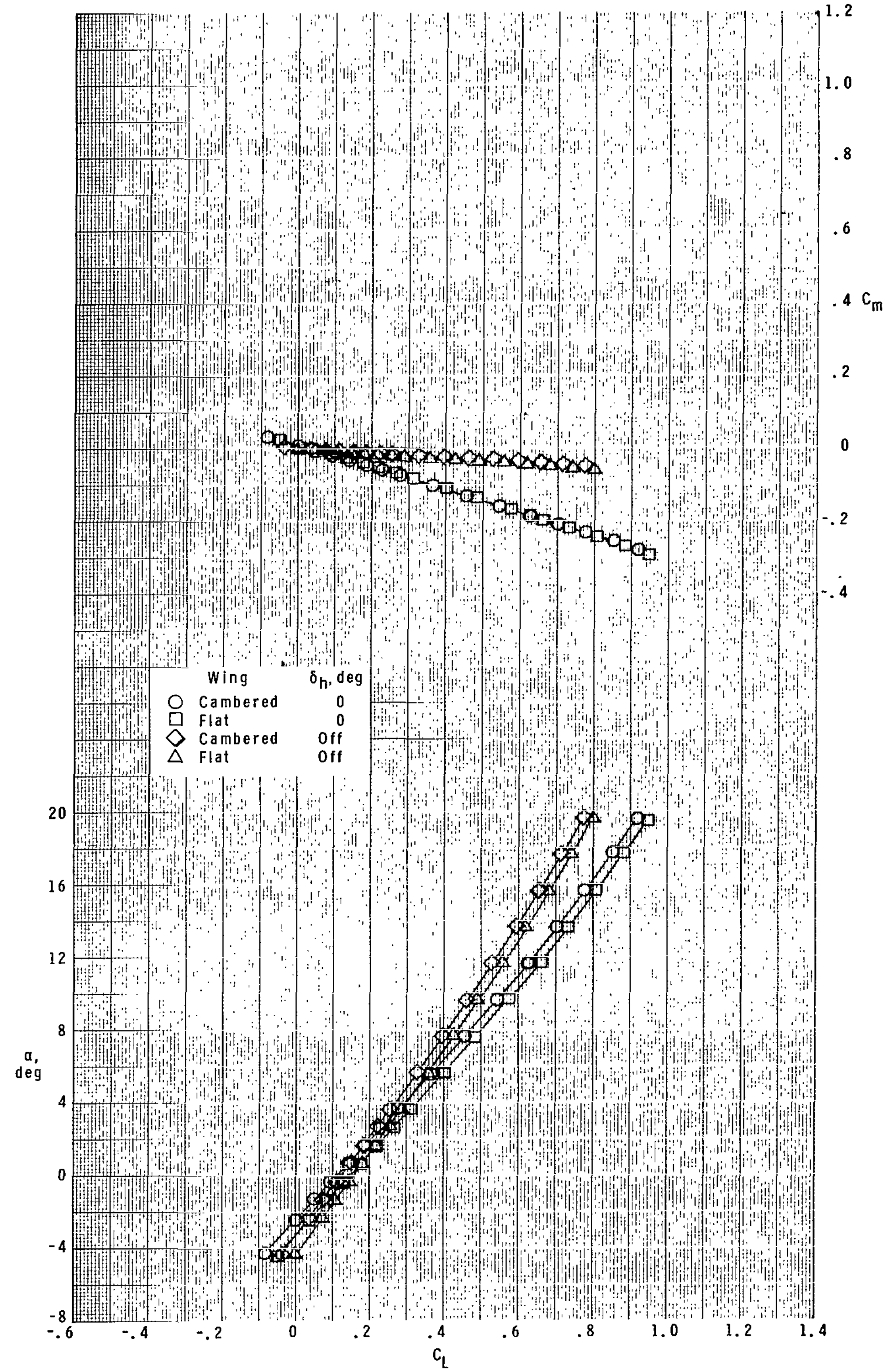

(h) M = 2.16.

Figure 4.- Continued.

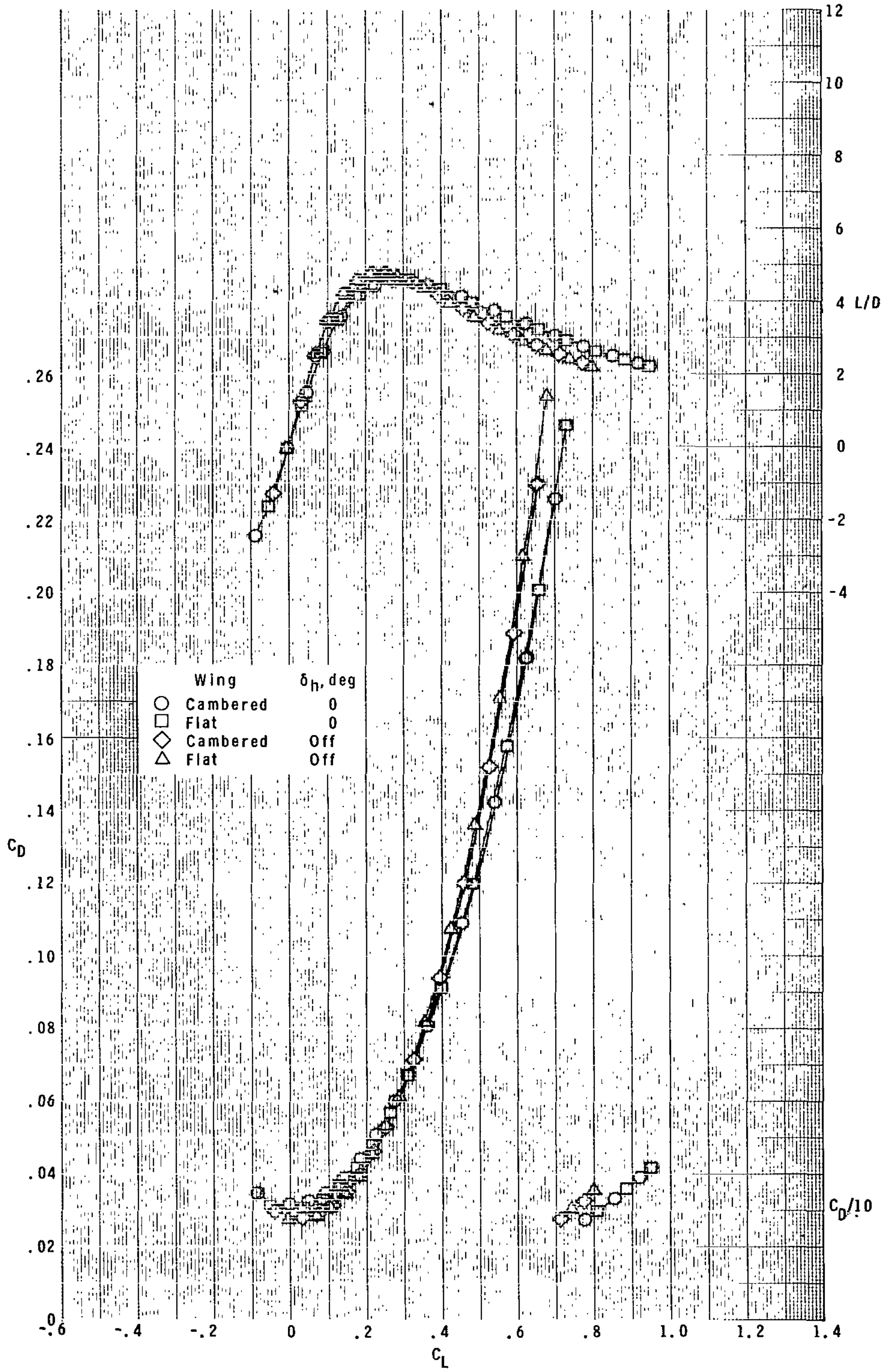

(h) M = 2.16. Concluded.

Figure 4.- Concluded.

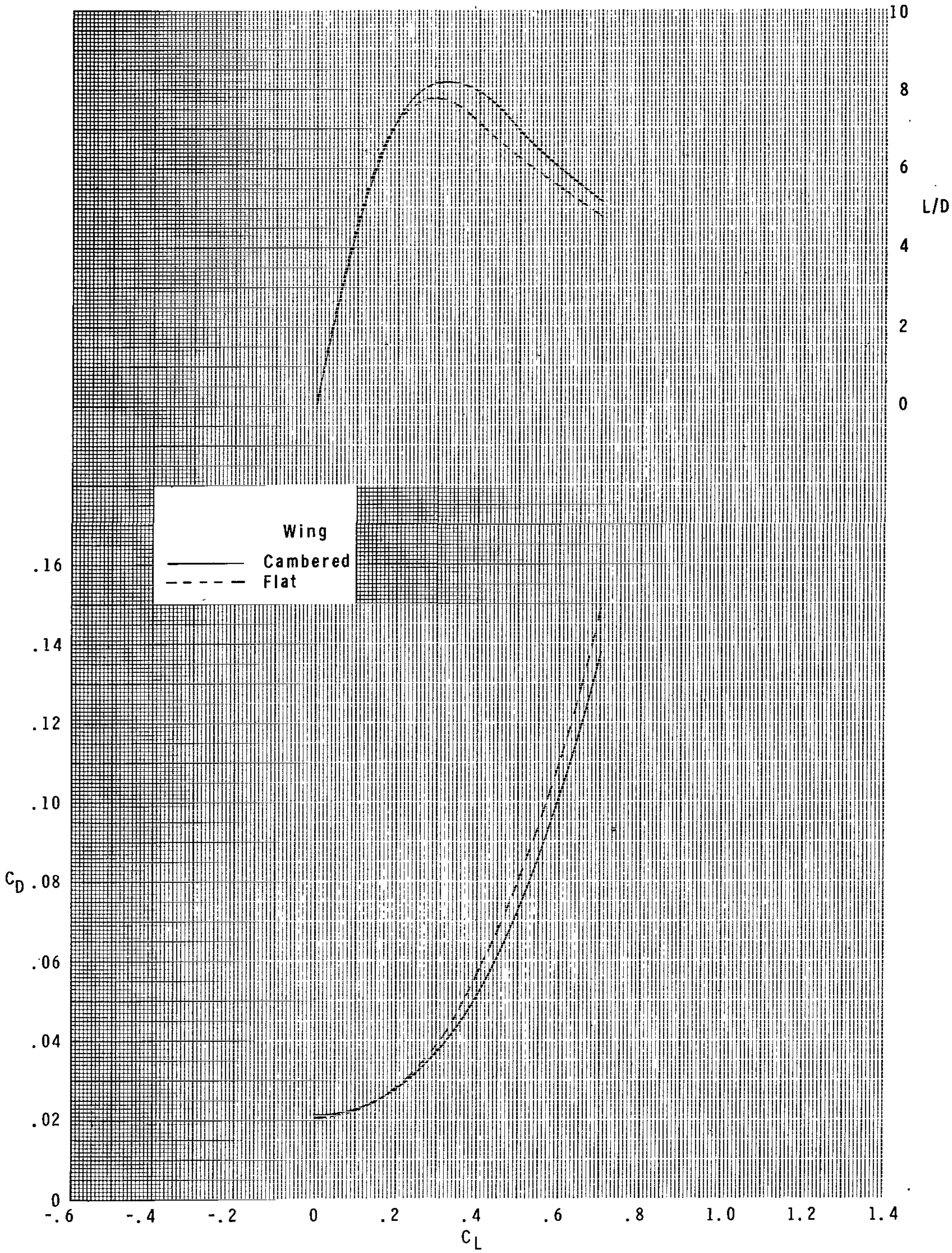

(a) M = 0.50.

Figure 5.- Trimmed drag polars and lift-drag ratios with cambered wing and flat wing.

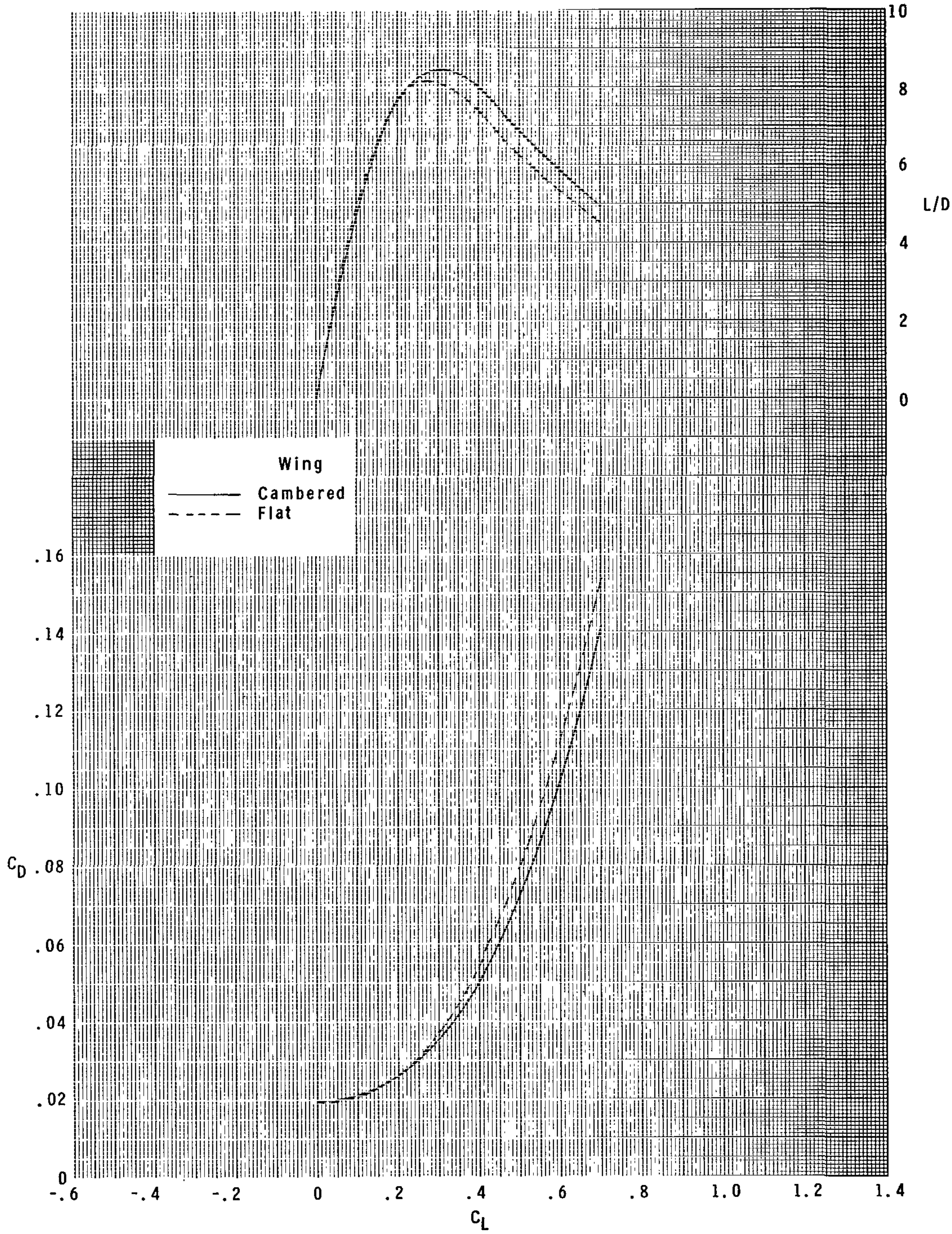

(b) M = 0.80.

Figure 5.- Continued.

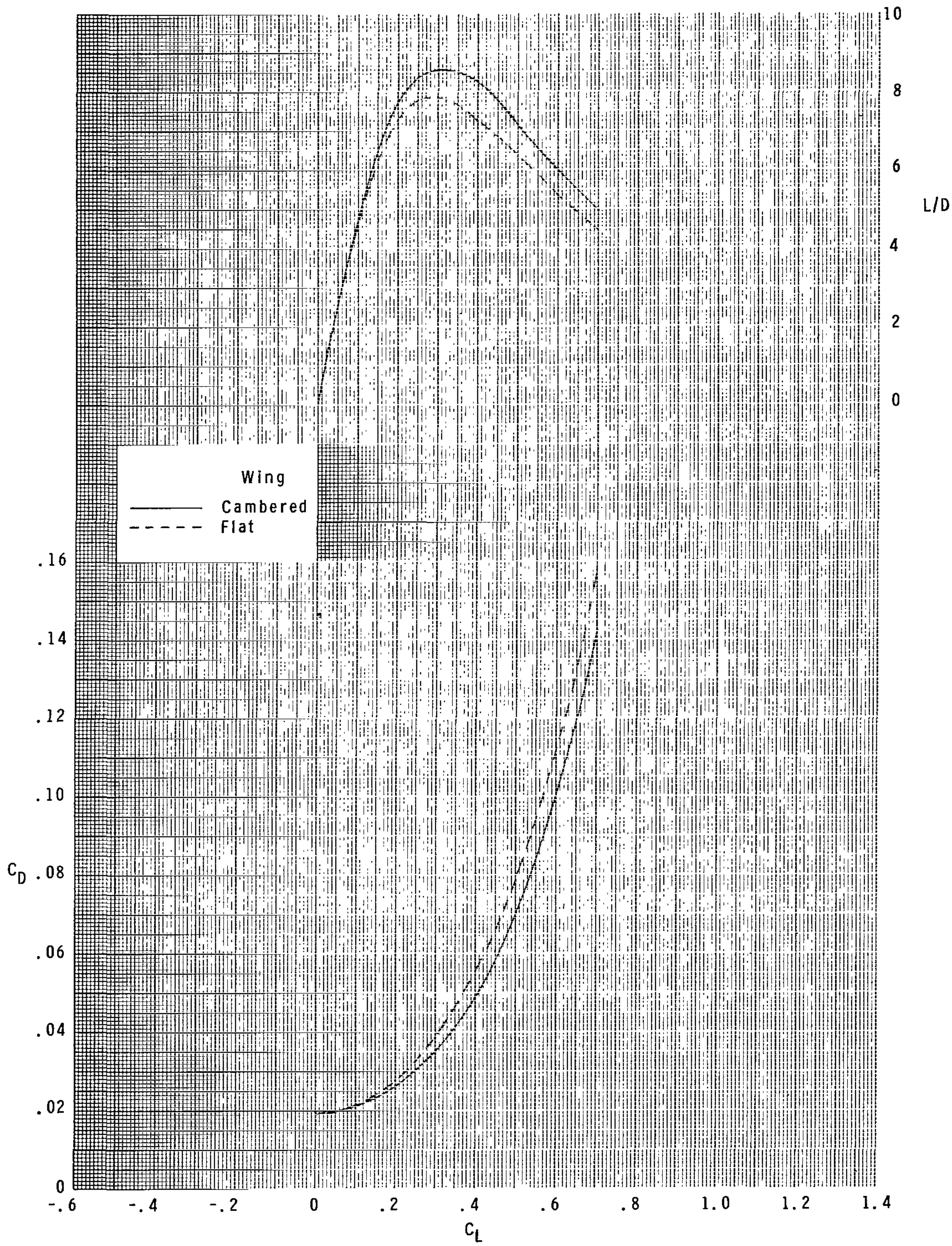

(c) M = 0.90.

Figure 5.- Continued.

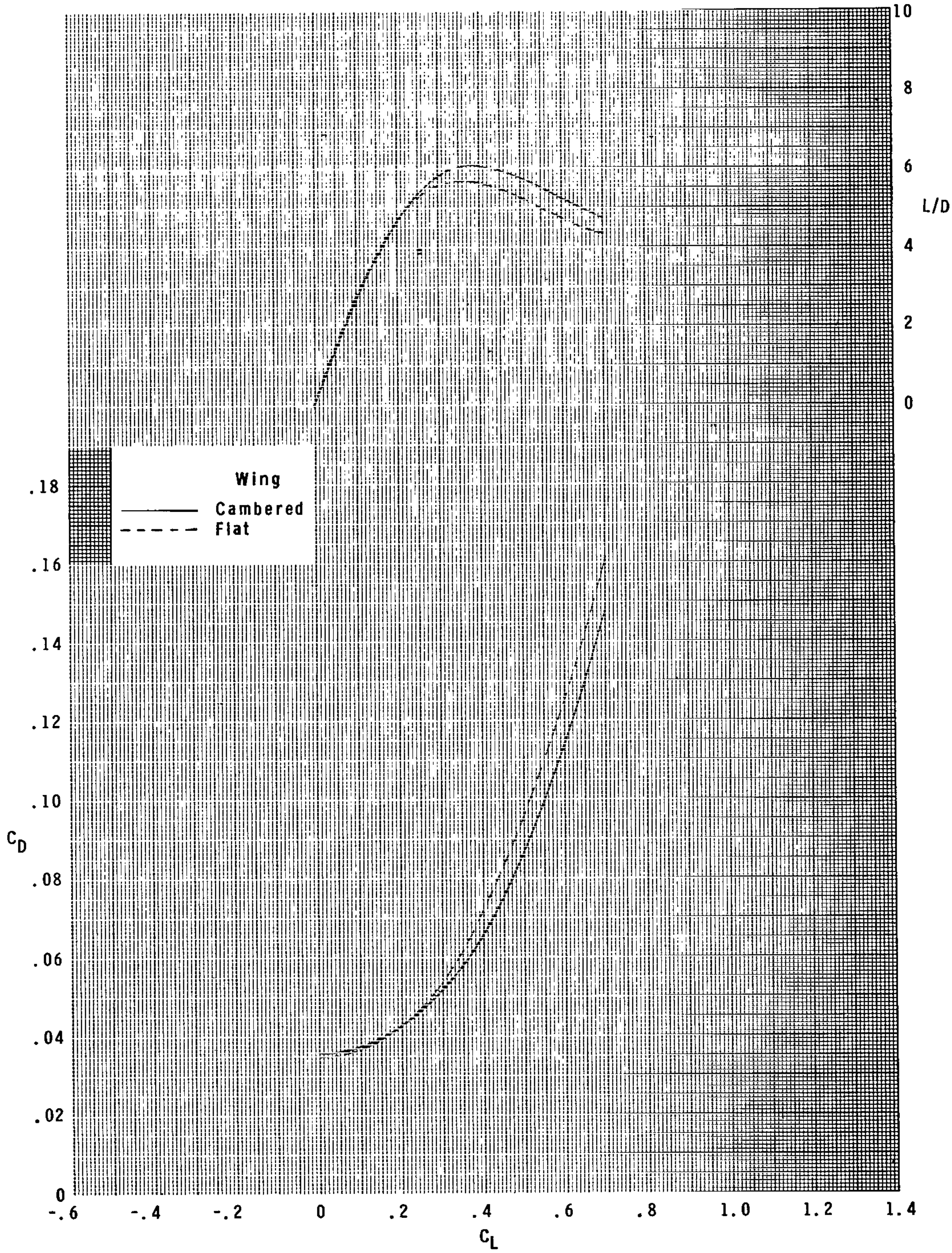

(d) M = 1.03.

Figure 5.- Continued.

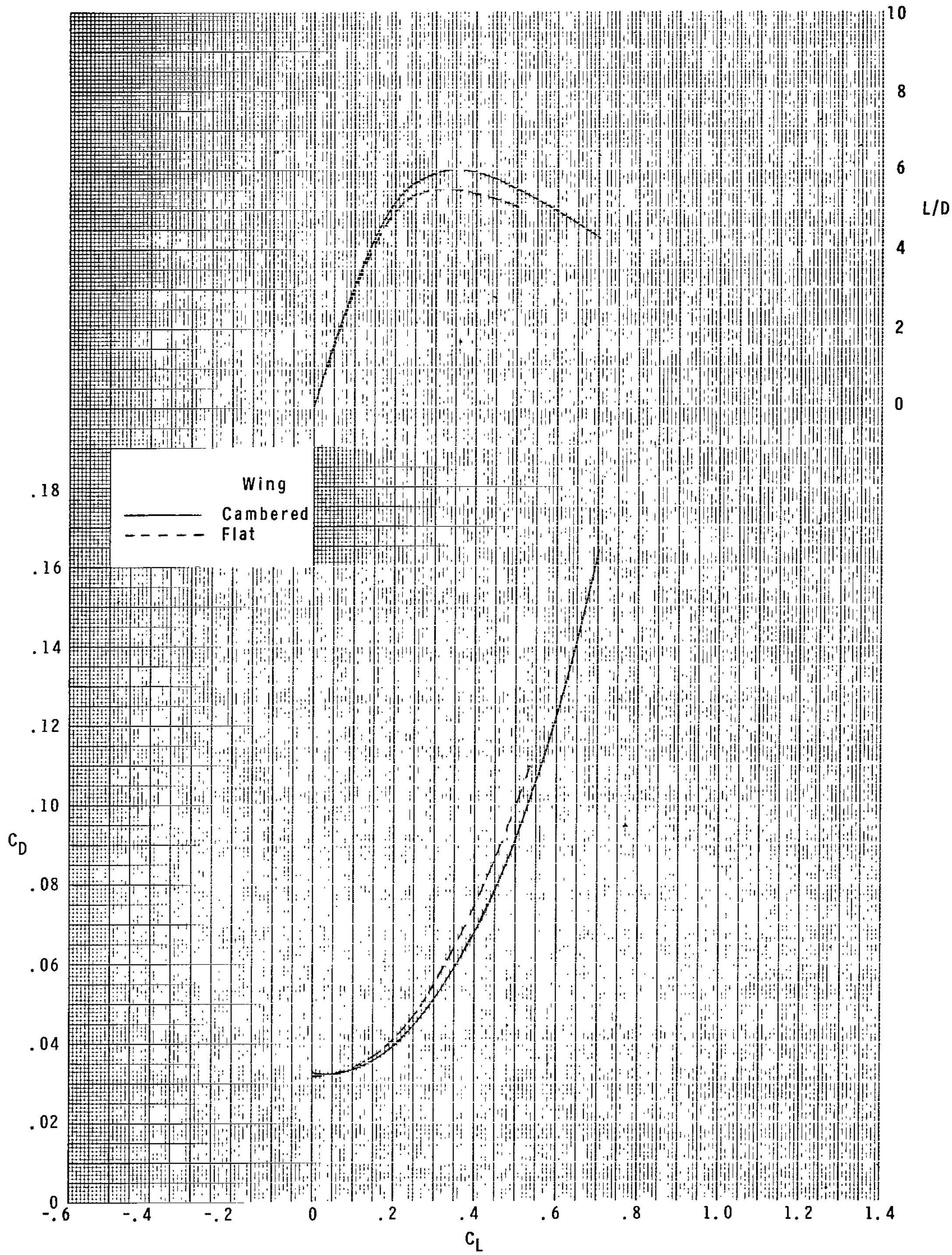

(e) M = 1.20.

Figure 5.- Continued.

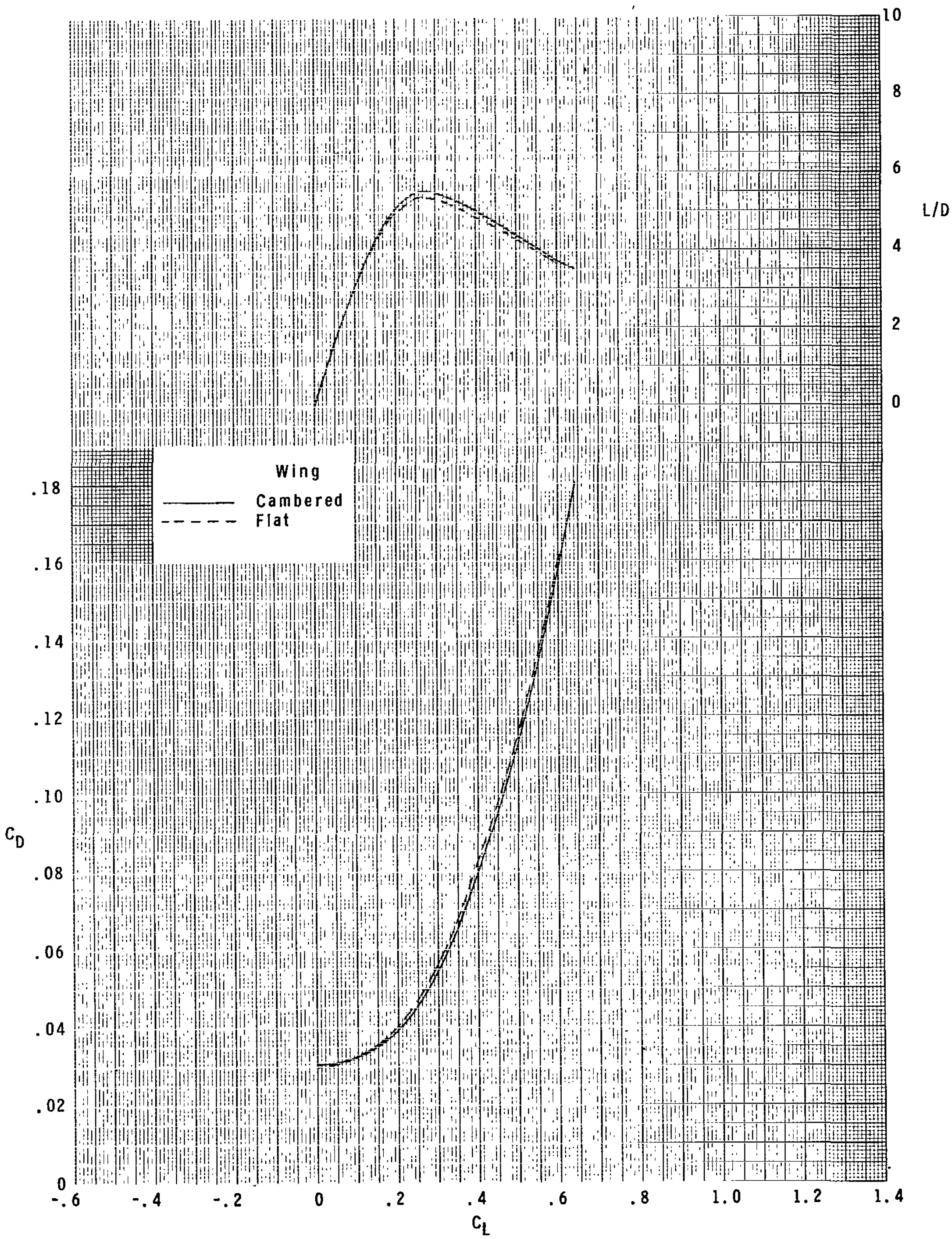

(f) M = 1.47.

Figure 5.- Continued.

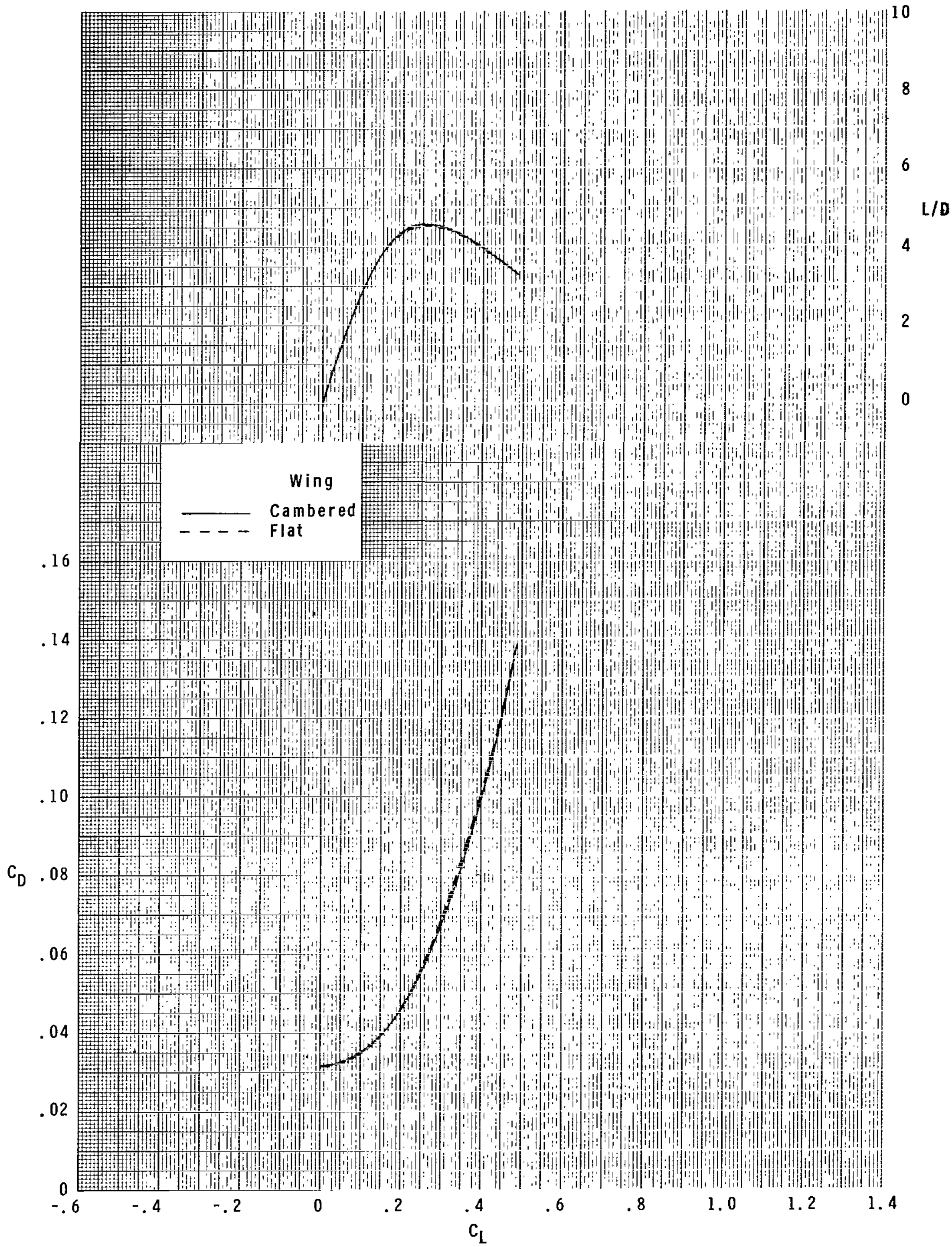

(g) M = 1.80.

Figure 5.- Continued.

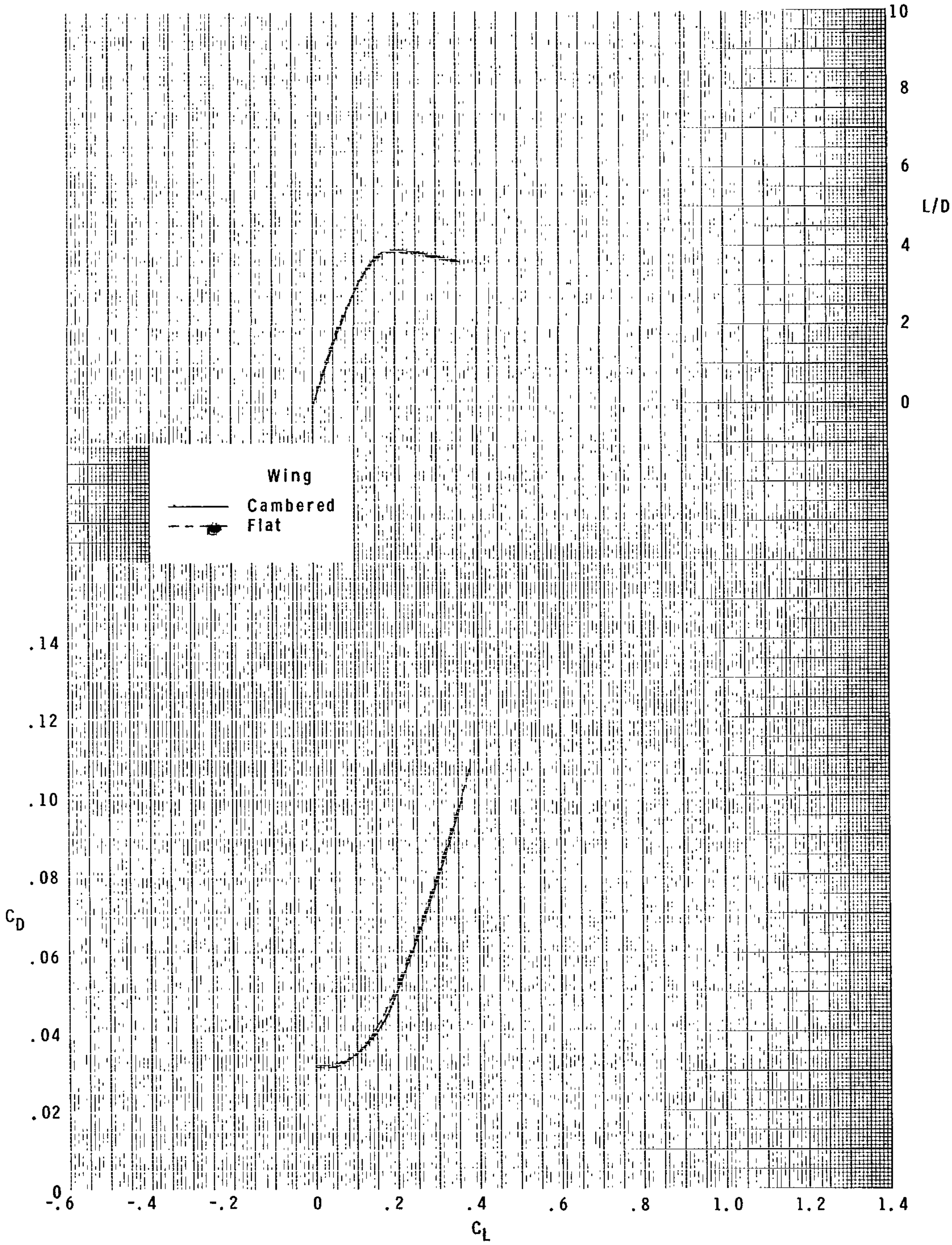

(h) M = 2.16.

Figure 5.- Concluded.

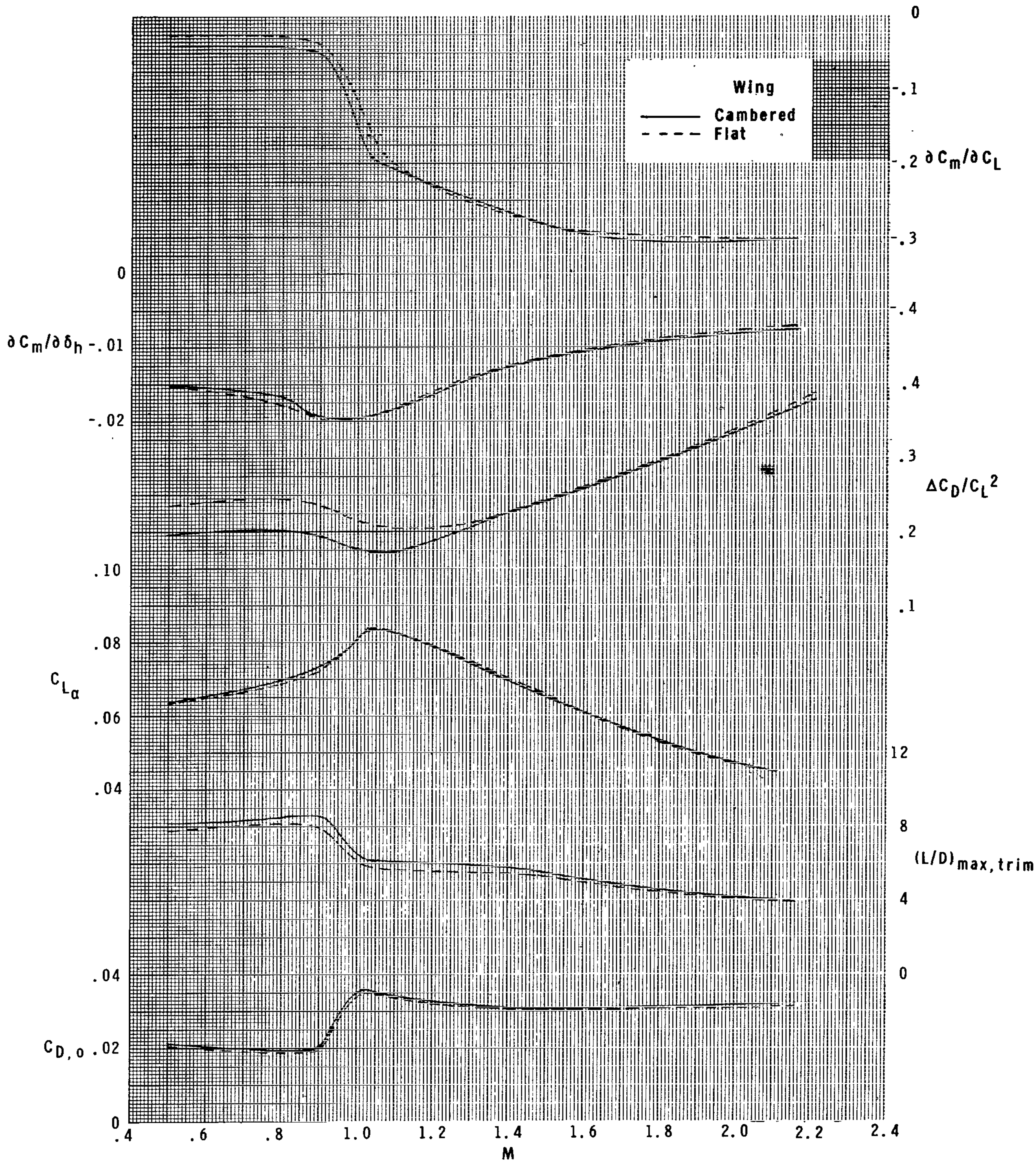

Figure 6.- Summary of pertinent longitudinal data.

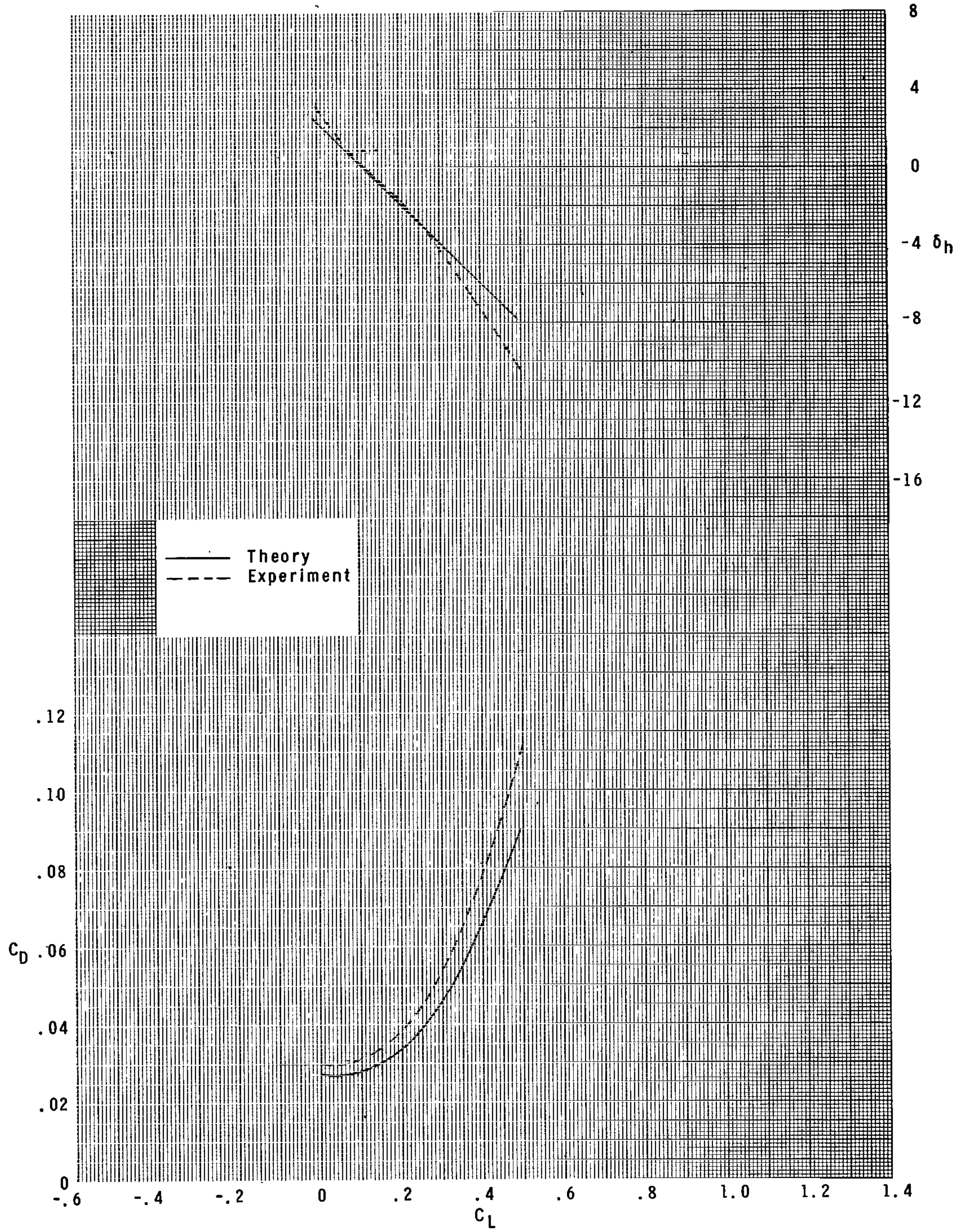

(a) M = 1.47.

Figure 7.- Comparison of experimental and theoretical trim curves for Mach 1.47, 1.80, and 2.16.

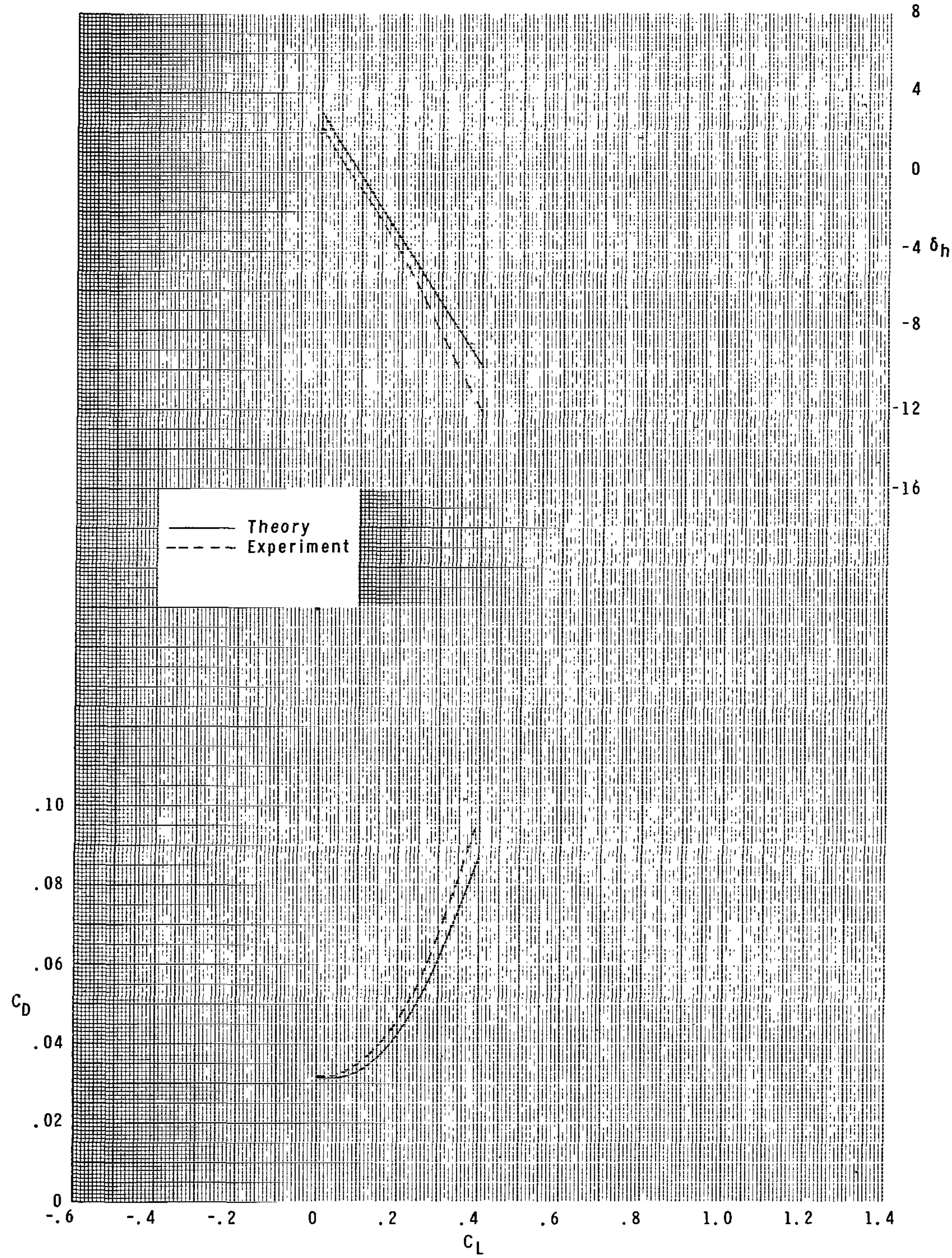

(b) M = 1.80.

Figure 7.- Continued.

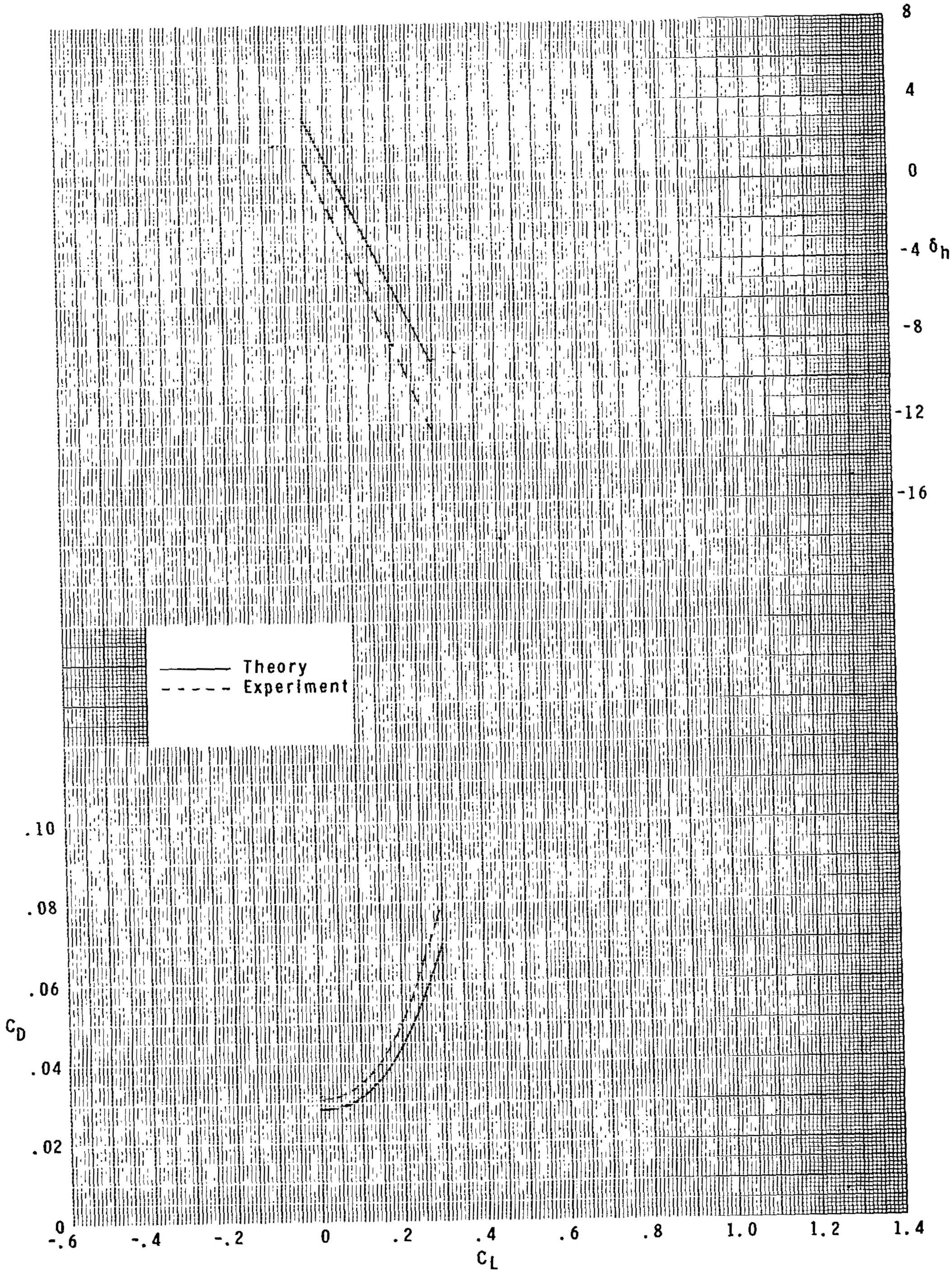

(c) M = 2.16.

Figure 7.- Concluded.

NASA-Langley, 1977

NATIONAL AERONAUTICS AND SPACE ADMINISTRATION
WASHINGTON, D.C. 20546

OFFICIAL BUSINESS
PENALTY FOR PRIVATE USE $300

THIRD-CLASS BULK RATE

POSTAGE AND FEES PAID
NATIONAL AERONAUTICS AND
SPACE ADMINISTRATION
451

U.S.MAIL

497 001 C1 U A 770708 S00903DS
DEPT OF THE AIR FORCE
AF WEAPONS LABORATORY
ATTN: TECHNICAL LIBRARY (SUL)
KIRTLAND AFB NM 87117

POSTMASTER: If Undeliverable (Section 158 Postal Manual) Do Not Return

"The aeronautical and space activities of the United States shall be conducted so as to contribute . . . to the expansion of human knowledge of phenomena in the atmosphere and space. The Administration shall provide for the widest practicable and appropriate dissemination of information concerning its activities and the results thereof."

—NATIONAL AERONAUTICS AND SPACE ACT OF 1958

NASA SCIENTIFIC AND TECHNICAL PUBLICATIONS

TECHNICAL REPORTS: Scientific and technical information considered important, complete, and a lasting contribution to existing knowledge.

TECHNICAL NOTES: Information less broad in scope but nevertheless of importance as a contribution to existing knowledge.

TECHNICAL MEMORANDUMS: Information receiving limited distribution because of preliminary data, security classification, or other reasons. Also includes conference proceedings with either limited or unlimited distribution.

CONTRACTOR REPORTS: Scientific and technical information generated under a NASA contract or grant and considered an important contribution to existing knowledge.

TECHNICAL TRANSLATIONS: Information published in a foreign language considered to merit NASA distribution in English.

SPECIAL PUBLICATIONS: Information derived from or of value to NASA activities. Publications include final reports of major projects, monographs, data compilations, handbooks, sourcebooks, and special bibliographies.

TECHNOLOGY UTILIZATION PUBLICATIONS: Information on technology used by NASA that may be of particular interest in commercial and other non-aerospace applications. Publications include Tech Briefs, Technology Utilization Reports and Technology Surveys.

Details on the availability of these publications may be obtained from:

SCIENTIFIC AND TECHNICAL INFORMATION OFFICE

NATIONAL AERONAUTICS AND SPACE ADMINISTRATION

Washington, D.C. 20546